MND-3607-239-3

SNAP 19 Phase III Final Report

VOLUME III
GENERATOR DEVELOPMENTAL ASPECTS

MARTIN MARIETTA NUCLEAR DIVISION

DISCLAIMER

This report has been prepared
under Contract AT(30-1)-3607
with the U.S. Atomic Energy
Commission

MND-3607-239-3 C-92A,
M3679, 55th Edition
AEC Research and
Development Report

SNAP 19 Phase III
Final Report

VOLUME III
GENERATOR DEVELOPMENTAL ASPECTS

MND-3607-239-3

May 1968

MARTIN MARIETTA CORPORATION NUCLEAR DIVISION

BALTIMORE, MD. 21203

LEGAL NOTICE

FOREWORD

This three-volume report, prepared by the Martin Marietta Corporation, is an account of the SNAP 19 radioisotope thermoelectric generator program performed under United States Atomic Energy Commission Contract AT(30-1)-3607.

PAGE BLANK

ABSTRACT

A. INTRODUCTION

This chapter indicates the purpose of SNAP 19 III Program and describes content of Volume III of the report and relationship to other volumes.

B. THERMOELECTRIC CONVERSION

Thermoelectric couple development, component selection criteria and the module criterion are described in this chapter.

C. GENERATOR FABRICATION

A description of development of advanced techniques for fuel handling, outgassing and leak testing generators is found in this chapter.

D. ELECTRICALLY POWERED HEAT SOURCE

Discusses heater element and heater block development, including problems encountered and method of resolution.

E. GENERATOR ENDURANCE TESTING

Described in this chapter are: the configuration of generators tested, preparation for the tests and the tests; results of pre-endurance and endurance tests; evaluation of thermoelectric components and conclusions drawn from endurance tests.

F. GENERATOR RELIABILITY DEMONSTRATION

Design features that provide reliability, and tests that provided reliability data are covered by this chapter.

G. GENERATOR SEAL PERFORMANCE

This chapter points out the performance of Viton A as generator seals.

H. HOT JUNCTION TEMPERATURE MEASUREMENT

Hot junction temperature measurement system, the problems experienced during its development and the means of problem resolution are discussed.

I. RADIATION SPECTRA

This chapter includes methods used in making neutron and gamma measurements, and gives spectra from these measurements.

J. FUEL CAPSULE SUPPORT

Described in this chapter are the method of capsule support, problems encountered with support design and means by which problems were corrected.

BLANK

SUMMARY

A. INTRODUCTION

The purpose of the SNAP 19 Phase III program was to qualify and deliver flight hardware for the Nimbus B spacecraft. Emphasis was not placed on technology development, but the program did result in advancements in generator technology.

B. THERMOELECTRIC CONVERSION

Methods of improving thermoelectric element control and measurements, couple fabrication processes and handling techniques, and test criteria and equipment were pursued throughout the SNAP 19 Phase III program. These efforts led to the establishment of a production process with an acceptable yield rate of couples meeting specification requirements.

In addition to the standard 2N-2P couples used in SNAP 19 generators, work was done on development of 2N-3P couples and 2N-2P couples with cups at the hot and cold ends.

C. GENERATOR FABRICATION

SNAP 19 generator fabrication involved many routine operations such as machining, welding and soldering. However, generator outgassing, fuel handling and generator leak testing processes needed development to meet requirements of the program. These process developments were successfully completed and employed in generator fabrication.

D. ELECTRICALLY POWERED HEAT SOURCE

Electrically powered cartridge heaters were used to simulate the isotopic heat source and to outgas generators which were subsequently to be fueled. Electrical heaters were also used for controlled heatup and cool-down in generator fueling and defueling operations.

Open- and short-circuit failures occurred in the initial version of the heaters, and the heater array wiring failed under vibration loads. Both of these problems were investigated, the causes were isolated and solutions were developed.

E. GENERATOR ENDURANCE TESTING

Eight electrically heated generators containing thermoelectric couples of the several configurations (2N-2P, 2N-3P and 2N-2P with cups) were endurance tested. Complete sets of data were obtained at regular intervals, and short sets were obtained daily during the tests. The power check data showed that all test generators performed satisfactorily. The test program yielded indications that the 2N-3P and 2N-2P (with cups) couples are superios to the 2N-2P couples with regard to stability and efficiency.

F. GENERATOR RELIABILITY DEMONSTRATION

There are no moving parts, and design redundancy minimizes sensitivity to critical static part failure. The series-parallel arrangement of the thermoelectric circuit enables the generator to withstand open-circuit thermoelectric couple failures, except for three couples in a single parallel array--an extremely unlikely event.

Tests accumulated 113,000 hours of operation without catastrophic failure. At 50% confidence, the demonstrated reliability is 0.95 for a one-year mission.

G. GENERATOR SEAL PERFORMANCE

A high temperature elastomer, Viton A, was selected to seal the generator cover plates and instrumentation penetrations. A multigas permeation model, an analytical model, tests and analyses verified the suitability of this material.

H. HOT JUNCTION TEMPERATURE MEASUREMENT

Resistance element sensors are used for hot junction temperature measurements. Erratic measurements during early testing led to discovery that breakdown of RTD electrical insulation was allowing the element to short to the case, and case voltage was impressed on the leads.

After experimentation with several approaches to correction of the problem, it was found that a hermetically sealed RTD spotwelded to an extension of the hot shoe operated satisfactorily.

I. RADIATION SPECTRA

Neutron measurements were made with a stilbene detector system. A data reduction program for the stilbene system was obtained from Mound Laboratory.

Gamma measurements were made with conventional gamma spectrometry techniques.

J. FUEL CAPSULE SUPPORT

Adequate support of the fuel capsule is essential to limit its motion relative to adjacent generator components. Disks of Min-K (Johns Manville Corporation) thermal insulating material constrain axial displacement. These disks are preloaded to provide the necessary constraint. The disks in an early generator were damaged because the preload was insufficient. Addition of shims to the design ensures proper preload.

CONTENTS

		Page
	Legal Notice	ii
	Foreword	iii
	Abstract	v
	Summary	vii
	Contents	ix
	List of Illustrations	xi
	List of Tables	xiii
I.	Introduction	I-1
II.	Thermoelectric Conversion	II-1
	A. Couple Development	II-1
	B. Thermoelectric Component Selection Criteria	II-3
III.	Generator Fabrication	III-1
	A. Generator Outgassing	III-1
	B. Fuel Handling Operations	III-2
	C. Leak Testing	III-6
IV.	Electrically Powered Heat Source	IV-1
	A. Heater Element Development	IV-1
	B. Heater Block Development	IV-3
V.	Generator Endurance Testing	V-1
	A. Generator Description	V-1
	B. Test Description and Preparation	V-3
	C. Pre-endurance Test Results	V-5
	D. Endurance Test Results	V-7
	E. Evaluation of T/E Performance	V-12
	F. Conclusions	V-16
VI.	Generator Reliability Demonstration	VI-1
VII.	Generator Seal Performance	VII-1
	A. Multigas Permeation Model	VII-1
	B. Results of Analysis	VII-5
VIII.	Hot Junction Temperature Measurement	VIII-1
IX.	Radiation Spectra	IX-1
	A. Neutron Measurements	IX-1
	B. Gamma Measurements	IX-1

CONTENTS (continued)

		Page
X.	Fuel Capsule Support	X-1
XI.	Bibliography of Topical Reports on SNAP 19 Generator Development	XI-1
	A. Thermoelectrics	XI-1
	B. Generator Design and Fabrication	XI-1
	C. Fuel Capsule Technology	XI-2
	D. Generator Subsystem Support Structure	XI-2
	E. Generator Performance and Endurance Tests	XI-2
	F. Generator Subsystem Environmental Tests	XI-3
	G. Mass Properties	XI-3
XII.	References	XII-1
Appendix A--Multigas Permeation Analysis		A-1

LIST OF ILLUSTRATIONS

Figure	Title	Page
II-1	Thermoelectric Couples--Exploded Views	II-2
II-2	Identification for Nine-Point Resistance Check	II-4
III-1	Outgassing Station	III-3
III-2	Fueling/Defueling Facility Arrangement	III-4
III-3	Generator Entering Thermal Vacuum Chamber	III-7
IV-1	Heating Element	IV-2
IV-2	Electrical Heater Block Configuration	IV-4
IV-3	Single Heater Circuit Connection	IV-5
IV-4	Typical Heater Connection Fracture	IV-5
IV-5	Redesigned Heater Array	IV-5
IV-6	Electrically Heated Generator and Dummy Unit Mounted for Roll Excitation	IV-6
IV-7	Tack Welding of Heaters to Block	IV-6
V-1	Thermoelectric Couples--Exploded Views	V-2
V-2	Endurance Test Arrangement for Electrically Heated Generator	V-4
V-3	Endurance Generator Test Chronologies	V-6
V-4	Endurance Test Generator Power Histories Comparison of Least Square Fit Curves	V-9
V-5	Endurance Test Generator Power Histories	V-10
V-6	Power Degradation Parameter Conversion Chart	V-11
V-7	T/E Efficiency of 2N-3P	V-13
V-8	T/E Efficiency of 2N-2P	V-13
V-9	Gross Output Power and Heat to Elements--2N-3P	V-14
V-10	Gross Output Power and Heat to Elements--2N-2P	V-15
VI-1	Demonstrated Reliability as a Function of Mission Duration	VI-3
VII-1	Multigas Permeation Model	VII-2
VII-2	Permeability Versus Temperature for Viton A	VII-4
VII-3	SNAP 19 Endurance Generator Pressure Decay	VII-6
VII-4	SNAP 19 Endurance Test Generator Pressure Predictions for Generator in Air	VII-8
VII-5	SNAP 19 Endurance Test Generator Nitrogen Pressure Buildup for Generator in Air	VII-9
VII-6	Endurance Generator Pressure Predictions and Experimental Data--Single Gas Versus Multigas Models	VII-10
VII-7	Fueled Dispersal Generator Pressure Profiles	VII-11
VII-8	Fueled IRHS Generator Pressure Profiles--Total Pressure	VII-13

LIST OF ILLUSTRATIONS (continued)

Figure	Title	Page
VII-9	Fueled IRHS Generator Pressure Profiles--Partial Pressures of Nitrogen and Helium	VII-14
VII-10	Fueled IRHS Generator Pressure Profiles--Partial Pressure of Argon	VII-15
VII-11	IRHS Generator Pressure Profiles for a Helium Fill Case	VII-16
VIII-1	Hot Junction Temperature Sensor (RTD)	VIII-2
VIII-2	RTD Installed Hot Shoe	VIII-2
VIII-3	RTD-TSCU Circuit Schematic	VIII-3
VIII-4	Encapsulated RTD	VIII-5
VIII-5	Hermetically Sealed RTD	VIII-5
VIII-6	Installation of Hermetically Sealed RTD's	VIII-6
IX-1	Typical Neutron Spectral Measurement	IX-2
IX-2	Gamma Spectrum	IX-3
IX-3	Gamma Spectrum	IX-4

LIST OF TABLES

Table	Title	Page
V-1	Pre-endurance Tests	V-3
V-2	Endurance Generator Test Times as of 11/30/67	V-5
V-3	Power Degradation Coefficients for Endurance Test Generators	V-8
V-4	Typical Efficiency Data	V-12
V-5	Comparison of T/E Efficiency and Stability Data	V-16
VI-1	Generator Operating Time Summary	VI-1
VII-1	Gas Permeability Constants for Viton A	VII-5
VII-2	Summary of Normalized Hot Argon Leak Rates for SNAP 19 Endurance Test Generators	VII-7
VII-3	Quantities of Oxygen Entering Generators for Various Test Conditions	VII-12

I. INTRODUCTION

The purpose of the SNAP 19 Phase III program was to qualify and deliver flight hardware for the Nimbus B spacecraft. Therefore, emphasis was not placed on the development of generator technology. The program did, however, contribute to generator technology, since (1) some developmental work, such as endurance testing and evaluation of new thermoelectric couple technology, were included in the program, (2) performance of the planned hardware aspects of the program yielded data and experience applicable to generator technology and (3) some development in specific areas was necessary to accomplish the program requirements.

This volume of the Phase III final report discusses generator technology developments. Additional development efforts relative to the isotopic heat sources are given in Volume II. Developmental aspects related to SNAP 19 safety are discussed in Ref. I-1. Chapter X of this volume presents a bibliography of topical reports related to technology development.

II. THERMOELECTRIC CONVERSION

A. COUPLE DEVELOPMENT

Throughout the SNAP 19 program, methods of improving thermoelectric element control and measurements, couple fabrication processes and handling techniques, and test criteria and equipment were constantly sought in a continuous development effort. The results of this effort have been the establishment of sophisticated element and couple specifications, discussed in the following section, and the numerous process specifications to implement this work. These controls have, in turn, resulted in consistency in performance of generators fabricated and tested under the program.

Most of the development work on the standard 2N-2P couple design (Fig. II-1) centered around the establishment of a qualified production process with acceptable yield rates and a product which meets all of the specification requirements.

In addition to the fabrication techniques and properties, the couple performance could also be affected by the spring pressure loads on the couple; consequently, special consideration was given to this area. Relatively simple interface conductance tests demonstrated the potential advantages of high pressure on nonbonded interfaces. The effectiveness on a bonded interface has not been determined but there is little doubt that, if the bond tends to degrade, a high spring load should certainly be advantageous relative to interface performance. On the other hand, excessively high spring pressure will result in undesirable element creep. At a room temperature element spring pressure of about 100 psi, for example, an unsatisfactory amount of material flow occurs with hot junction operating temperatures of 950° F. This has been demonstrated in short duration testing. The 60-psi spring pressure specified for each SNAP 19 element is considered near optimum, well below the level at which creep becomes a problem and still provides good thermal contact.

Also, under the SNAP 19 program, Martin Marietta Corporation fabricated two endurance test generators which incorporated two variations (Fig. II-1) of thermoelectric conversion material and bonding techniques. The purpose of these units was to obtain long-term performance data and to compare it with similar data from standard 2N-2P SNAP 19 generators.

One unit, generator S/N 20, was assembled using 2N-3P thermoelectric elements. Extensive development work was required to realize a satisfactory preproduction qualification run for the couples. The first bonding attempts of the 3P material resulted in internal cracking of the P type elements. Experimental work on the bonding materials and temperatures subsequently resulted in an acceptable couple with good yield rates.

Generator S/N 21 was assembled using 2N-2P type thermoelectric elements, but employing a thin metal cup at both the hot and cold ends in the bonding technique. The cup feature is expected to produce a more stable 2N-2P couple. In addition, because the cup design provides more area in contact with the element bond, the bond joints will have greater strength. Development on these couples involved not only various brazing materials and cup thicknesses, but variations in hot shoe material itself. New bonding jigs were also employed. Martin Marietta Drawing 452A2300001 depicts the couple details and refers to the Nuclear Process Specifications employed to fabricate these components.

Data on the thermoelectric performance characteristics are presented in Ref. II-1, which is summarized in Chapter V of this report.

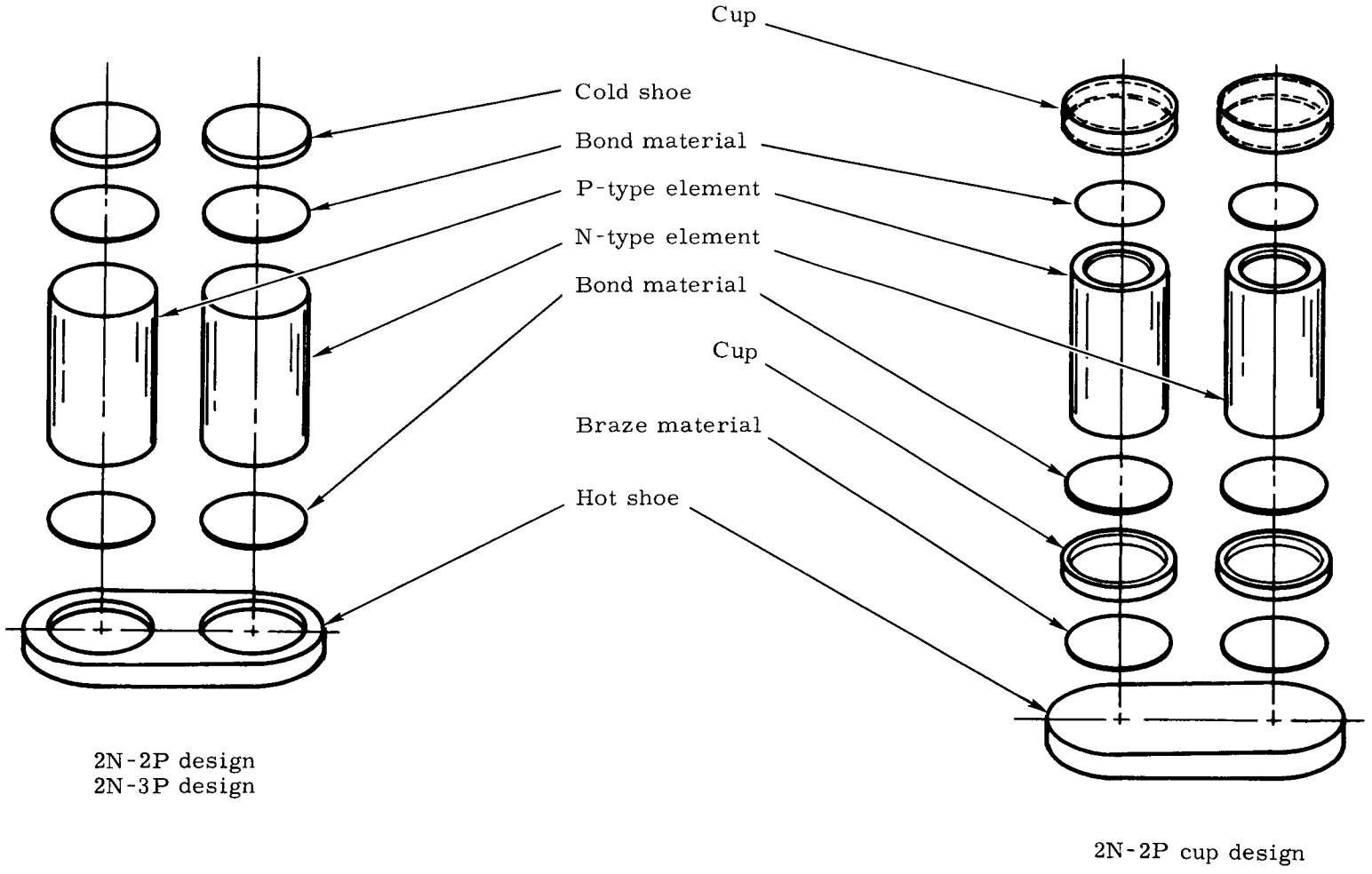

FIG. II-1. THERMOELECTRIC COUPLES--EXPLODED VIEWS

B. THERMOELECTRIC COMPONENT SELECTION CRITERIA

1. Element Specification

All SNAP 19 Phase III generators (S/N 7 through 23A) were built with thermoelectric elements purchased under the requirements of Ref. II-2. The preliminary version of this specification was written in August 1965 and Revision 4 was issued in July 1966. However, the additional criterion of significance contained in Revision 4 was the quality factor (Seebeck voltage squared divided by electrical resistivity) and this requirement was made retroactive to the beginning of Phase III. Some additional data were taken on elements under Revision 4 (e.g., thermal conductivity, compressive strength, etc.) but these data are for information purposes only and do not affect the selection or rejection of element batches. Therefore, elements for all Phase III generators were, in effect, inspected to Revision 4 requirements although in some cases certain informational-type data on element samples do not exist. A brief discussion of Revision 4 follows.

All elements must conform to the dimensions and tolerances defined on the element design drawing. There are five nondestructive surface finish requirements on chipping, pitting, grain grooves, surface deposits and cracking. There are three nondestructive electrical requirements on Seebeck voltage, room temperature, electrical resistivity and quality factors. For informational purposes only, sampling destructive tests were conducted to determine thermal conductivity, internal defects, compressive strength and minor constituent impurity levels (spectrographic analysis). In addition, there are requirements on element cleanliness and storage of finished elements.

2. Couple Specification

All Phase III thermoelectric couples were inspected according to Ref. II-3 except that visual criteria were waived for endurance generator S/N 19. In addition to the nine-point (Fig. II-2) couple resistance check (four bonds, two elements, two legs, whole couple), this specification includes destructive test requirements on output power and internal resistance (both at hot and cold junction operating temperatures of 900° F $\pm$ 10° and 200° F $\pm$ 10°, respectively), internal cracking (metallographic sectioning) and nondestructive requirements on surface finish, cleanliness and storage.

3. Module Criterion

The thermoelectric module criterion that was applied to all SNAP 19 generators (S/N 1 through 23A) is that module resistance must not exceed 4.8, 6.0 and 4.2 milliohms for 2N-2P, 2N-3P and 2N-2P cupped material, respectively.

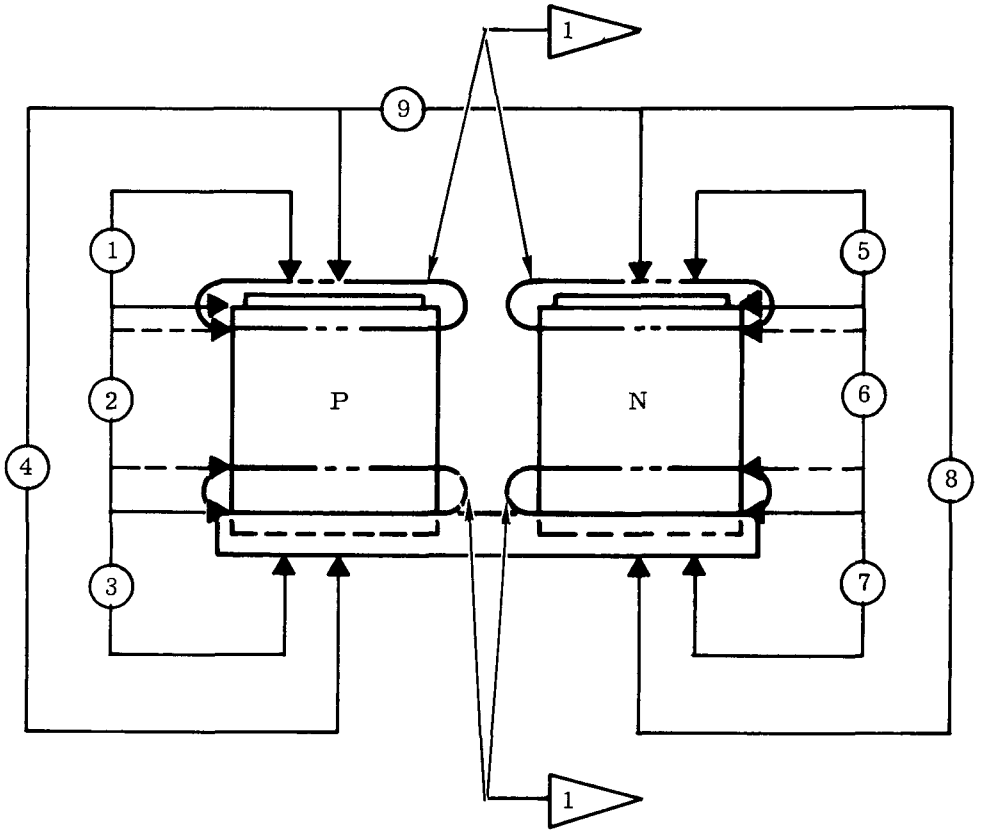

Positions for Nine-Point Check

1 Phantom lines applicable to cup-type couples only

Legend

1, 5 Cold end bonds
2, 6 Elements
3, 7 Hot end bonds
4, 8 P and N legs
9 Couple

FIG. II-2. IDENTIFICATION FOR NINE-POINT RESISTANCE CHECK

III. GENERATOR FABRICATION

SNAP 19 generator fabrication involves many routine operations including machining, welding, soldering, etc. However, several steps in the fabrication process required further development during the program. These included generator outgassing, fuel handling operations and generator leak testing. These are discussed in the following sections.

A. GENERATOR OUTGASSING

Contaminants within a radioisotope thermoelectric generator (RTG) when present in sufficient quantities, can be detrimental to performance time. Several methods have been employed in the development of RTG assembly techniques to minimize the contamination present at the time of assembly. These have included individual, thorough cleaning of each component prior to assembly and final assembly in a clean, argon-filled dry box.

Outgassing techniques have been employed on many thermoelectric generator programs to ensure a degree of cleanliness unobtainable by other means. In theory, outgassing consists of reducing the RTG internal pressure and raising the temperature until contaminants are driven of by vaporization or thermal excitation.

In practice, however, the process is restricted by:

(1) Maximum allowable temperatures within the RTG

(2) Changes in heat transfer capability as a result of reduced gas pressure within the generator core

(3) Allowable rates of temperature change to avoid thermal shock at the thermoelectric couple bonds.

The SNAP 19 outgassing process evolved in a series of developments. Each development was undertaken either to improve the overall cleanliness or to reduce the risk to the RTG as it underwent the process. Maximum temperature limits were established for both the hot and cold junctions of the thermoelectric couples. Changes in heat transfer capability under reduced gas pressure were anticipated. Allowable rates of temperature change were established to minimize thermal shock and still apply a realistic time criterion to the process. The present outgassing procedure consists of the following steps:

(1) The electrically heated generator is evacuated while at room temperature until the internal pressure is 200 microns or less. This step removes the major portion of free contaminants before heat is applied, thus limiting chemical reaction between the contaminants and generator components.

(2) The generator hot junction temperature is raised to 300° F and held for four hours. This step drives off most of the available hydrocarbons at temperatures below their cracking temperature; cracking usually starts at 350° F and above. A significant quantity of water vapor is also removed during this hold period.

(3) The generator is backfilled with argon to 20 mm Hg and the hot junction temperature is raised to 975° F. This is higher than the anticipated operating temperature of flight generators and drives off most of the

remaining reactionable materials. The increase in internal pressure minimizes the potential for an overtemperature or thermal shock during the transition. The internal pressure is never reduced below 20 mm Hg while the generator is at the high temperature level.

(4) The generator is held at these conditions for four hours, flushed with clean argon, held again, and finally reflushed and backfilled.

The argon employed in the generator backfilling and flushing operations is purchased as laboratory grade (99.99% pure) and is passed through both a cold trap and a chip furnace prior to entering the generator. A residual gas analyzer (RGA) and a Beckman hygrometer are employed to verify the cleanliness of the argon and to inspect the gaseous effluents during the outgassing process.

Figure III-1 shows a typical RTG installed on the outgassing station. The port employed for pumping out the generator is part of a special outgassing assembly designed to facilitate the outgassing sequence and to be easily removable during fueling.

B. FUEL HANDLING OPERATIONS

Fuel handling operations have been subdivided into two categories: the initial inspection of the fuel capsule or heat source as received at Martin Marietta from Mound Laboratory and fueling or defueling the RTG. Many of the dispersal heat source handling operations are performed in air, but all intact re-entry heat source (IRHS) handling is performed in a glove box. The slight differences in heat source configuration also pose varying problems and a requirement for different handling tools.

1. Radiological Inspections

Each fuel capsule or heat source is inspected for contamination as soon as possible after being received at Martin Marietta. Dispersal heat sources are not sealed in transit, and are handled freely in air once removed from the shipping cask. The inspection is performed in a previously prepared glove box facility with provisions for air-tight sealing of the inspection area if contamination is discovered. A series of swipes are taken on the capsule surface and evaluated with alpha sensitive meters to determine the extent, if any, of surface contamination. The swipes are counted twice, once in a short count which detects large quantities of contaminants quickly and once in a long count, for a more precise measurement. After the swipe tests have shown that the surface contamination is within the allowable limits, the capsule is returned to the shipping cask for storage until generator fueling.

Intact re-entry heat sources, because of their more sensitive materials, are never handled outside a clean, low oxygen environment (see Volume II for a more detailed discussion). The intact re-entry heat source is received at Martin Marietta in a sealed container and is withdrawn from that container only in a controlled environment (Fig. III-2). The sealed container is equipped with purge valves that are utilized in sampling the gas within the sealed container before it is opened.

When the initial purge check is complete, the container is opened to permit swipe tests of the IRHS which are similar to those employed for the dispersal capsule. The same counting techniques are employed and the container is resealed for storage when they are complete.

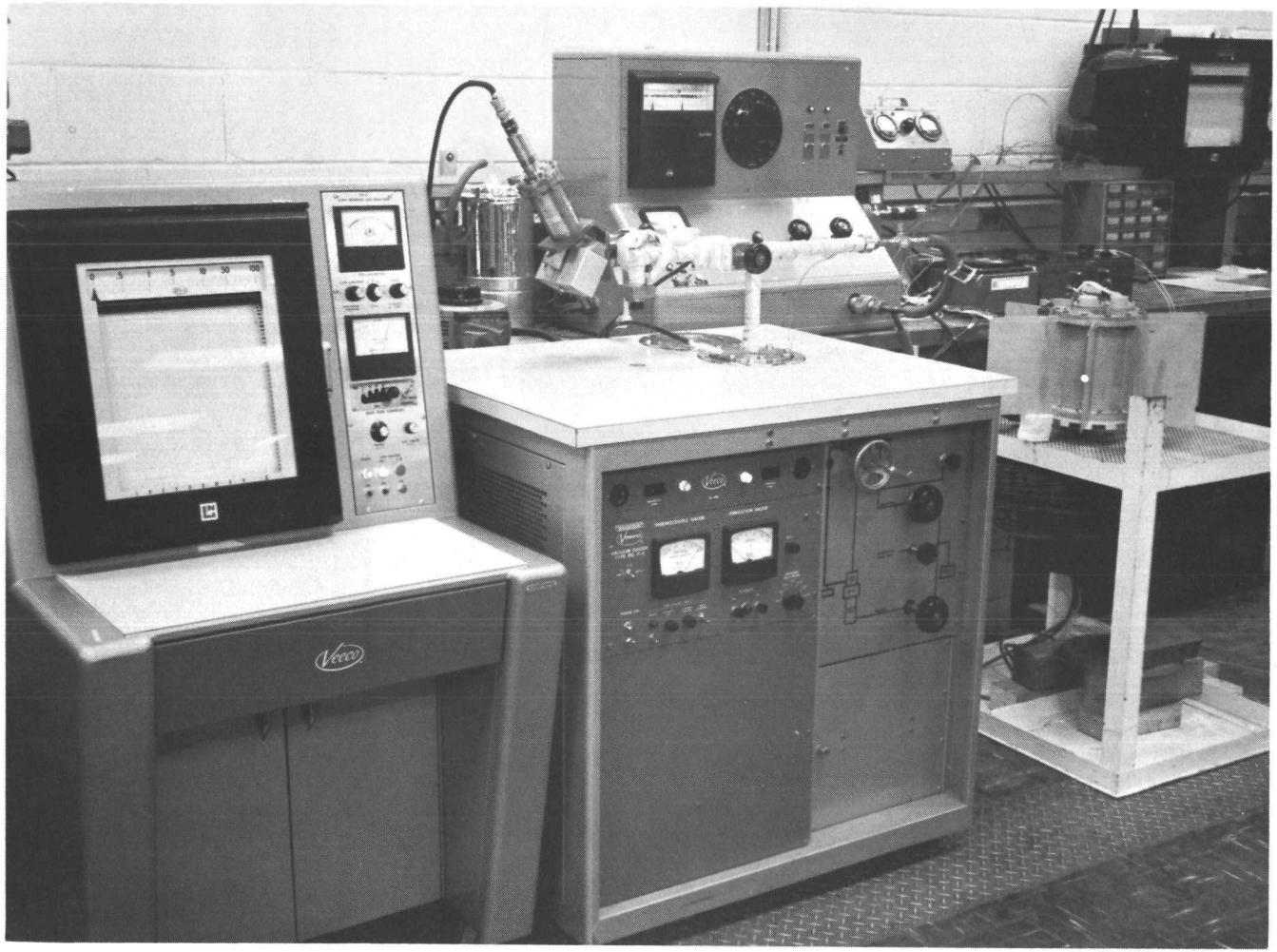

FIG. III-1. OUTGASSING STATION

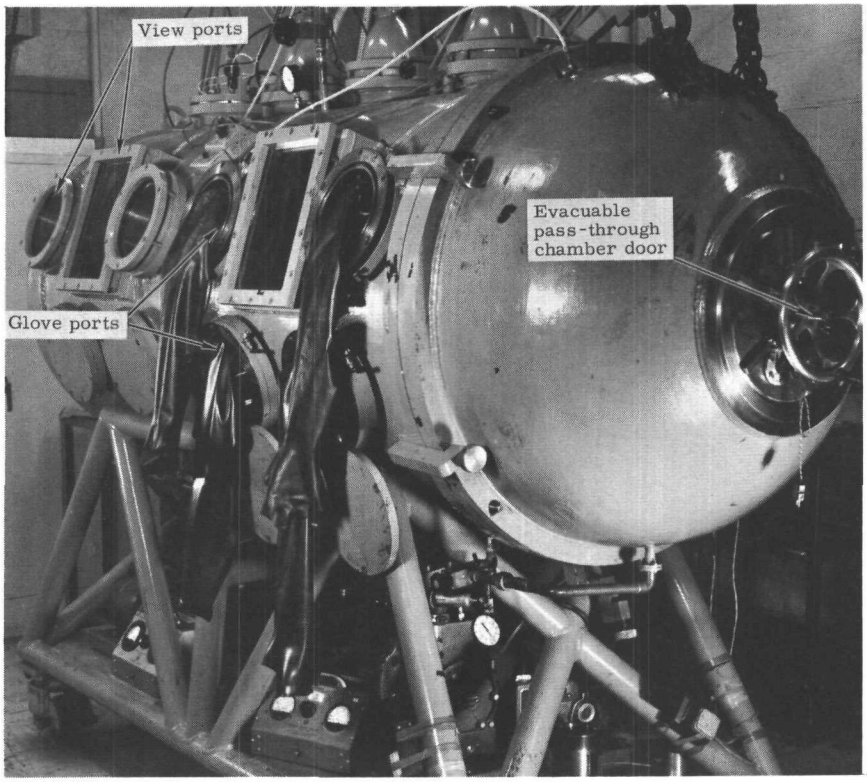

Fueling/Defueling Chamber

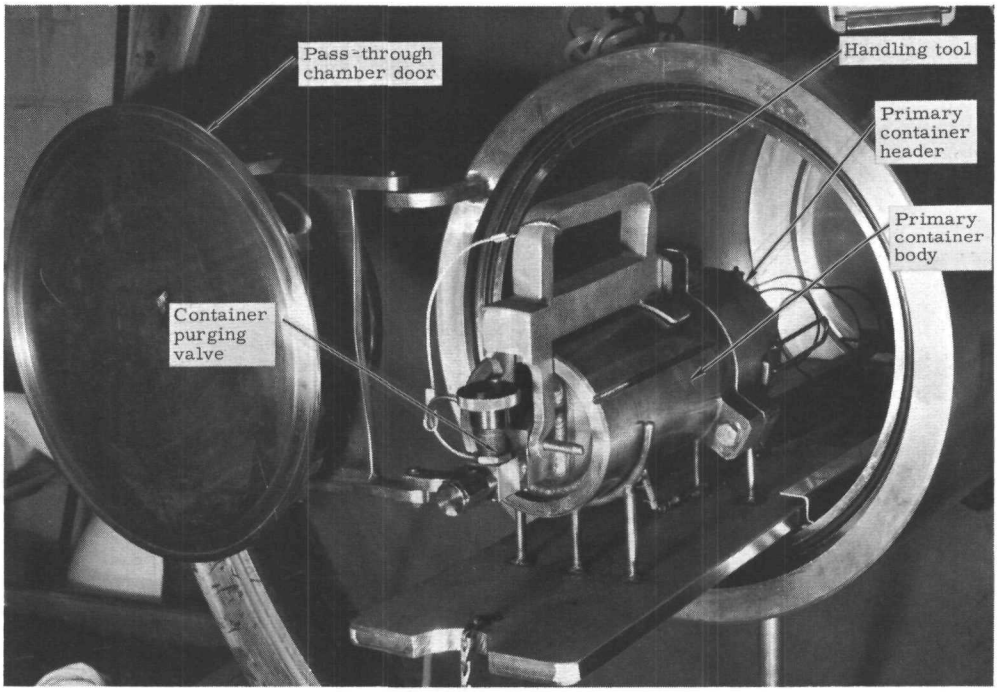

Heat Source Primary Shipping Container in Fueling Facility Pass-Through

FIG. III-2. FUELING/DEFUELING FACILITY ARRANGEMENT

The swipe tests are repeated on heat sources each time they are removed from storage or withdrawn from an RTG.

2. Fueling and Defueling

During the fabrication and outgassing phases of its construction, each generator is equipped with an electrically powered heat source. During the fueling operations this electrically powered heat source heats the generator to operating temperature and maintains the generator at that temperature until the isotopic heat source can be inserted. It is presently felt that the less thermal shock the generator experiences during the fueling operation, the more successful the operation will be. The degree of success attained in any given fueling is measured by a series of power checks (functional power output measurements) performed before and after the fueling.

The differences between dispersal and intact re-entry heat sources stem from the external configuration of each. The dispersal capsule permits the installation of a positive locking tool for handling. The IRHS is completely smooth surfaced. Its aerodynamic design does not permit the use of positive locking tools. To facilitate IRHS handling, a three-fingered gripping tool was designed for fueling.

The typical SNAP 19 fueling sequence followed these steps:

(1) Install the electrically heated generator in the fueling facility.

(2) Purge the fueling facility with a series of evacuations and backfills.

(3) Pass the heat source into the fueling facility.

(4) Open the generator from the top and prepare the electrically powered heat source for removal.

(5) Inspect the isotope heat source for surface contamination.

(6) Remove the electrical heat source and insert the isotope heat source.

(7) Install the RTG flight cover and reseal when temperature equilibrium is reached.

During the final closure operation, shims were employed to adjust the heat source preload within predetermined limits. The same basic pattern was followed with both the IRHS and dispersal heat sources.

Defueling operations were essentially similar to this technique. Starting with a fueled RTG, the steps were:

(1) Install the fueled RTG in the fueling facility.

(2) Purge the facility with a series of evacuations and backfills.

(3) Bring the electrical heat source up to temperature.

(4) Open the generator and remove the isotope heat source.

(5) Install the electrical heat source.

(6) Inspect the isotope heat source and remove it for storage.

(7) Cool the generator by slowly reducing the power input to the electrical heaters, seal the generator and remove it from the fueling facility.

The three-fingered handling tool, designed for fueling an IRHS generator, was not sufficient for defueling. The clearance between the heat source and the RTG heat accumulator block is not adequate to permit installing the tool when the heat source is fully inserted in the generator. Instead, a vacuum tool was employed to partially withdraw the IRHS until the three-fingered tool could be installed.

The success attained in many fueling and defueling operations throughout the program is attributed to the extensive and thorough training received by each man working as part of a fueling or defueling team. Each operation was practiced until every man was totally familiar not only with his own task but also with the tasks of the other team members.

In all, six dispersal generators were fueled and six were defueled, seven IRHS generators were fueled and five were defueled for a total of 24 successful operations.

C. LEAK TESTING

During fabrication and test, each flight or fueled prototype RTG receives three leak tests. The first two are performed on the individual generators, and the third test is performed in the subsystem configuration. This last leak test is done during thermal vacuum testing and is discussed in Volume I.

1. Helium Cold Leak Tests

Prior to any heating of the RTG, and at the completion of the generator assembly, each seal is tested with helium. Utilizing the outgassing cover and pressure port, the pressure within the RTG is pumped down to 200 microns or less. The operator directs a helium probe at each potential leak point around the RTG seals and welded closures. When the probing is complete, the generator is bagged and immersed in helium.

The probe operation permits the operator to search for gross leakage at various points on the RTG. The total immersion or bagging technique yields a total RTG leak rate. Should that leak rate exceed 5.5×10^{-6} 5 cm^3/sec of helium, the generator is returned for rework.

2. Argon Hot Leak Tests

Subsequent to the fueling operation, each RTG is tested for final seal integrity. This test is performed with the generator hot and in short circuit condition.

When the generator is fueled, all outgassing ports and pressure penetrations are removed. The leak test, therefore, must be performed from the outside of the generator. Each RTG is suspended inside a small thermal vacuum chamber (Fig. III-3), the chamber is pumped down, and a residual gas analyzer measurement is made of the quantity of argon leaking through the generator seals. A liquid nitrogen-cooled shroud maintains the generator at a safe operating temperature throughout the test.

A numerical value is obtained for the quantitative argon leak rate by comparing the measured data against a known argon standard and deducting a value derived from empty chamber measurements. This value is then normalized for the variations which occur in internal pressure and seal temperature between different generators. Finally it is compared against an acceptance standard of 1×10^{-4} scc/sec.

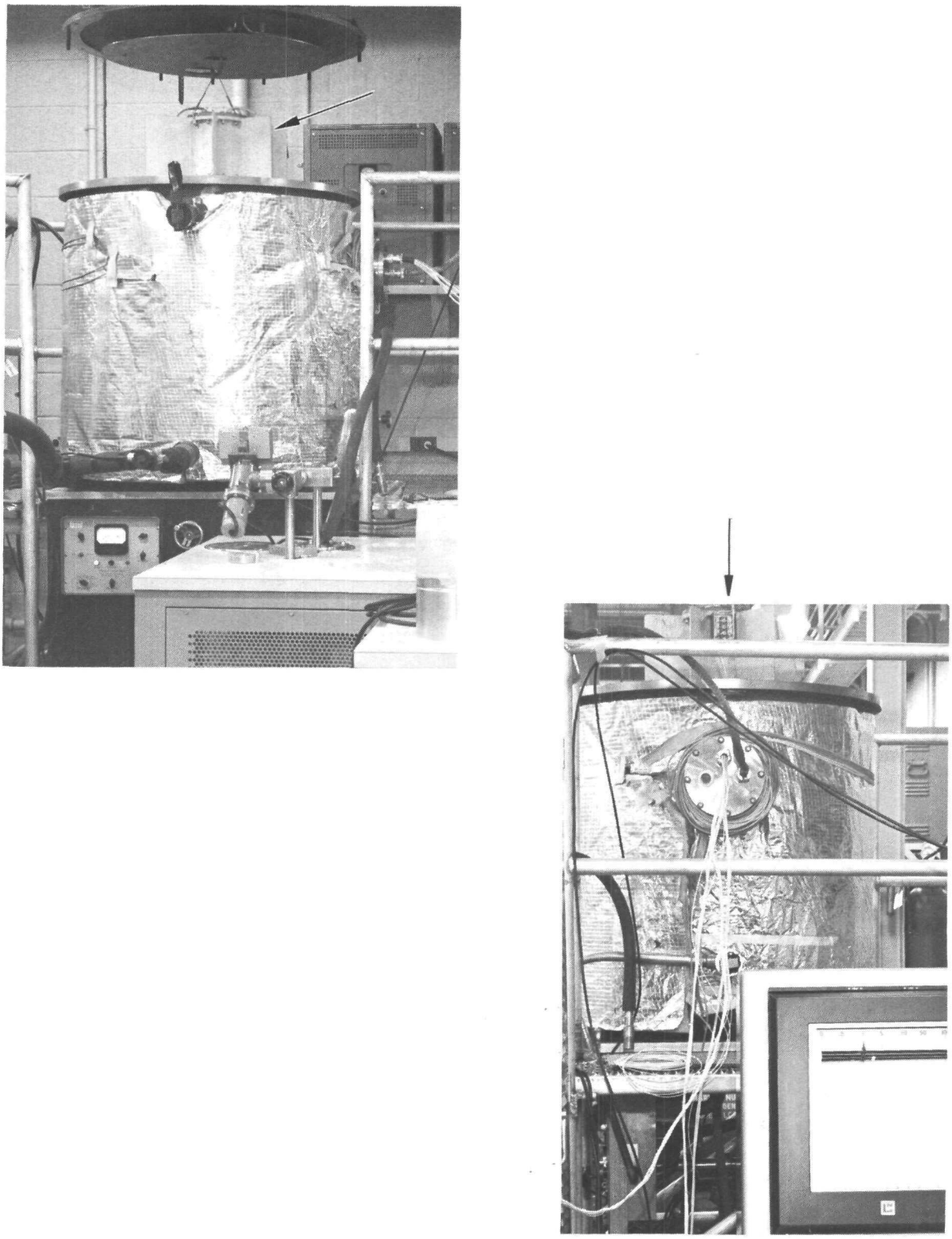

FIG. III-3. GENERATOR ENTERING THERMAL VACUUM CHAMBER

IV. ELECTRICALLY POWERED HEAT SOURCE

In electrically powered SNAP 19 generators, cartridge heaters were used to simulate the isotopic heat source. These heaters were also used for outgassing of the generators which were to be fueled later. Electrical heaters were used for controlled heatup and cooldown in generator fueling and defueling operations.

Two problems encountered early in the program on the initial version of the heaters were cartridge heater open or short circuit failures, and failures of the heater array wiring under vibration loads (during generator subsystems S/N 2 and 5 prototype testing). Both of these problems were investigated, the causes were isolated, and solutions were developed.

The heater failure was traced to arcing between internal power leads. The wiring failures were caused by inadequate heater and wiring structural support. Redesign of both the heater element and heater block array resulted in a heat source with an operating life in argon at 1075° F of many thousands of hours. In addition, these were capable of withstanding the complete spectrum of generator subsytem environmental tests.

A. HEATER ELEMENT DEVELOPMENT

An array of six heaters was used to simulate the 570-watt(t) inventory of a single fueled SNAP 19 generator. Each heater was capable of producing 225 watts using a 115-volt a-c source. The heaters were electrically wired in parallel so that each drew only about five amperes, although the wiring could safety carry about 12 amperes.

The heater element was designed to minimize arcing by having only one power lead exit from each end of the element. The element was a cartridge unit with an Inconel sheath and 15-gage, electronic grade, solid nickel leads. Because of their flexibility, stranded leads were desired, but an extensive development program would have been required, and scheduling would not permit this.

Shorted heater circuit failures began to occur in September 1966. Failure analysis indicated the origin of the trouble to be in the heater element design. Sauereisen No. 29 cement was used to hold in place a ceramic plug at both ends of the heater cartridge. (See original design in Fig. IV-1.) It was determined that the cement became conductive during curing and, in addition, produced a highly corrosive precipitate. The failure process occurred as follows:

(1) The Sauereisen cement became conductive and allowed current leakage between the two internal power leads.

(2) The reaction between the lead wires and Sauereisen cement eroded material from the lead wires, forming a deposit and lowering the resistance between leads.

(3) When the resistance between the leads became low enough, arc-over occurred, causing either an open or short circuit. The point of arc-over in every failure of this type was inside the heater at the innermost end of the ceramic plug.

A joint Martin Marietta-vendor effort resulted in a heater element redesign, (Fig. IV-1) which proved to be trouble free. The power leads were altered so that

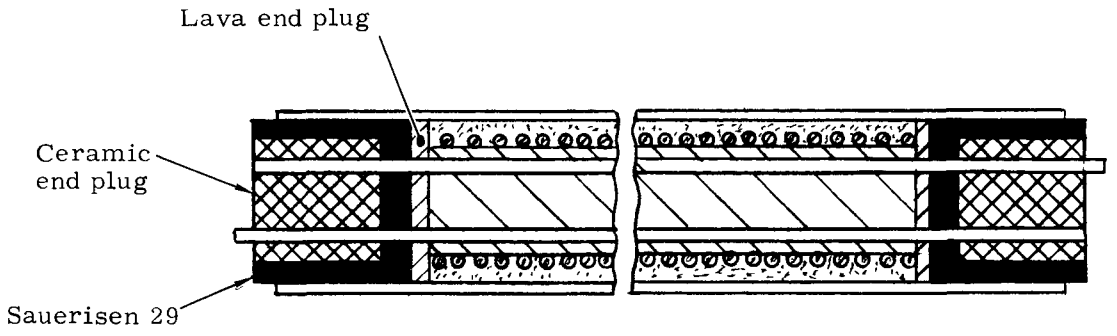

a. Original Design

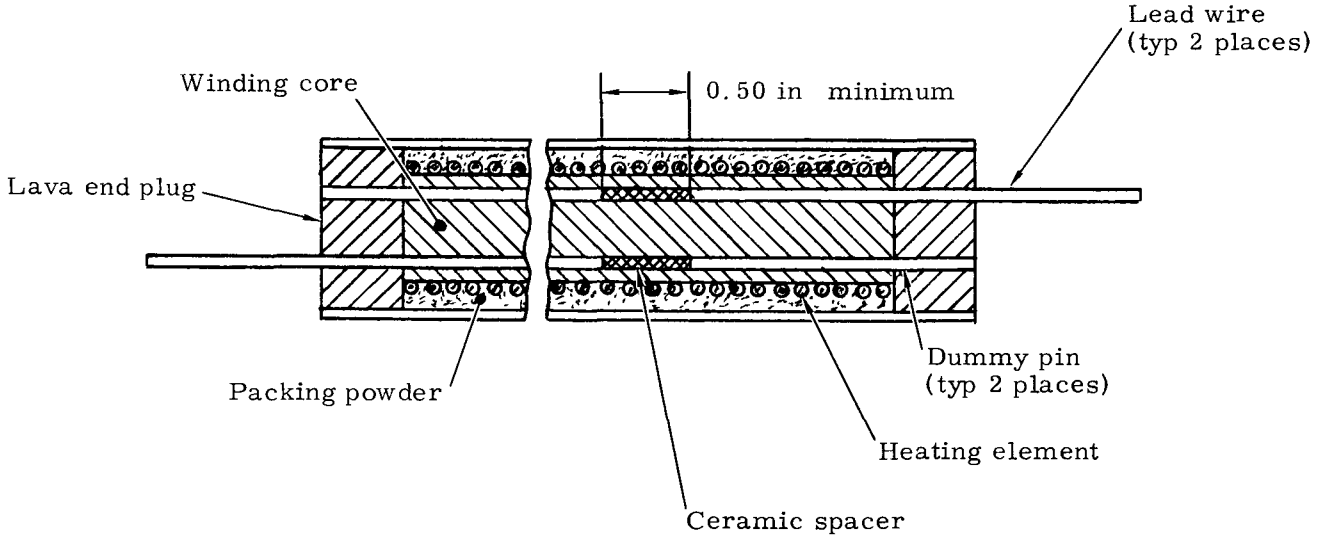

b. Redesign

FIG. IV-1. HEATING ELEMENT

only one lead at each end of the cartridge was active. As noted previously in the original design only one lead at each end protruded from the cartridge. The other wire, although flush with the end, was electrically active. The ceramic spacer is shown in the lower sketch of Fig. IV-1 and the Sauereisen No. 29 cement and ceramic plugs were replaced with a Grade A lava plug swaged into the heater sheath as an integral part of the element.

Process specifications were issued for the redesign heater element that required a heater block burn-in with a complete heater array at 1000° F for eight hours to assure bakeout or outgassing of the complete assembly prior to use in a SNAP 19 generator.

During the analysis of the heater elements, traces of a hydrocarbon atmosphere were found in the generator. The source of hydrocarbon was found to be cleaning agents (acetone and toluene) and oil vapors from the vacuum pump used in the generator outgassing operation. The use of these cleaning agents was eliminated from all generator operations and molecular sieve-type vapor traps were added to the outgassing stations to further reduce the hydrocarbon environment.

B. HEATER BLOCK DEVELOPMENT

The electrical heat source used during Phase III of the SNAP 19 Program is a cylindrical steel block housing six electrical heaters (Fig. IV-2). This block and heater assembly simulates the size, weight, center of gravity and thermal inventory of the SNAP 19 dispersal fuel capsule. The evolution of this heat source design is traced in this section.

The Phase II electrical heat source employed a seven-piece graphite block (instead of steel) with steel inserts around the cartridge heaters.

On two occasions during Phase II, heater lead wire failures occurred during dynamic qualification testing on subsystem S/N 2 (generators S/N 3 and 4). The heaters were wired in parallel using a solid nickel wire connection, heliarc welded as shown in Fig. IV-3. Examination of the failures showed that these had occurred at the lead connection adjacent to the weld (see Fig. IV-4). The failure was caused by insufficient compliance in the wiring and by the embrittlement of the welded joint. The heater was redesigned (Fig. IV-5) to increase compliance by use of stranded wire, and to avoid embrittlement by crimped connections rather than welding.

During the initial phase of prototype vibration testing of subsystem S/N 5, heater wiring failure occurred. Subsequent internal inspection of the upper generator disclosed crushed and fractured heater wiring. This condition was caused by impacts on the ends of the heater block assembly when the supporting Min-K insulation surfaces fractured and pulverized during vibration.

Several design iterations were subjected to vibration testing using a dummy unit as the lower generator as shown in Fig. IV-6. The initial redesign incorporated end caps for the heater block to protect the heater leads and to provide greater load bearing contact surface for support under load. During the vibration testing, heater failure again occurred. Internal inspection showed that although the heater block assembly was sufficiently restrained from movement under vibration loads, the individual heaters moved relative to the block, resulting in fracture of the lead wiring. This problem was resolved by tack welding the heater sheath to the block at one end (Fig. IV-7).

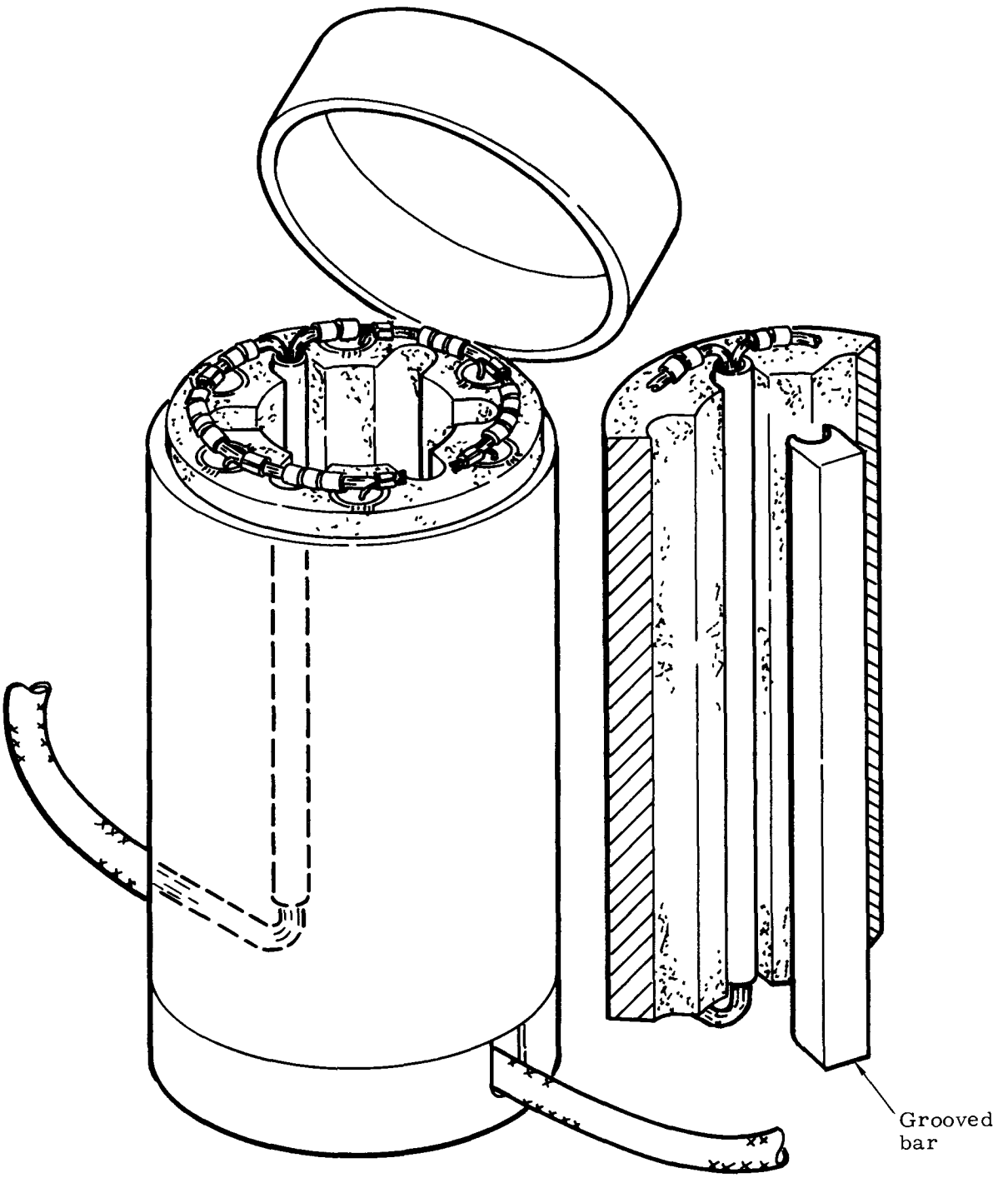

FIG. IV-2. ELECTRICAL HEATER BLOCK CONFIGURATION

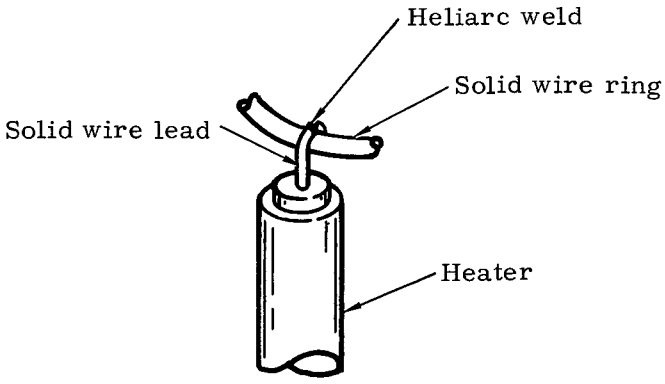

FIG. IV-3. SINGLE HEATER CIRCUIT CONNECTION

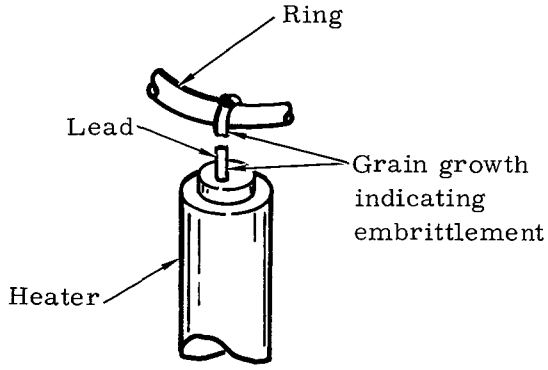

FIG. IV-4. TYPICAL HEATER CONNECTION FRACTURE

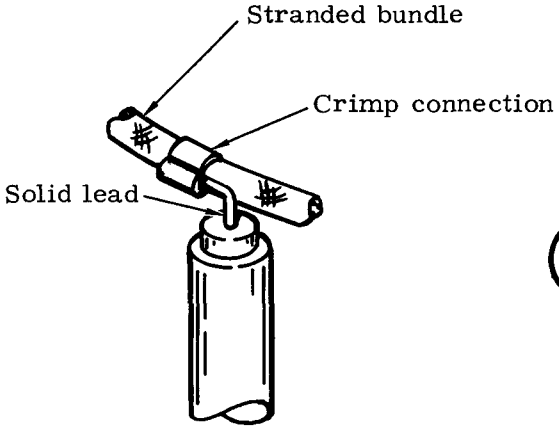

Note:
Ceramic beads (not shown) are installed over the stranded bundle

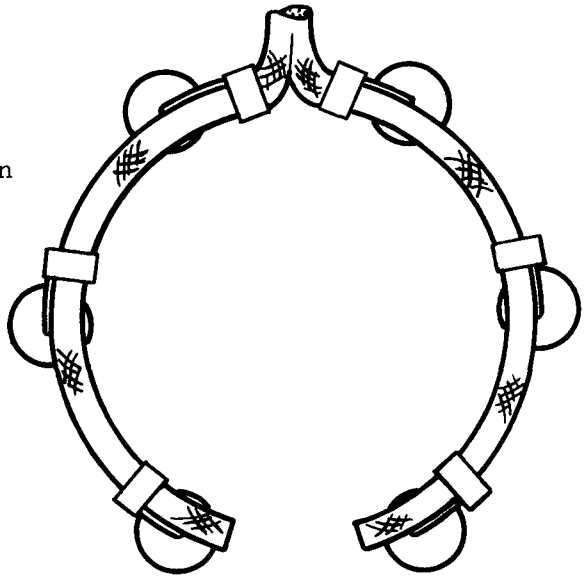

FIG. IV-5. REDESIGNED HEATER ARRAY

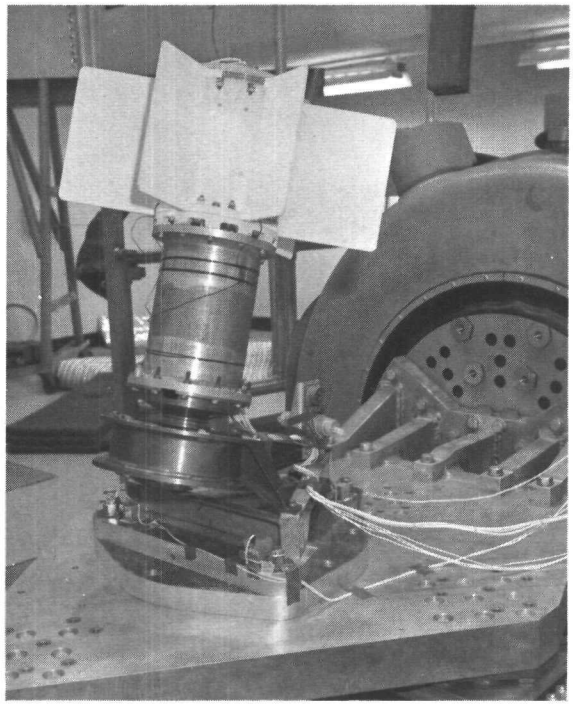

FIG. IV-6. ELECTRICALLY HEATED GENERATOR AND DUMMY UNIT MOUNTED FOR ROLL EXCITATION

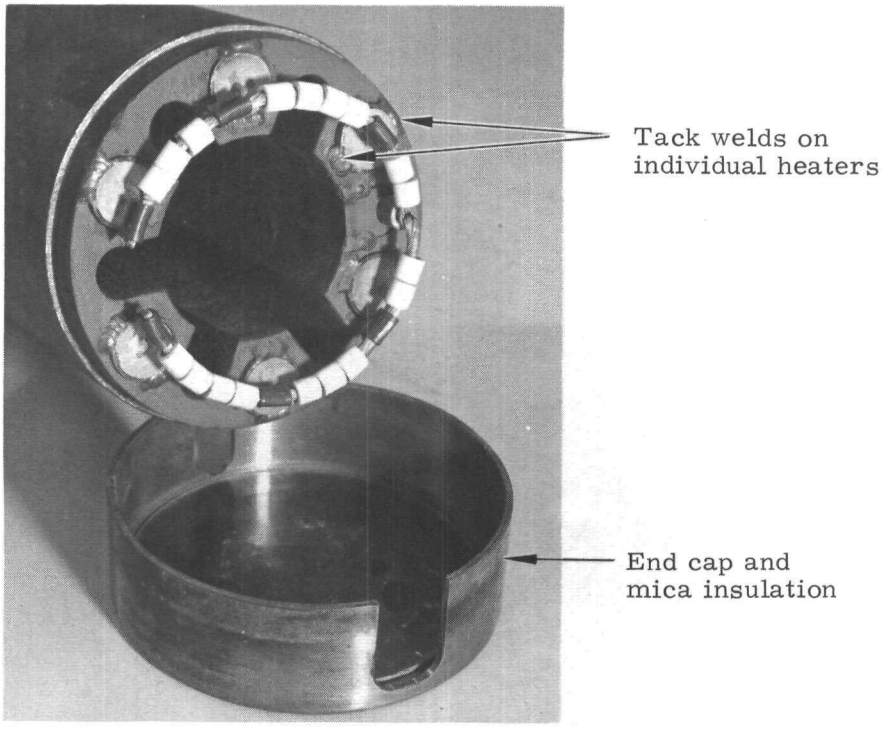

FIG. IV-7. TACK WELDING OF HEATERS TO BLOCK

Development vibration testing was resumed and the design successfully completed the sinusoidal vibration tests. However, during the final two minutes of random vibration failure again occured. The failure was due to fatigue of the unrestrained stranded nickel lead wire routed from the bottom of the heater block up through a hole in the block. This problem was resolved by tack welding a grooved metal bar to the heater block around this lead wire to provide support as shown in Fig. IV-2.

Vibration tests were successfully completed on this final configuration. The unit was disassembled and the internal components visually inspected following the tests. There were no indications to suggest that a change in the original Min-K preload had occurred and the heater block assembly details exhibited no change or damage as a result of the dynamic loading. The final design review concluded that the redesigned heater block provided sufficient restraint to assure proper functioning under the vibration environment.

This design was incorporated into generator subsystem No. 5 and environmental testing was successfully completed.

V. GENERATOR ENDURANCE TESTING

The delivery of flight subsystem No. 8A was preceded by over one year of extensive endurance testing involving eight electrically heated SNAP 19 generators. This activity is summarized here and reported in detail in Ref. V-1. The objectives of Ref. V-1 were to:

(1) Present an orderly display of the endurance test data.

(2) Characterize SNAP 19 2N-2P, 2N-3P and 2N-2P (cupped) generator performance versus time at orbital thermal conditions and provide comprehensive data on parameters such as hot junction temperature variation, open circuit voltage and contact resistivity which aid in RTG design.

(3) Compare 2N-2P, 2N-3P and 2N-2P (cupped) generator performance with regard to RTG design and mission utilization; i.e., efficiency, power stability and power level. All units used for the Nimbus B application contained 2N-2P thermoelectrics.

(4) Provide a demonstrated reliability assessment.

(5) Characterize the performance of the elastomeric seals by comparing the experimental endurance test results with the multigas permeability analysis developed for SNAP 19 generators.

Reference V-1 includes all data on generators S/N 4, 5, 6, 17, 19, 20 and 21 taken at Martin Marietta and all in-air test data on S/N 18 (part at Martin Marietta; part at Naval Ship Research and Development Center). The endurance test program was terminated on November 30, 1967.

A. GENERATOR DESCRIPTION

A complete description of generators (S/N 4, 5, 6, 17, 18 and 19) with 2N-2P thermoelectric couples is provided in Volume I, Section II of this report. The electrical heat source used in all endurance generators is discussed in Volume III, Chapter IV.

The couples used in endurance test generator S/N 20 (Fig. V-1) are identical in configuration to the 2N-2P couples except that the P-type elements used are designated TEGS-3P by the 3M Company and the P bonding materials are different. The 3P material was used in this unit to compare long term power stability and efficiency data with similar data from generators containing 2P material.

The couple configuration used on endurance generator S/N 21 differs from the others in that cups are used at both the hot and cold side of each element as shown at the right of Fig. V-1. No cold shoes are employed. The purpose of the cups is to produce a more stable 2N-2P couple. In addition to greater power stability, the bond joints are stronger.

Developmental activities on all three couple configurations and element and couple specifications are covered in Chapter II of this volume.

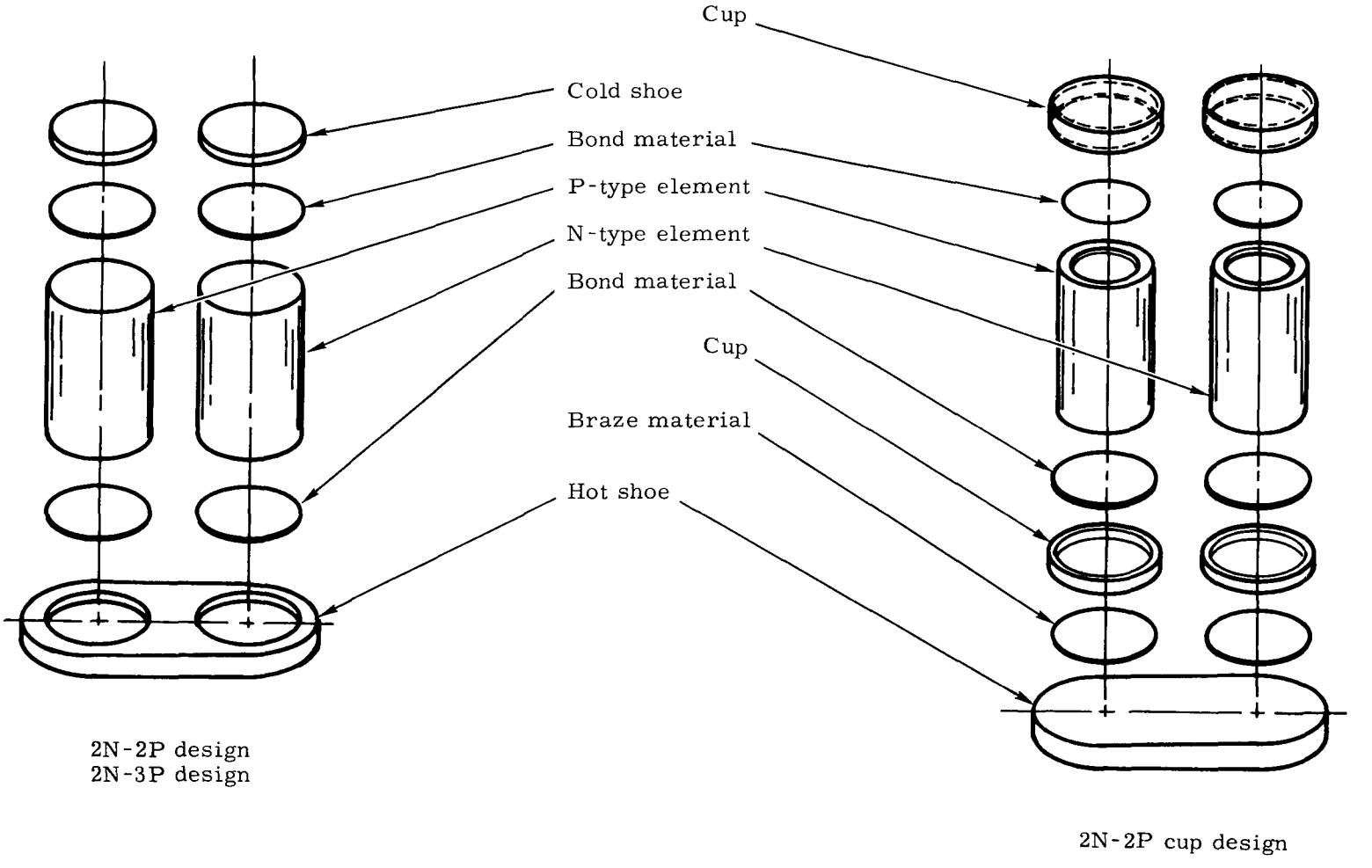

FIG. V-1. THERMOELECTRIC COUPLES--EXPLODED VIEWS

B. TEST DESCRIPTION AND PREPARATION

SNAP 19 generators were subjected to a series of short term tests and preparatory activities prior to endurance testing to assure satisfactory initial performance. These are listed in Table V-1. Further details on these activities are given in Ref. V-1. Outgassing and leak testing are also discussed in Chapter III of this volume.

TABLE V-1

Pre-endurance Tests

Test	Purpose	Comments
Helium cold leak	Verify integrity of generator seals	Performed at room temperature after generator assembly but prior to outgassing
Outgassing	Remove contaminant gases	Series of purging operations at successively higher temperatures
Power check	Determine approximate initial performance	
Argon leak	Determine argon permeation rate through generator seals	Performed in evacuated chamber with residual gas analyzer and calibrated leak. Performed either at room temperature or in the heated condition (~340° F seal temperature, flight condition).
Parametric	Determine BOL performance characteristics as function of load voltage	Used to identify peak power voltage

The generators were endurance tested at operating conditions which approximate those of orbital flight. Accordingly, the input power was specified at 570 watts and the fin root (housing) temperature at 350° F. The 2N-2P generators were tested at a load voltage of 2.6 volts. The developmental units using 2N-3P and 2N-2P (cupped) thermoelectric couples were tested at optimum voltages of 2.3 and 2.4 volts, respectively.

A typical endurance test arrangement for the electrically heated generators is illustrated in Fig. V-2. Power to the heaters was provided by regulated power supplies. Controllers were connected to input power and hot junction temperature indicators which activated alarms at monitoring posts whenever controller set limits were exceeded. Similar control devices monitored fin root temperatures and load voltages in later stages of endurance testing as power and instrumentation consoles were modified to improve generator test control.

At first, complete sets of data were obtained twice weekly, and short sets were taken each working day for test integrity monitoring. In the later stages of the test program, the frequency of data acquisition was reduced to one complete set of data per month, supported by daily short data sets. Logs of accumulated time were maintained for each generator; the results are summarized in Table V-2. The definition of endurance test time is the time accrued while the generator was on load at or near design test conditions, exclusive of parametric time. Parametric

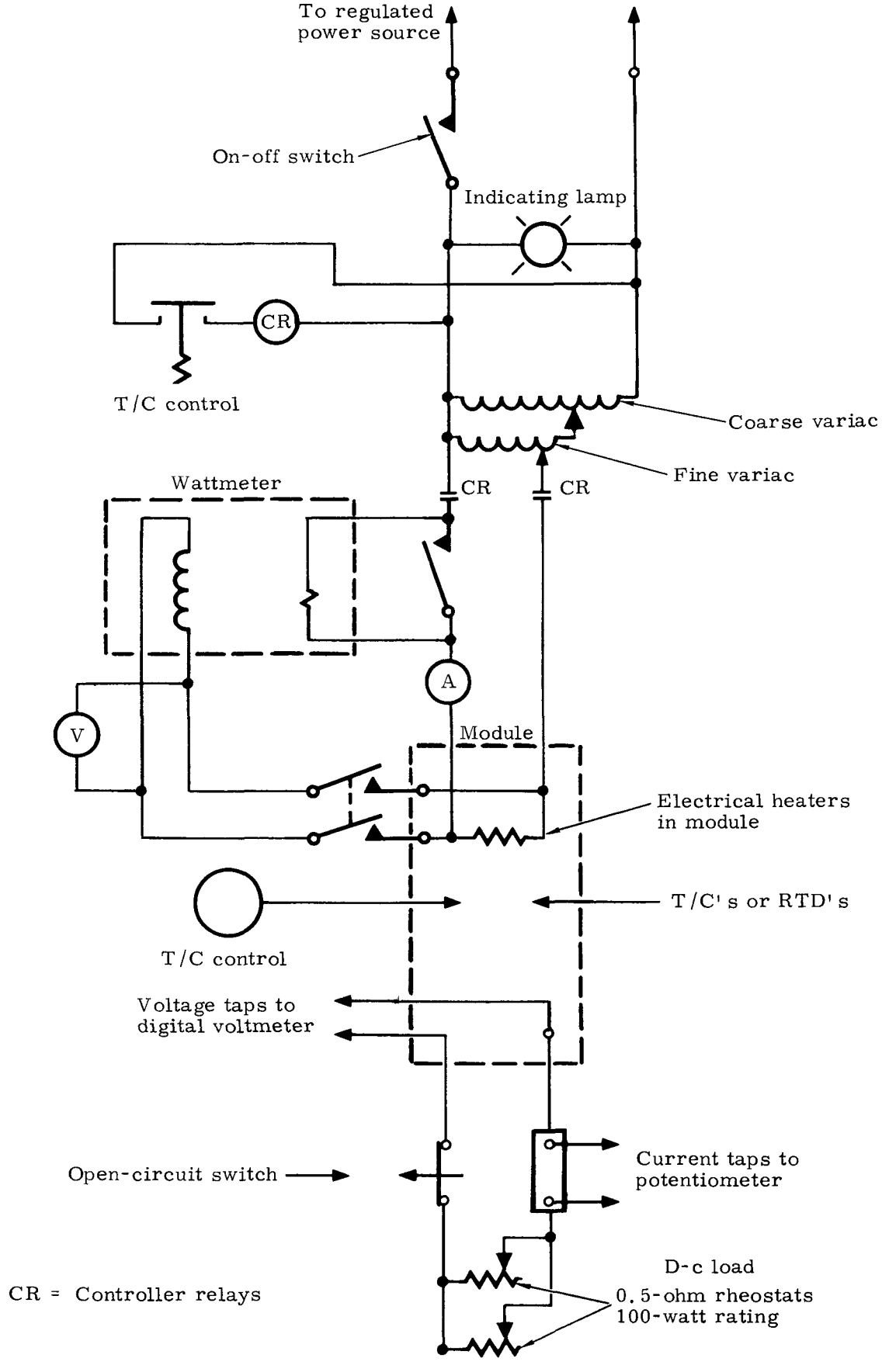

FIG. V-2. ENDURANCE TEST ARRANGEMENT FOR ELECTRICALLY HEATED GENERATOR

time is that spent at load voltages other than the endurance test voltage and transition periods between parametric test points. A few generators were maintained on short circuit and this time was recorded. Partial power operation includes all normal heatup, cooldown, and transient periods incurred due to power outages and equipment failures. Generator downtime applies to periods between start and termination of endurance testing when generators were cold for various reasons. Test chronologies of the endurance generators are presented in Fig. V-3.

TABLE V-2

Endurance Generator Test Times as of 11/30/67

Generator S/N	Endurance Test (hr)	Parametrics (hr)	Short Circuit (hr)	Partial Power (hr)	Down Time (hr)
4	10,270	50	0	160	0
5	9,450	140	1920	530	2240
6	12,170	280	790	500	104
17	5,610	110	0	140	0
18(1)	3,160	110	0	230	0
19(2)	5,460	190	0	230	0
20	5,620	300	0	110	0
21	2,900	180	2	30	0

Notes:

(1) Total test time in air (terminated 5/24/67).

(2) As of 8/14/67, prior to shipment to NASA, Huntsville.

C. PRE-ENDURANCE TEST RESULTS

The results of all leak tests, power checks and parametric load voltage tests are presented in the topical report on the endurance generators (Ref. V-1).

Hot argon leak data showed that the endurance generators had elastomeric seal leak rates of from 2×10^{-5} to 4.4×10^{-5} scc/sec of argon, as normalized to a 337° F seal temperature (nominal flight condition) and 14.7 psia generator pressure. Discussions of generator seal performance and the multigas permeation model developed on the SNAP 19 program are in Section VII of this volume.

The power check data showed that all eight endurance generators were satisfactorily fabricated and assembled. The data also showed that output power is somewhat dependent on fin root temperature and that for meaningful comparisons between generators or of a given generator at different times, data must be correlated at the same fin root temperature.

The parametric load voltage data led to the following conclusions:

(1) A SNAP 19 2N-2P generator with a hot junction temperature of ~900° F initially produces a peak power of ~ 30 watts at about 2.6 volts. After one year, the peak power voltage is about 2.5 volts with a hot junction temperature of ~ 935° F.

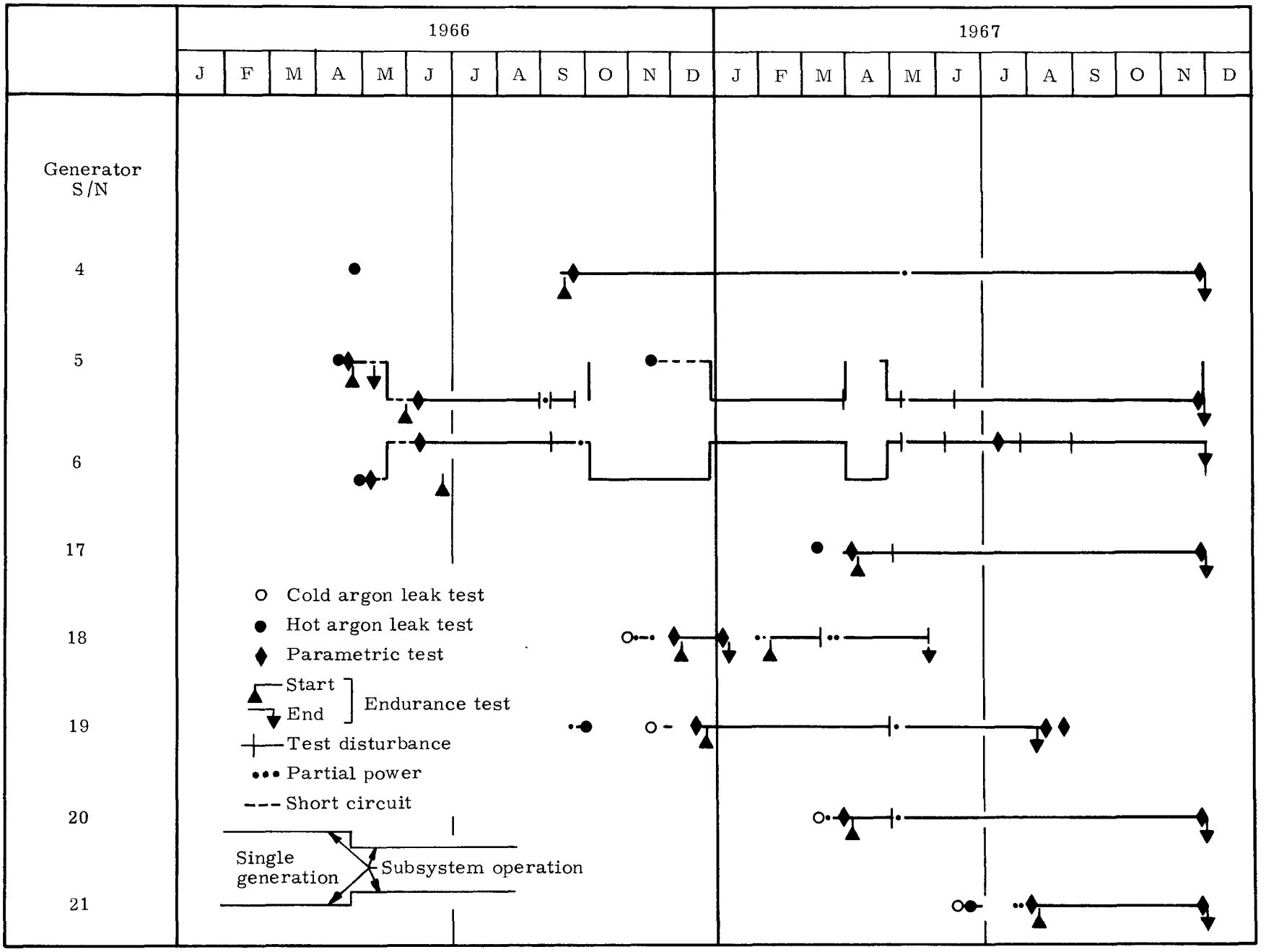

FIG. V-3. ENDURANCE GENERATOR TEST CHRONOLOGIES

(2) A SNAP 19 2N-3P generator (e.g., S/N 20) initially produces ~ 26 watts at ~ 2.3 volts with a 900° F hot junction. After one year, the peak voltage will be ~ 2.2 volts, with the hot junction remaining at 900° F (since 2N-3P degradation at this temperature is small).

(3) A SNAP 19, 2N-2P (cupped) generator (e.g., S/N 21) initially produces ~ 27 watts at ~ 2.4 volts with an 850° F hot junction temperature. Although only 2900 hours had accrued on this unit prior to shutdown, it is apparent that the degradation for the one year has a negligible effect on initial optimum voltage and hot junction temperature.

(4) With 2N-2P, 2N-3P, or 2N-2P (cupped) thermoelectric elements, the penalty for failure to operate exactly at optimum voltage is small. For example, a voltage shift of 0.3 volt from optimum creates only a 0.5-watt loss.

D. ENDURANCE TEST RESULTS

1. Data

Significant data accumulated during generator endurance testing was documented on IBM punched cards. A computer program was written to effect display of these data, reduce the data and list the converted data. All raw and converted data and the computer program used are presented in Ref. V-1.

Data presented in Ref. V-1 are:

(1) Time on test

(2) Average fin root temperature

(3) Average hot junction temperature

(4) Load voltage

(5) Load current

(6) Open circuit voltage

(7) Pressure transducer resistances

(8) Date

(9) Adjusted hot junction temperature

(10) Hot-to-cold junction delta temperature

(11) Output power

(12) Ratio of output power to initial output power

(13) Output power as determined by least squares fit

(14) Generator internal pressure

(15) Internal electrical resistance

(16) Load resistance

(17) Thermoelectric contact resistivity per couple

(18) Seebeck coefficient.

These data are presented in tables for each endurance test generator as a function of time. Selected data such as generator power, pressure, temperatures, voltage and contact resistivity were plotted versus time.

2. Power

Comparisons of endurance test generator power histories are presented in Figs. V-4 and V-5. Figure V-4 presents absolute power and Fig. V-5 presents power normalized to the beginning of the test.

The power output of generator S/N 6 can be well represented by the equation,

$$P = P_o \exp(-\gamma t)$$

where the power degradation coefficient, γ, is a constant with a value of 4.9×10^{-5} throughout the 12,200-hour test period. The remaining 2N-2P generators (exclusive of S/N 21) exhibited a period of burn-in, characterized by coefficients near 4×10^{-5}/hr during the initial 3000 hours on load, followed by periods of essentially constant γ below 3×10^{-5} hour^{-1} until test termination. The analytic fit of a single γ value to test data by the method of least squares provides comparative constants for power stability, but it tends to penalize the short-time test generators in which the burn-in period is a significant portion of total test time. The curves in Figs. V-4 and V-5 were constructed using single-valued γ. The power degradation coefficients are tabulated in Table V-3. Figure V-6 presents conversion factors relating the power degradation coefficient, γ, to the power degradation in watts/1000 hr.

TABLE V-3

Power Degradation Coefficients for Endurance Test Generators

Generator S/N	4	5	6	17	18	19	20	21
Endurance test time (hr)	10,270	9450	12,170	5610	3160	5460	5620	2900
Average hot junction temperature (°F)	910	930	930	915	890	900	905	855
Burn in γ, 0 to 3000 hours (hour^{-1} x 10^5)	4.5	7.7(1)	4.9	3.9	4.1	3.5	1.2	1.0
Steady state γ, 3000 hours to end of test (hour^{-1} x 10^5)	2.6	2.3(1)	4.9	2.6	--	3.0	1.2	--
Overall γ, 0 to end of test (hour^{-1} x 10^5)	3.0	3.5	4.9	3.1	4.1	3.0	0.9	1.0

Notes:

(1) Includes effect of thermal cycling and/or rework following heater failure.

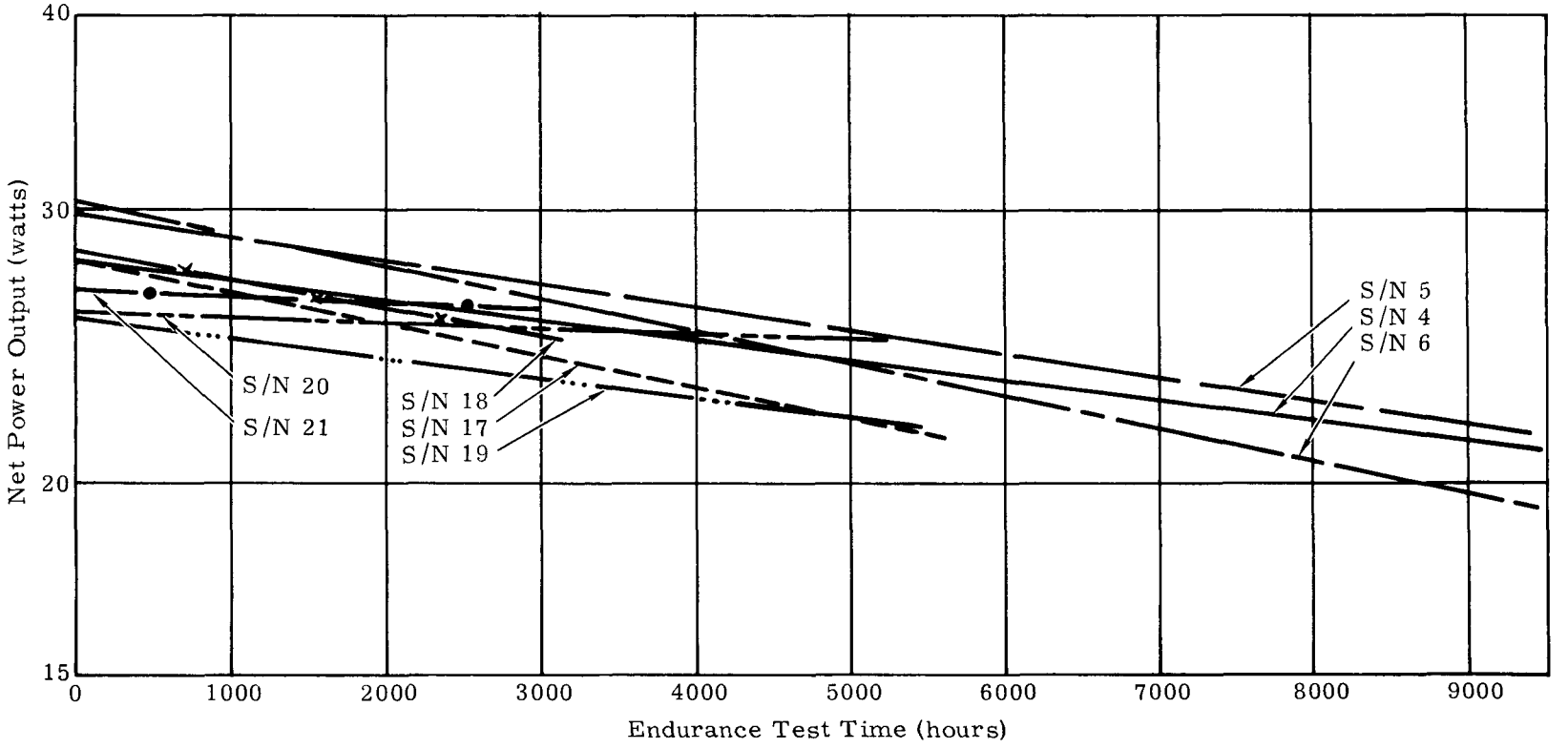

FIG. V-4. ENDURANCE TEST GENERATOR POWER HISTORIES COMPARISON OF LEAST SQUARE FIT CURVES

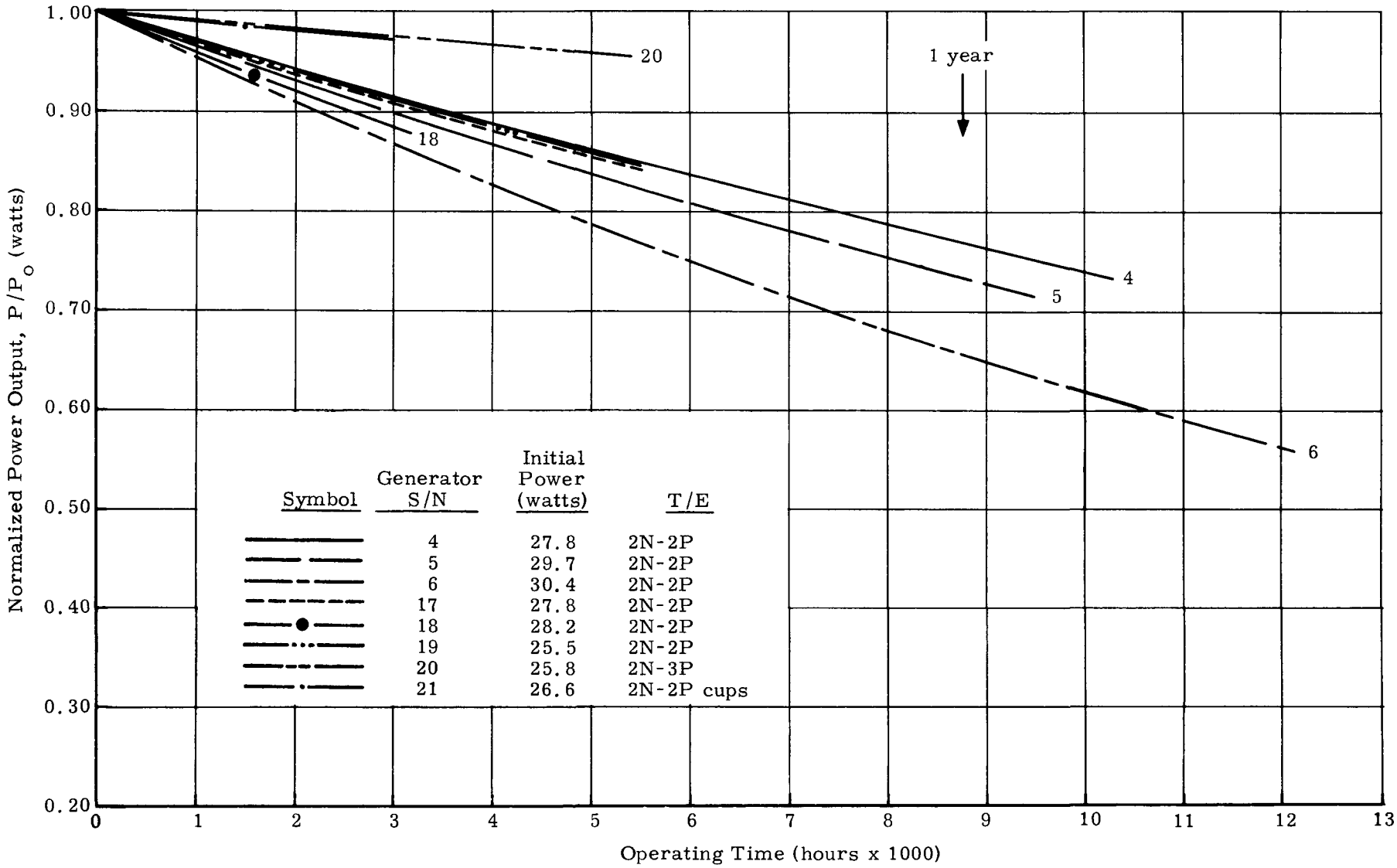

FIG. V-5. SNAP 19 ENDURANCE TEST GENERATOR POWER HISTORIES

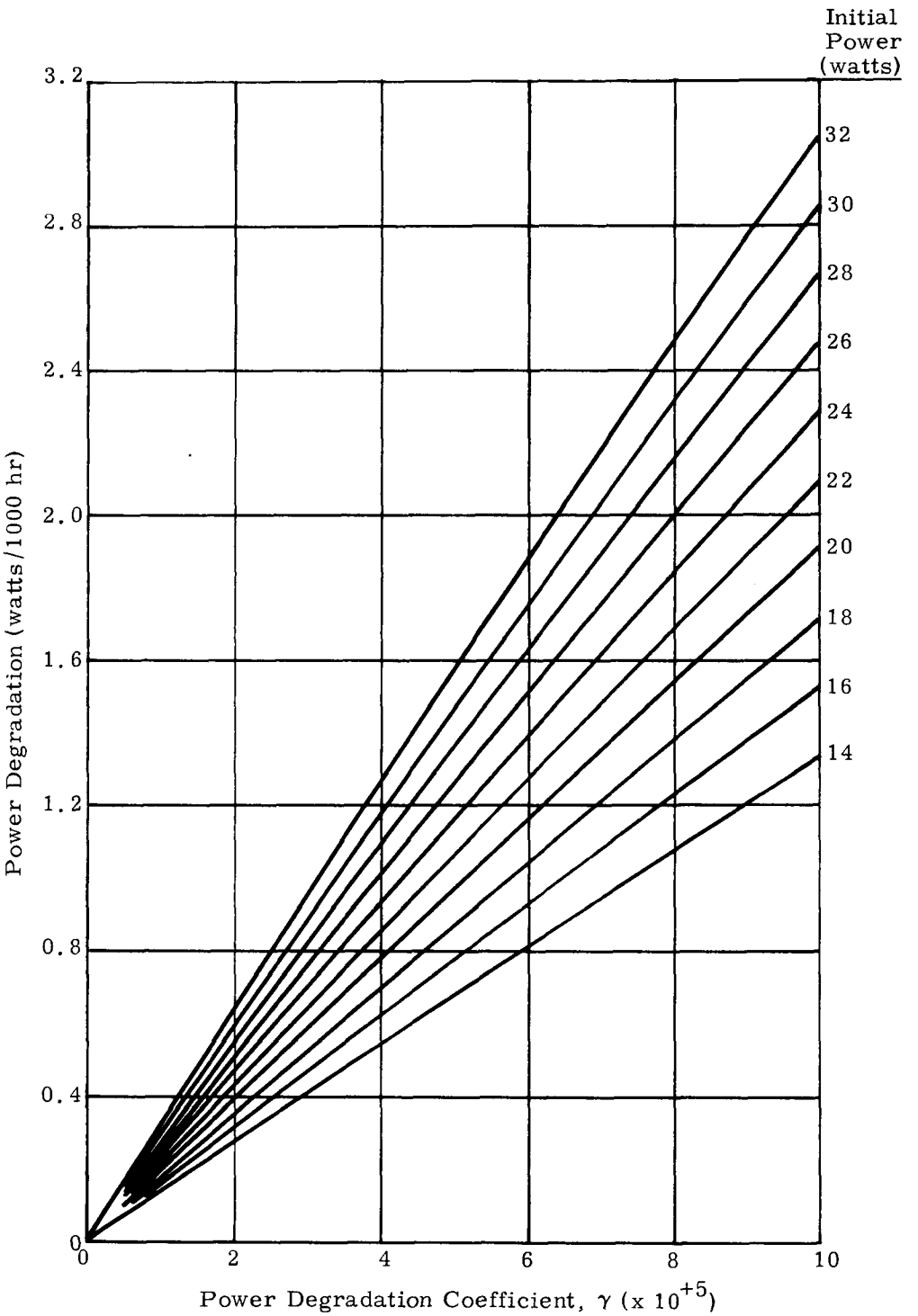

FIG. V-6. POWER DEGRADATION PARAMETER CONVERSION CHART (WATTS/1000 HR VERSUS γ)

Power produced by generators S/N 20 and S/N 21 was more stable than the power output of the standard 2N-2P generators. Least-square lines to these data have coefficients of about 1×10^{-5}/hr as illustrated in Figs. V-4 and V-5 and Table V-3. No burn-in periods were evident for either the 2N-3P or 2N-2P cupped thermoelectric element configuration.

E. EVALUATION OF T/E PERFORMANCE

Two criteria, efficiency and power stability, can be used to evaluate the three types of couples tested. Typical efficiency results are presented in Table V-4; power-time coefficients are given in Table V-3.

TABLE V-4

Typical Efficiency Data

Generator	Time (hr)	T/E Material	Contact Resistivity (μ -cm^2)	Junction Temperature (°F) Hot	Junction Temperature (°F) Cold	Efficiencies (%) Overall	Efficiencies (%) T/E	Efficiencies (%) Joule
4	710	2N-2P	2350	897	404	4.9	5.9	97
	8770		7250	925	409	3.9	4.6	98
5	800		2400	931	410	5.3	6.1	97
	8737		7300	946	408	4.0	4.7	98
6	672		2400	914	406	5.1	6.0	97
	8638		9000	935	408	3.5	4.3	98
17	480		2600	915	417	4.8	5.9	97
	5610		6000	930	401	4.1	5.0	98
18	545		2900	915	401	5.0	5.9	97
	3119		5200	938	410	4.4	5.2	98
19	227		3000	891	401	4.5	5.7	97
	5377	2N-2P	6100	916	408	3.9	4.9	97
20	336	2N-3P	600	910	402	4.5	5.2	96
	5139	2N-3P	600	893	397	4.3	5.1	96
21	115	2N-2P, cups	1300	854	398	4.7	5.9	96
	2900	2N-2P, cups	1500	849	398	4.5	5.9	97

Thermoelectric efficiencies defined as output power divided by heat to the elements were obtained from the data in Figs. V-7 and V-8 after determining the appropriate contact resistivities from Figs. V-9 and V-10. Figures V-7 and V-8 were constructed using the techniques described in Ref. V-1. Gross output power in Figs. V-9 and V-10 was calculated from measured net power output by adding the Joule (I^2R) loss using the SNAP 19 internal module resistance (hot and cold shoes, module wiring) of eight milliohms. The overall efficiency, based on a net power at the module taps and 570 watts input, was computed from measured powers.

Figures V-7 and V-8 are based on Seebeck coefficient, electrical resistivity and thermal conductivity property data. The initial temperature data on 2N-2P generators S/N 4, 5, 6, 17, 18 and 19, however, clearly show that Phase III thermoelectric

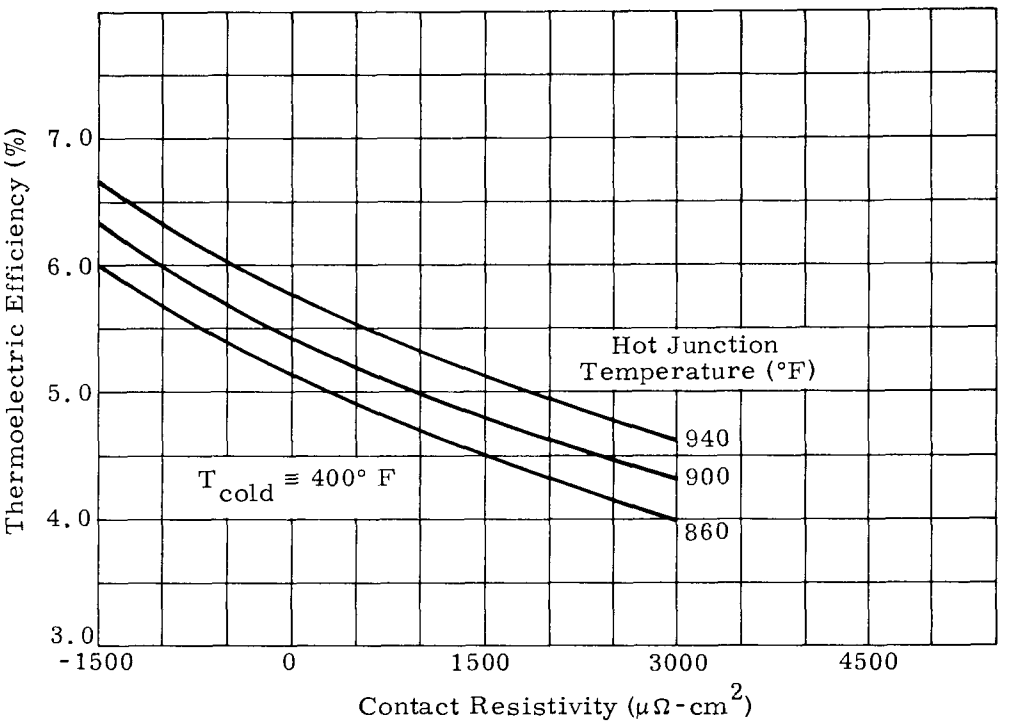

FIG. V-7. T/E EFFICIENCY OF 2N-3P

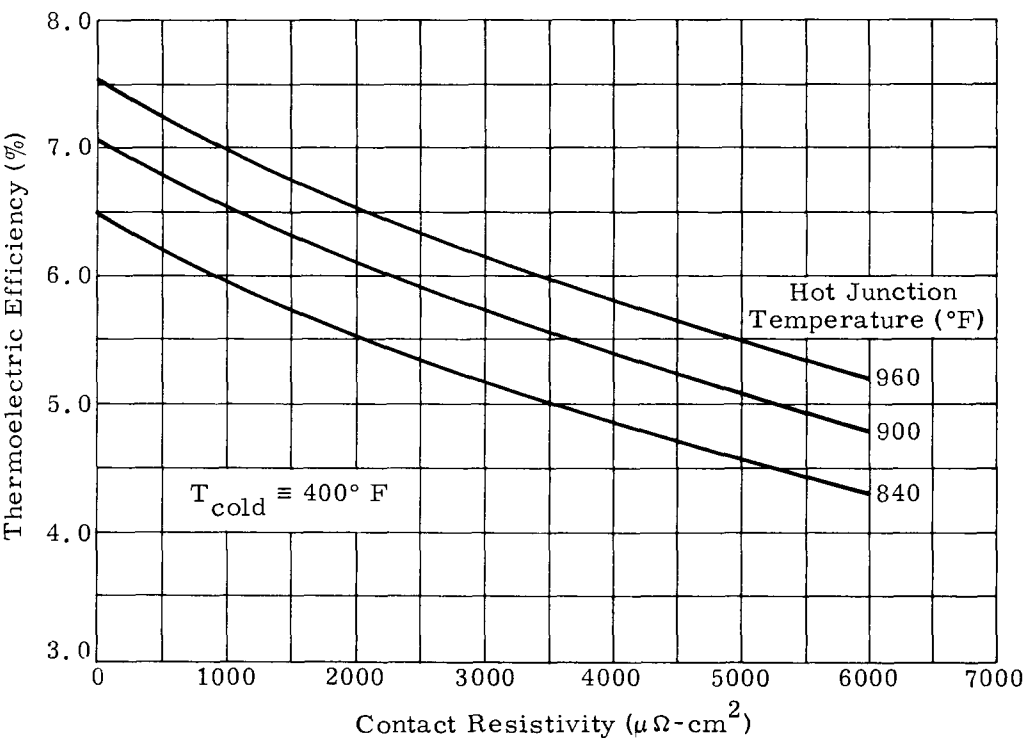

FIG. V-8. T/E EFFICIENCY OF 2N-2P

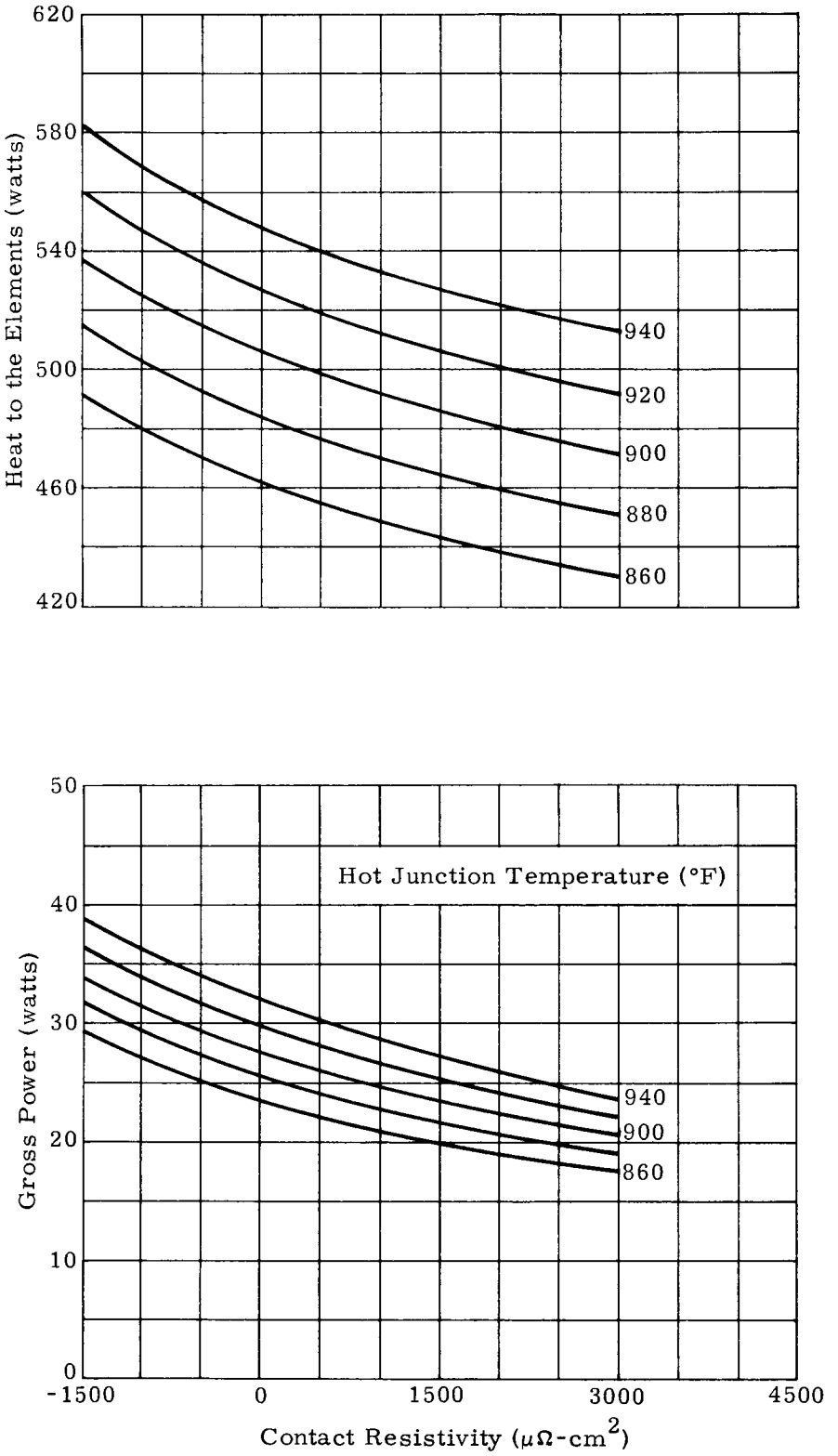

FIG. V-9. SNAP 19B GROSS OUTPUT POWER AND HEAT TO ELEMENTS--2N-3P

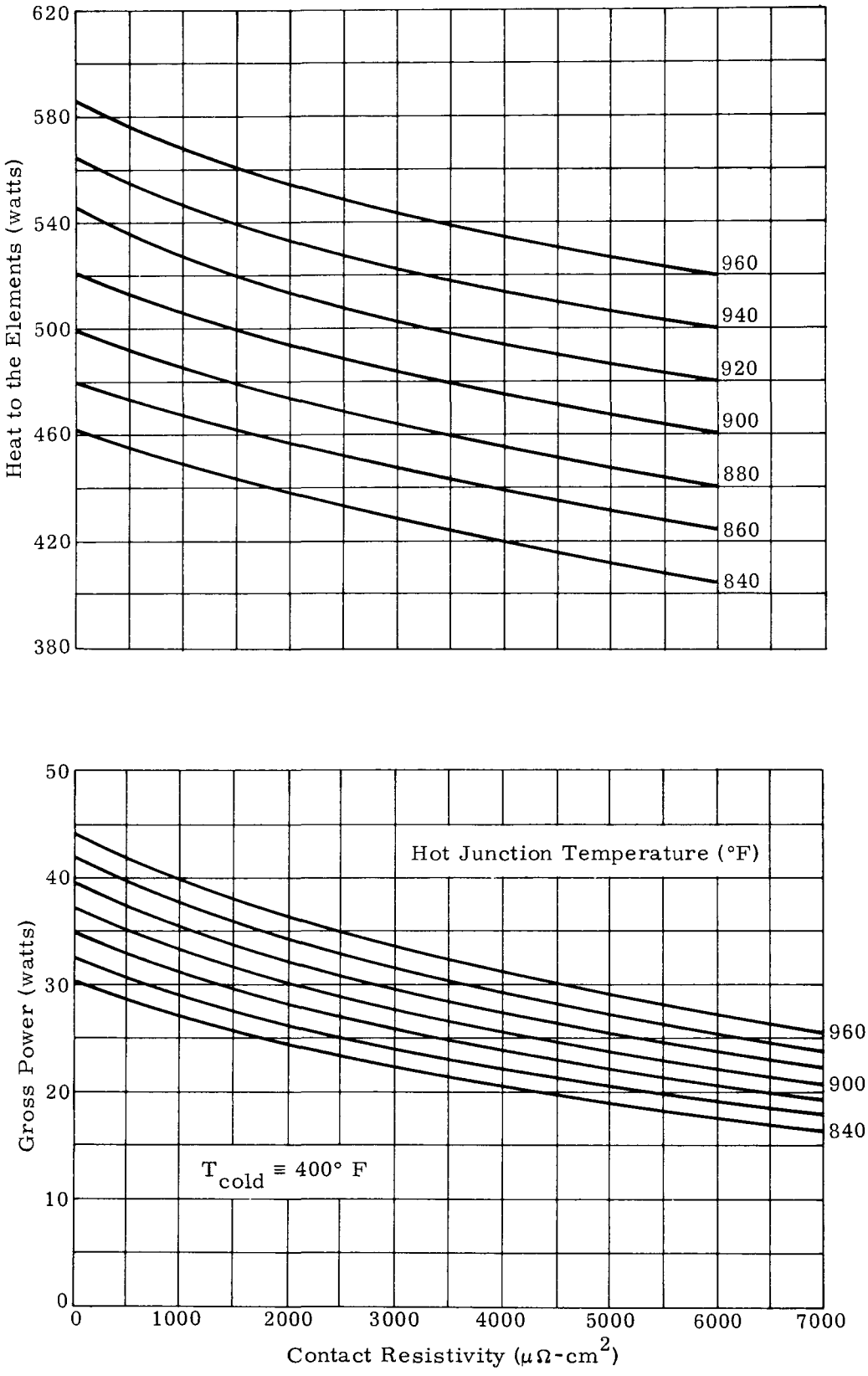

FIG. V-10. SNAP 19B GROSS OUTPUT POWER AND HEAT TO ELEMENTS--2N-2P

material has a higher thermal conductivity than Phase II material (about 10% on the couple although not necessarily equally divided between the N and P elements). This material property difference may account for differences of as high as 8% in the thermoelectric efficiency and heat to the elements as determined from Figs. V-7 through V-10. The gross output correlations on Figs. V-9 and V-10 are independent of thermal conductivity. Differences in initial Seebeck coefficient between generators, as evaluated by the hot junction temperature comparisons between instrumentation reading and open circuit voltage determination, are small.

A comparison of Tables V-3 and V-4 reveals that the efficiency and stability of 2N-2P material at hot junction temperatures around 900° F are lower than those of 2N-3P at 900° F or 2N-2P with cups at 850° F. The better of the latter two configurations is not obvious. The degradation coefficient on the 3P material has always been slightly lower but so have thermoelectric efficiencies. Further testing of generators S/N 20 and S/N 21 can resolve which couple configuration is superior.

Generator S/N 19 is of particular interest in that this unit's thermoelectric couples did not meet visual standards (see Chapter II). A review of S/N 19 data shows that the initial power was one to two watts lower than other Phase III 2N-2P generators (i.e., S/N 4, 17 and 18). This is a 3 to 6% loss in initial power that could correspond to a 3 to 6% loss in cross sectional thermoelectric area because of the couple defects (i.e., pits, chips, grooves, etc.) that were not screened by the visual criteria. The power stability on S/N 19 is as expected and closely duplicates the stability observed on S/N 4.

F. CONCLUSIONS

The following conclusions were drawn from the SNAP 19 endurance generator test program:

(1) Thermoelectric material 2N-3P at 900° F hot junction and 2N-2P with cups at 850° F are both superior to 2N-2P at 900° to 950° F on the basis of efficiency and power stability except that in the first 2000 hours (approximately), there is a slight efficiency advantage to 2N-2P. A comparison is given in Table V-5. The long term (over one year) relative merits of 2N-2P with cups are not yet clear due to a lack of sufficient endurance test data. The stability of 2N-3P is slightly greater but the efficiency and output power are slightly less. Additional data should resolve which couple is superior.

TABLE V-5

Comparison of T/E Efficiency and Stability Data

T/E	Generator S/N	Test Hours	Generator Power Loss (%)	Efficiency at End of Test Period (%)
2N-2P	4, 5, 6	8760	23 to 35	3.5 to 3.8
2N-2P	4, 5, 6, 17, 19	5500	15 to 23	3.8 to 4.3
2N-2P	4, 5, 6, 17, 18, 19	2900	8 to 13	4.1 to 4.7
2N-3P	20	5500	5	4.3
2N-2P	21	2900	3	4.5

(2) The data from generator S/N 19 indicate a need for retaining couple visual criteria.

(3) The optimum load voltage did not shift strongly with time, even with 2N-2P material, as evidenced by initial and final current-voltage parametric test results. Furthermore, the power penalty for failure to operate exactly at optimum voltage is small. The flatness of the power curve, as a function of voltage, near the optimum value is a characteristic of PbTe material.

(4) Seebeck coefficient of 2N-2P materials at 900° to 950° F decreased sharply during the first year (typically 7%). This change prevents the use of beginning-of-life Seebeck data at later times in life for evaluation of hot junction temperatures in conjunction with measured open circuit voltage data.

(5) Phase III 2N-2P generators (i.e., S/N 4, 17, 18 and 19) were fabricated with thermoelectric materials of slightly different physical properties than Phase II generators (i.e., S/N 5 and 6) as evidenced by the lower thermal conductivity and, hence, higher operating temperatures of the Phase II units. The result was that Phase II generators had higher initial power (1 to 2 watts) but lower stability.

(6) Output power for 2N-2P generators is a function of fin root temperature. This behavior has also been observed on SNAP 19 prototype and flight generators and is due to the temperature-dependent thermoelectric properties (Seebeck coefficient, electrical resistivity and thermal conductivity).

(7) Demonstrated generator reliability at 50% confidence is 0.95 for a one-year mission and 0.90 for a two-year mission based on accumulated hours as of 1/1/68. Predicted reliability of a generator to experience no catastrophic failures is 0.9961 for one year and 0.9922 for two years.

(8) Generators operated in an air environment will admit both oxygen and nitrogen gases by permeation through elastomeric seals. The in-leaking oxygen reacts with the zirconium getter. The introgen is not reacted and contributes to the measured total internal pressure. Leakage on the endurance generators varied from 2×10^{-5} to 4.4×10^{-5} scc/sec of argon, as normalized to a 337° F seal temperature and 14.7 psia internal pressure.

(9) The multigas permeability model presented in Chapter VII adequately describes the behavior of generator pressure as a function of time in both air and vacuum environments.

VI. GENERATOR RELIABILITY DEMONSTRATION

High reliability is inherent in radioisotope-fueled thermoelectric generators such as SNAP 19. The unit is a static device and therefore not subject to mechanical wear-type failures. Redundancy has been designed into the generator to minimize sensitivity to critical part failure. The thermoelectric circuit, for example, is series-parallel; therefore, the generator can withstand open-circuit thermoelectric couple failure except with three couples in a single parallel array--an extremely low-probability event. In addition, the couples are under mechanical load, which will assure continuity.

The SNAP 19 generator endurance test program afforded an excellent opportunity to accumulate operating time on many generators (see Chapter V and Ref. VI-1). A number of units were bench tested (Chapter V) at the SNAP 19/Nimbus operating conditions of thermal input, load voltage and housing temperature. Further, additional operating hours were realized during environmental and performance testing of prototype, flight and electrically heated generator subsystems. This included vacuum chamber testing (ranging from two weeks to one month) of some of the generator subsystems. Fueled units were, of course, in operation from time of fueling.

Operational time of 24 generators was considered in the evaluation of demonstrated reliability. Nearly all of the time was obtained during Phase III. A relatively small amount, less than 10% of the total, was accumulated during the Phase II Program. An operating time summary is given in Table VI-1. Time applicable to reliability assessment is 113,000 hours. Of this, 69,100 hours were gained in endurance testing and 43,900 hours in test operations on generator subsystems and storage of fueled units.

TABLE VI-1

Generator Operating Time Summary

Generator Usage	Serial Number	Operating time as of January 1, 1968 (hr)
Endurance testing	1	4,000
	2	4,000
	4	10,400
	5	11,900
	6	13,400
	17	5,800
	18	5,100
	19	5,800
		Subtotal 60,400
Endurance and thermoelectric development	20	5,600
	21	8,700
		Subtotal 8,700

TABLE VI-1 (continued)

Generator Usage	Serial Number	Operating time as of January 1, 1968 (hr)
Prototype, flight and electrically heated systems test units	3	3,800
	4	3,800
	7	4,300
	8	4,400
	9	800
	10	800
	11, 11A	5,700
	12, 12A	5,700
	13	4,600
	14	4,600
	15	1,500
	16	1,500
	22, 22A	1,200
	23, 23A	1,200
	Subtotal	43,900
	Total	113,000

Generators S/N 20 and S/N 21 contained developmental couples, that is, relative to the SNAP 19. Time data for these units are included since the assessment is based on catastrophic failure and, in this regard, the couple detail differences are not significant.

The cutoff time for the present assessment is January 1, 1968. Some of the units provide operational data beyond that date. The flight subsystem (generators S/N 22A and S/N 23A) accrues 1440 generator-hours per month. Generator S/N 18 is currently under test at the Naval Ship Research and Development Center, S/N 19 is being tested at Marshall Space Flight Center and S/N 20 and 21 will be tested further at Jet Propulsion Laboratory.

As of January 1, 1968, there have been no catastrophic failures. At 50% confidence, the demonstrated reliability is 0.95 for a one-year mission. A plot of reliability versus mission time on this basis is given in Fig. VI-1.

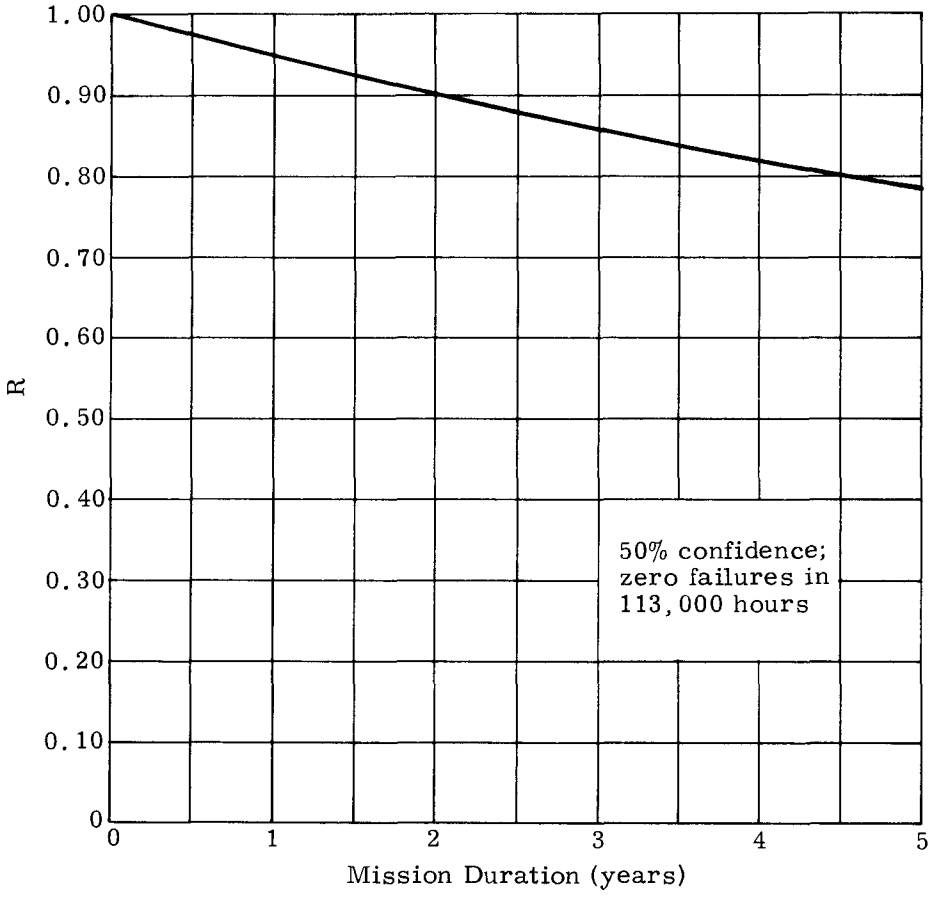

FIG. VI-1. DEMONSTRATED RELIABILITY AS A FUNCTION OF MISSION DURATION

VII. GENERATOR SEAL PERFORMANCE

The permeation of gases through the seals of SNAP 19 thermoelectric generators is of interest for two reasons:

(1) Loss of conductive gases from a generator will result in increased hot junction temperatures and excessive thermoelectric material sublimation rates. Both of these adverse changes will result in a deterioration of electrical performance.

(2) Influx of free oxygen from the atmosphere, unless completely reacted, will reduce couple and bond life and result in accelerated power degradation.

Because of its compliance and temperature compatibility, an elastomer, Viton A, was selected to seal the generator cover plates and instrumentation penetrations. A compliant seal was necessary due to the numerous thermal cycles which the generator would experience during its operational lifetime. To reduce the possibility of oxidation from in-leakage of air, an oxygen getter was provided within the generator housing. After an accumulated total of more than 60,000 hours under heat, SNAP 19 generators give no indication of seal deterioration nor couple degradation due to oxidation.

During the latter portion of the SNAP 19 program, a comprehensive permeation model was developed that accurately predicts generator pressure history during storage, test and flight. Prior development of a complete permeation model was not possible because of the lack of research data on variations of permeation rates through Viton A for the various gases of interest. Even today, there is no known source of data for the permeation of argon through the Viton compound. This lack of data has been compensated for by analysis of SNAP 19 endurance generator test data. Development of this permeation model and its subsequent use has substantiated the existing seal leakage acceptance criterion, i.e., that the argon leak rate, referenced to 337° F seal temperature and 14.7 psia argon pressure, be no greater than 1.0×10^{-4} scc/sec for each RTG.

A. MULTIGAS PERMEATION MODEL

The multigas permeation model treats the permeation of oxygen, nitrogen, helium and argon through the SNAP 19 Viton seals. In-leakage of air is treated as permeation of the two primary constituent gases, nitrogen and oxygen. While the nitrogen contributes to increased pressures within the generator void volume, the oxygen diffusing into the generator can be reacted to form zirconium oxide by an oxygen getter. The chemical process

$$O_2 + Ar \Rightarrow Zr\,O_2$$

requires ~ 0.1 pound (48 grams) of oxygen to entirely oxidize the 0.3 pound (136 grams) of zirconium chips which constitute the getter. The maximum quantity of oxygen permeated under the temperatures and leakage rates considered is less than 1 gm/yr. At approximately 900° F getter temperature, the rate of reaction is assumed to prevent any significant partial pressure buildup of oxygen within the generators.

The multigas permeation model, schematically illustrated in Fig. VII-1, is based on the SNAP 19 generator drawing 452B1000000. Leakage through the elastomeric seals (Ref. VII-1) depends on the seal installation geometry, the difference of partial pressures across the seal, and the permeability of the seal at a given seal temperature, expressed as

$$Q = \frac{A}{d}\,\Delta p\,P \qquad \text{(VII-1)}$$

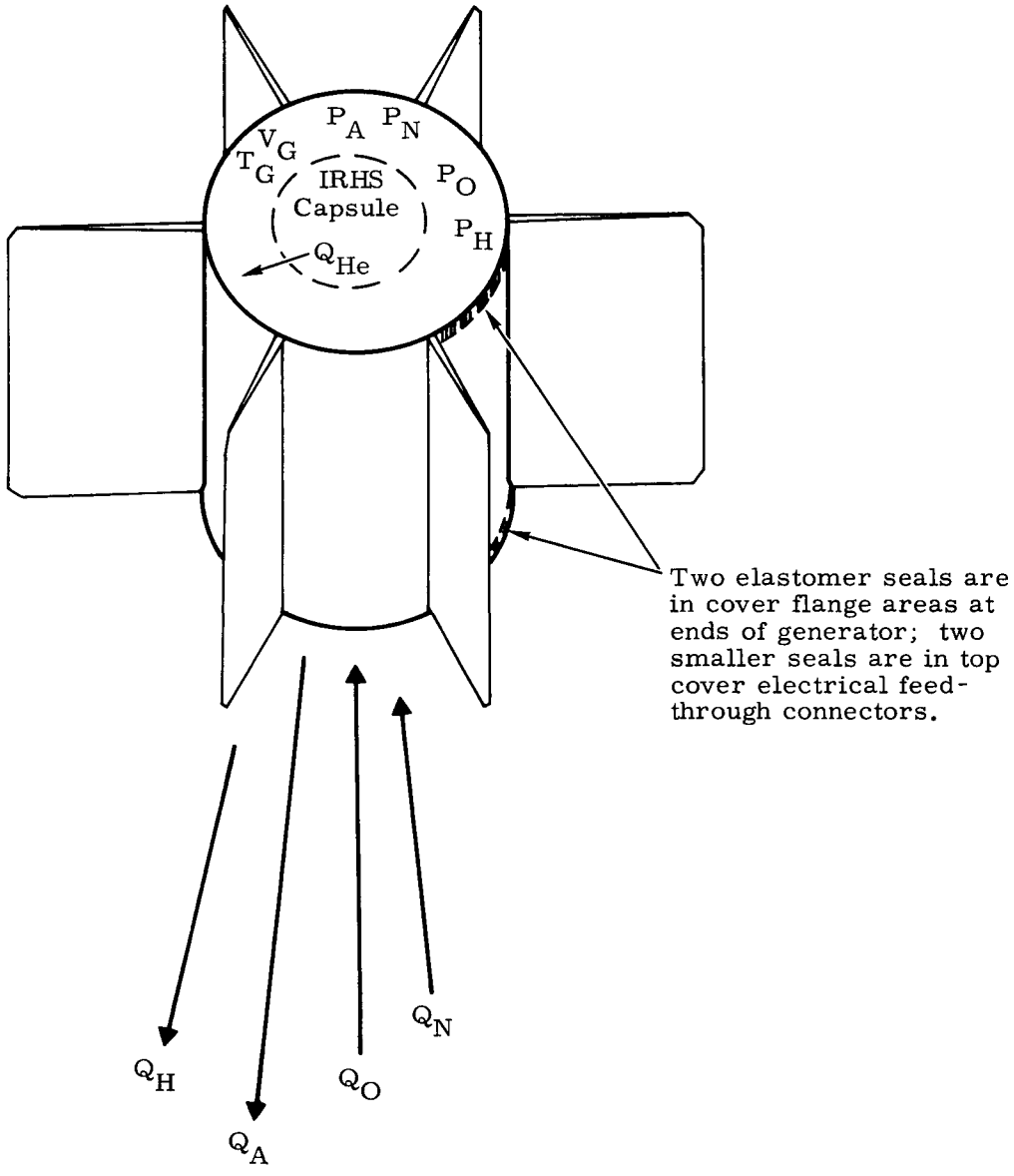

FIG. VII-1. MULTIGAS PERMEATION MODEL

where

Q = volumetric flow (leakage rate)

A = seal area normal to permeation flow

d = width of seal

Δp = partial pressure difference between generator and environment

P = permeability constant

1. Seal Installation Geometry

The observed leakage rate difference between generators under similar test conditions is attributed to variations in seal installation geometry, such as seal compression. Reference VII-2 states that the geometry term A/d is approximately proportional to the square of seal compression in percent of the original seal diameter. Test data indicate an A/d variation from approximately 6 centimeters for a very tight SNAP 19 seal to 30 centimeters for a seal with maximum acceptable leakage rates.

2. Partial Pressures

Generator net leakage rates are the sums of individual permeation rates of the gases involved. The generator in an air environment loses argon and helium at rates essentially proportional to their absolute internal partial pressures while gaining nitrogen at a rate proportional to the difference between the partial pressure of nitrogen in air (approximately 11.2 psi) and the absolute nitrogen partial pressure within the generator.

Similarly, oxygen penetrates the seal at a rate proportional to the difference between its partial pressure in air (approximately 3.5 psi) and the absolute oxygen partial pressure in the generator. The elemental zirconium getter is capable of reacting oxygen at rates considerably greater than may enter through an acceptable seal. Partial pressures of oxygen within the generator therefore remain essentially zero. The combined gas permeation rate of a generator in vacuum is the sum of individual gas rates out of the unit at existing internal partial pressures.

3. Seal Permeability

The permeability of elastomers increases greatly with a temperature increase and is significantly affected by elastomer compounding and curing methods. The permeability constants compiled in Table VII-1 are based on data published in Refs. VII-3, VII-4 and VII-5, and on analyses of pertinent in-house test data.

The variation of permeability with seal temperature is illustrated in Fig. VII-2. A semilog scale was used to obtain permeability-temperature curves which are approximately exponential within the 200° to 350° F temperature range. Hot argon leakage tests and generator storage and flight operation fall within this temperature range. The SNAP 19 seal temperature is approximately equal to fin root temperature.

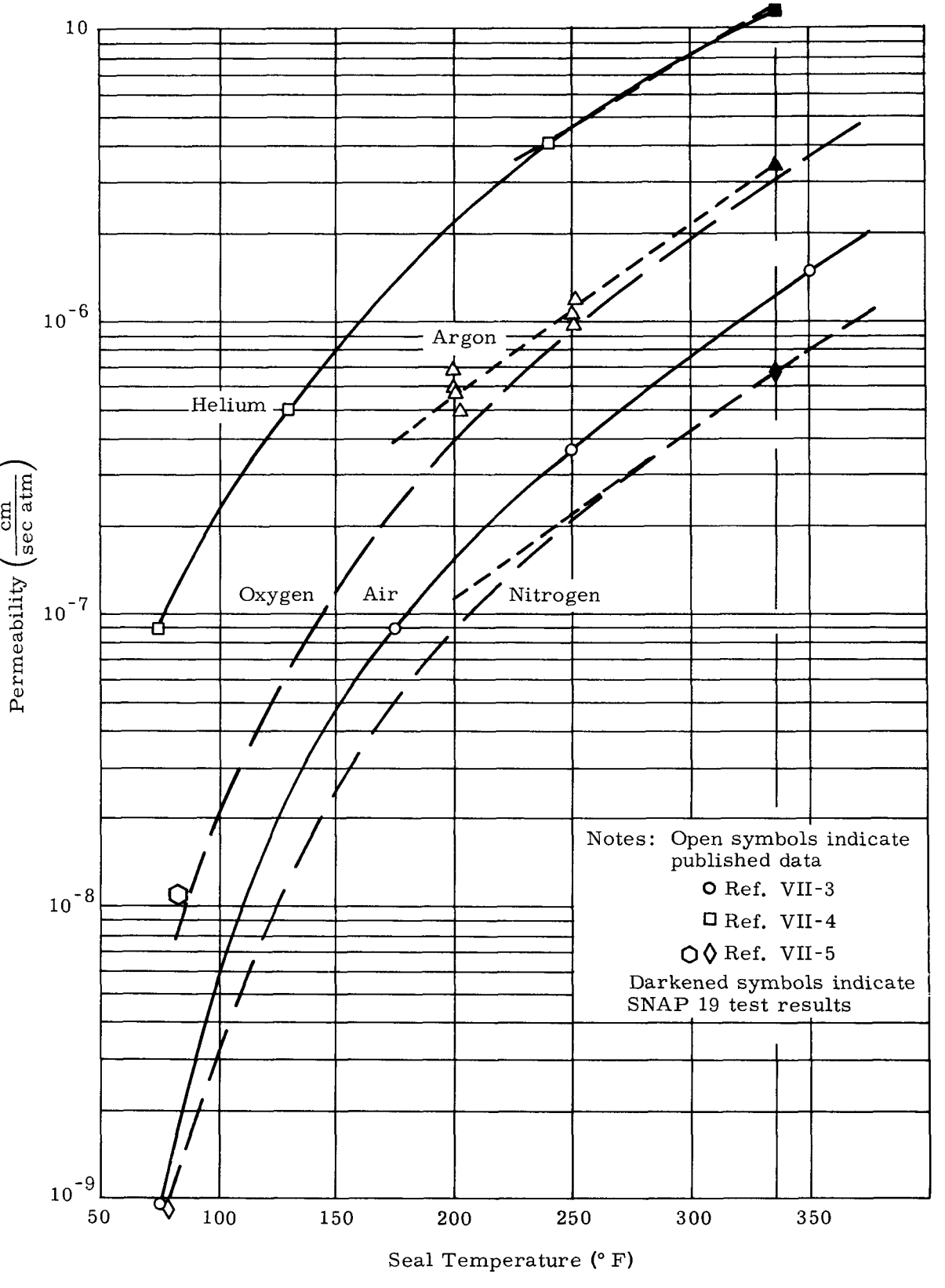

FIG. VII-2. PERMEABILITY VERSUS TEMPERATURE FOR VITON A

TABLE VII-1

Gas Permeability Constants for Viton A

Seal Temperature (° F)	Air $\frac{cm^2}{sec\text{-}atm}$	N_2 $\frac{cm^2}{sec\text{-}atm}$	O_2 $\frac{cm^2}{sec\text{-}atm}$	A $\frac{cm^2}{sec\text{-}atm}$	He $\frac{cm^2}{sec\text{-}atm}$
75	9.9×10^{-10}	5.4×10^{-10}	4.0×19^{-9}	6.0×10^{-8}	1.0×10^{-7}
220	2.2×10^{-7}	1.3×10^{-7}	5.5×10^{-7}	7.2×10^{-7}	3.0×10^{-6}
260	4.2×10^{-7}	2.4×10^{-7}	1.1×10^{-6}	1.2×10^{-6}	5.2×10^{-6}
300	7.5×10^{-7}	4.2×10^{-7}	1.9×10^{-6}	2.1×10^{-6}	7.9×10^{-6}
337	1.2×10^{-6}	6.6×10^{-7}	3.0×10^{-6}	3.3×10^{-6}	1.1×10^{-5}

4. Analytical Model

Based on the permeability equation, (Eq. VII-1), and the ideal gas law, the equations in Appendix A were developed to describe the pressure profiles of the various SNAP 19 generators (endurance, dispersal and flight-IRHS), both for vacuum and air ambient environments. The model is completely general in that it covers the permeation of oxygen, nitrogen, argon and helium as well as the internal production of helium due to the decay of the plutonium fuel. (In the IRHS design, helium is released from the capsule to the generator housing and ultimately diffuses through the seals to the environment.)

The equations in Appendix A represent closed form solutions to the multigas permeation problem and are amenable to manual calculations. An equivalent system of equations, developed first, was also programmed on a digital computer for rapid parametric studies, the results of which follow.

B. RESULTS OF ANALYSIS

1. Endurance Test Generators

Decay of gas pressure within the SNAP 19 generators is dependent on the generator external pressure environment (air or vacuum). This is illustrated in Fig. VII-3. A normalized argon leakage rate of 1.0×10^{-4} cm^3/sec at standard temperature and pressure results in a decay of endurance (dispersal type) generator pressure from 30 to 1.0 psia in 11,000 hours of vacuum environment. The same generator, when operated in air, will reach a minimum internal pressure of 6.5 psia after 10,500 hours. At this point, the partial pressure of argon is approximately 1.1 psia, as it would be after a similar test period in vacuum. The remaining 5.4 psia in the generator results from nitrogen diffusion into the generator. A similar process is shown for three relatively tighter seals which leak argon at normalized rates of 5×10^{-5}, 3.5×10^{-5} and 2×10^{-5} scc/sec.

A summary of normalized hot argon leak rates for the SNAP 19 endurance test generators is presented in Table VII-2.

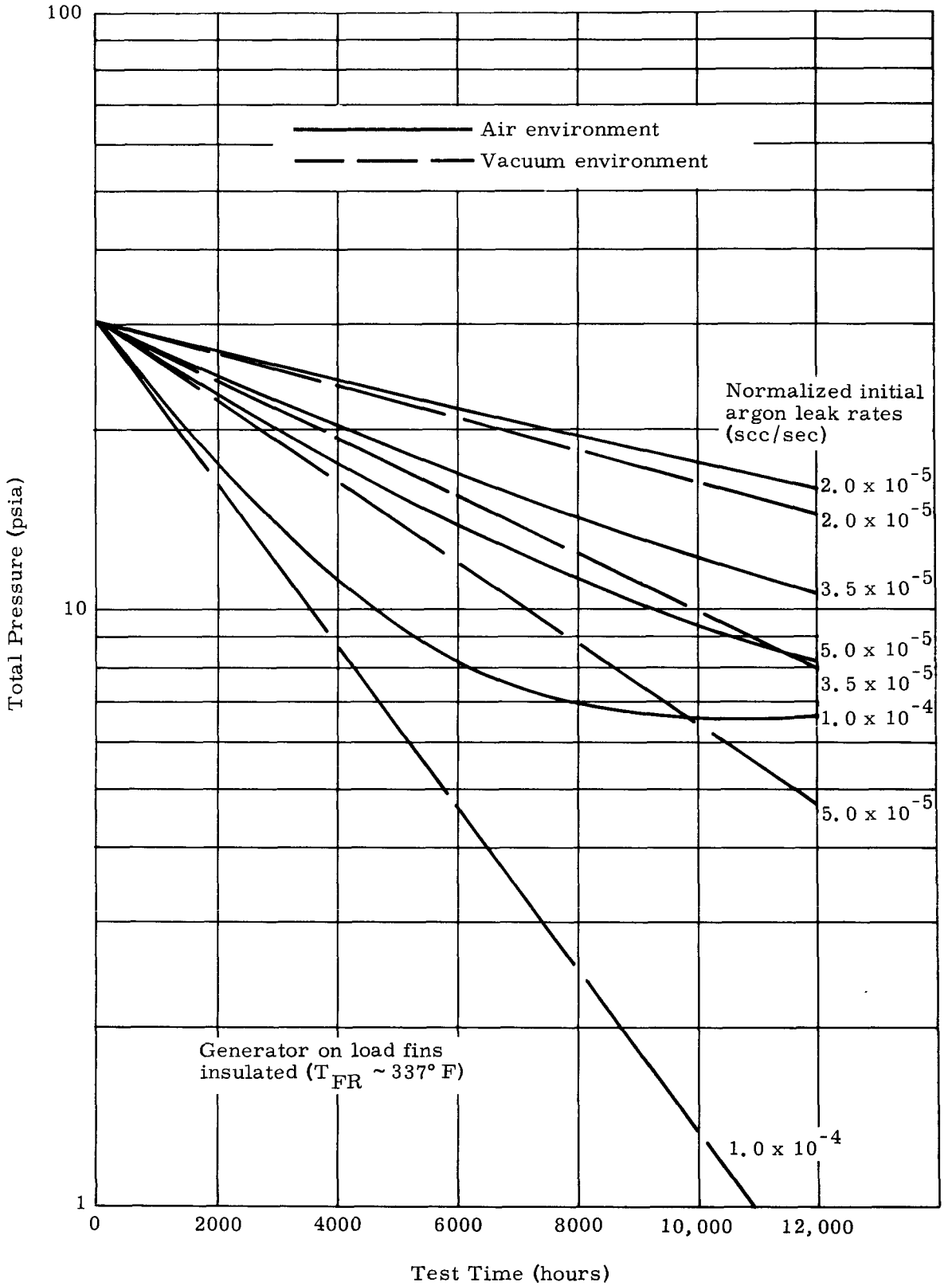

FIG. VII-3. SNAP 19 ENDURANCE GENERATOR PRESSURE DECAY

TABLE VII-2

Summary of Normalized Hot Argon Leak Rates
for SNAP 19 Endurance Test Generators
(14.7 psia, fin root temperature = 337° F)

Generator S/N	Normalized Argon Leakage Rate (scc/sec)
4	3.4×10^{-5}
5	2.9×10^{-5}
6	3.1×10^{-5}
17	2.0×10^{-5}
18	3.5×10^{-5}
19	4.0×10^{-5}
20	3.3×10^{-5}
21	4.4×10^{-5}

Analysis shows that the minimum composite generator pressure in an air environment is the same for a given seal temperature and initial gas inventory, but this minimum pressure occurs later for the lower rates. This is illustrated by the projected maximum/minimum endurance test generator pressure profiles shown in Fig. VII-4. Partial nitrogen pressures are shown in Fig. VII-5. SNAP 19 generators are filled with argon so that the initial gas inventory may be expressed as an argon generator pressure for stated conditions of generator gas temperature.

Equally as important for purposes of pressure predictions are the relative permeabilities of the various gases at test temperatures. Dependence of permeability of argon, nitrogen, oxygen and helium through Viton A on temperature is illustrated in Fig. VII-2 and compared in Table VII-1. At a seal temperature of 337° F (the average flight condition) the permeability of argon is five times that of nitrogen and approximately one-third that of helium. At a seal temperature of 260° F, the relative permeabilities of argon to nitrogen are unchanged but argon permeability is one-quarter that of helium. At room temperatures the argon permeability exceeds nitrogen permeability by two orders of magnitude and is approximately one-half that of helium.

Figure VII-6 shows that the multigas model pressure predictions match test data for endurance test generators S/N 4 and S/N 7. Similar agreement is obtained for other generators where consistent pressure transducer data are available.

2. Dispersal Generators

SNAP 19 generators fueled with the dispersal heat source experience a pressure decay during storage periods in air prior to flight. This is illustrated in Fig. VII-7 for generators with normalized argon leakages of 2.0×10^{-5} scc/sec (minimum expected, causing maximum pressure) and 1.0×10^{-4} scc/sec (maximum acceptable, causing minimum pressure). Storage temperatures of 260° F on fin roots and 740° F on hot junctions were selected for the storage periods of 6 to 12 months. The end-of-storage pressure spikes indicate generator gas temperature increases to 337° F on the fin root

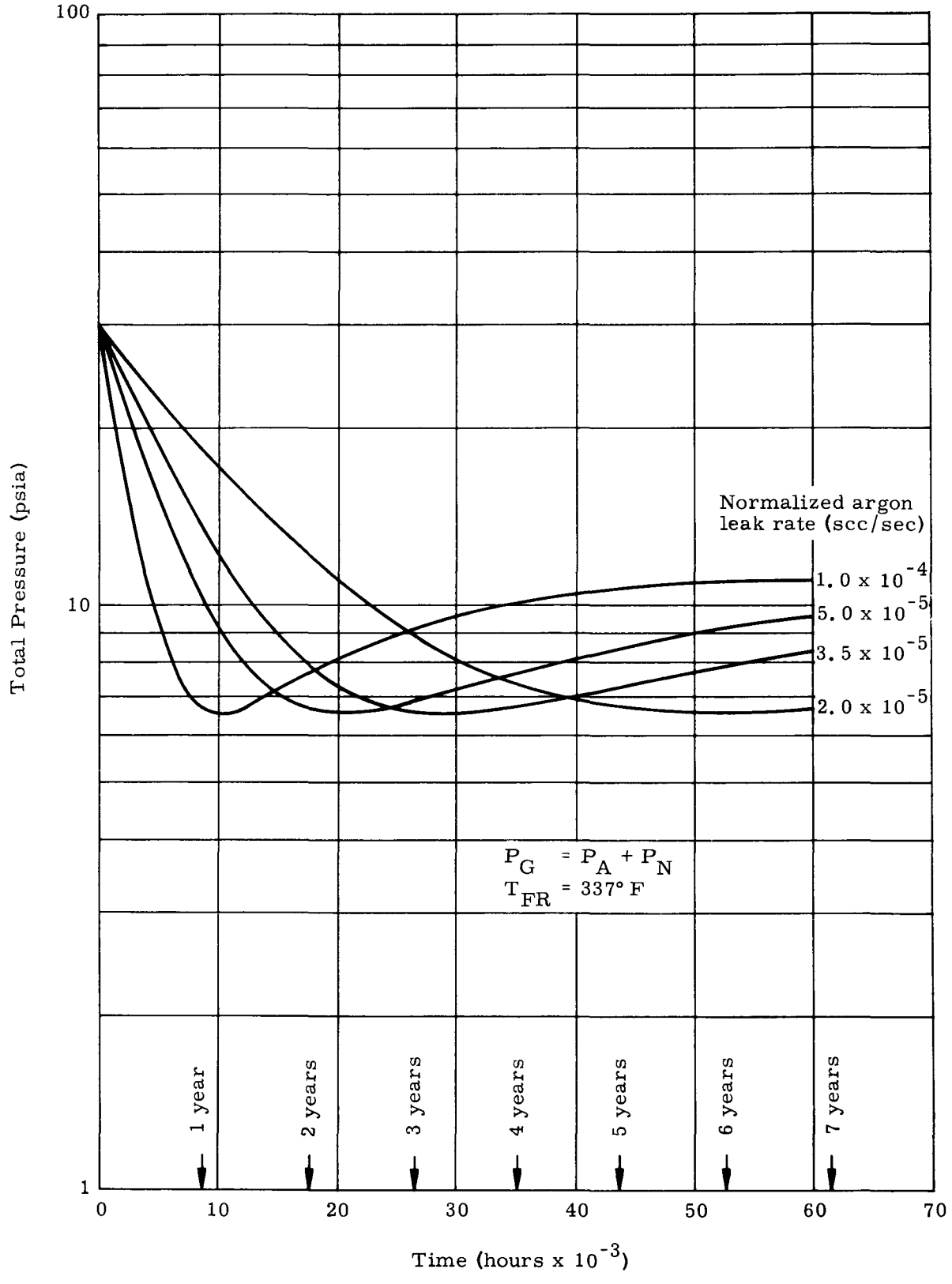

FIG. VII-4. SNAP 19 ENDURANCE TEST GENERATOR PRESSURE PREDICTIONS FOR GENERATOR IN AIR

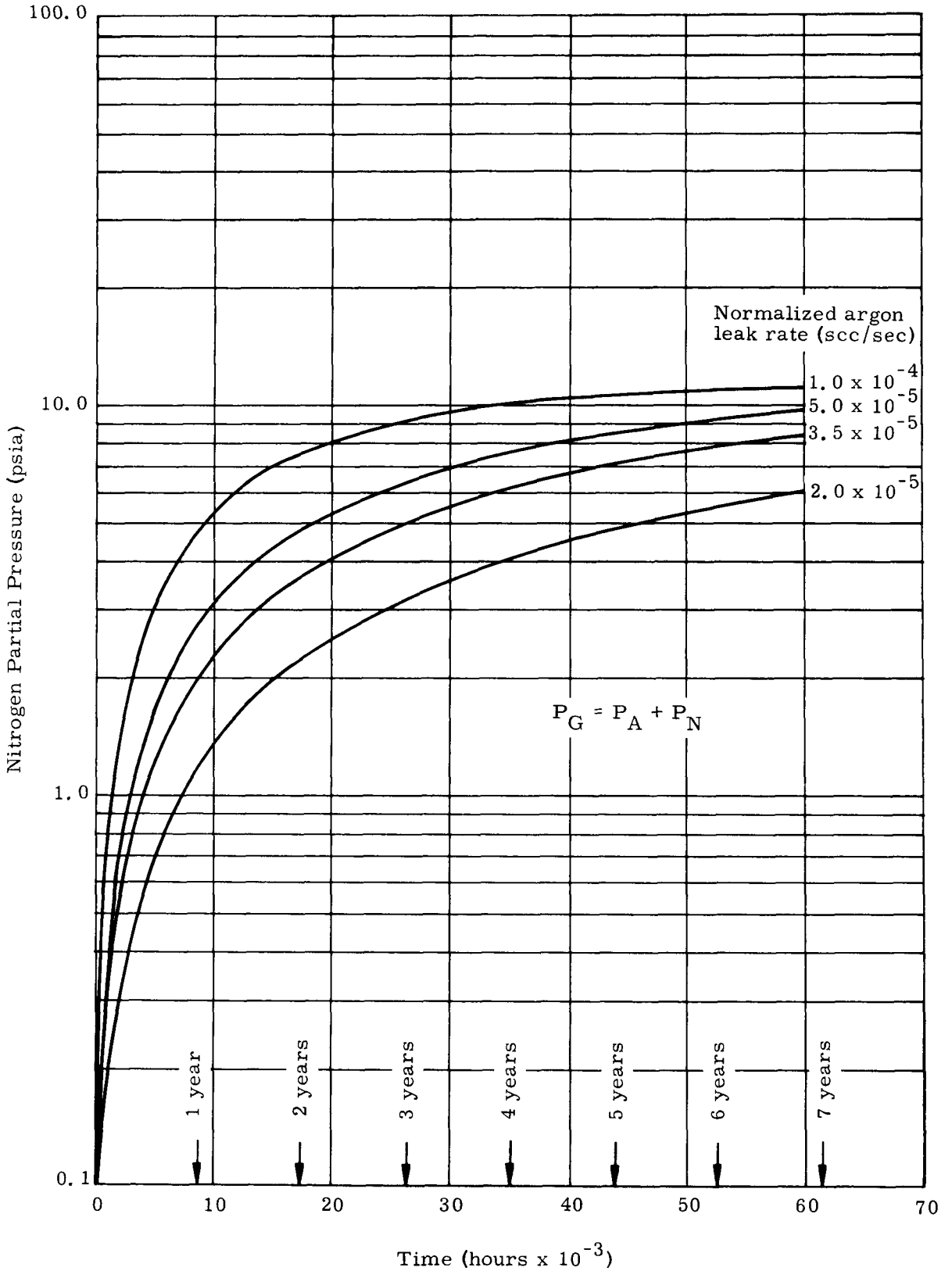

FIG. VII-5. SNAP 19 ENDURANCE TEST GENERATOR NITROGEN PRESSURE BUILDUP FOR GENERATOR IN AIR

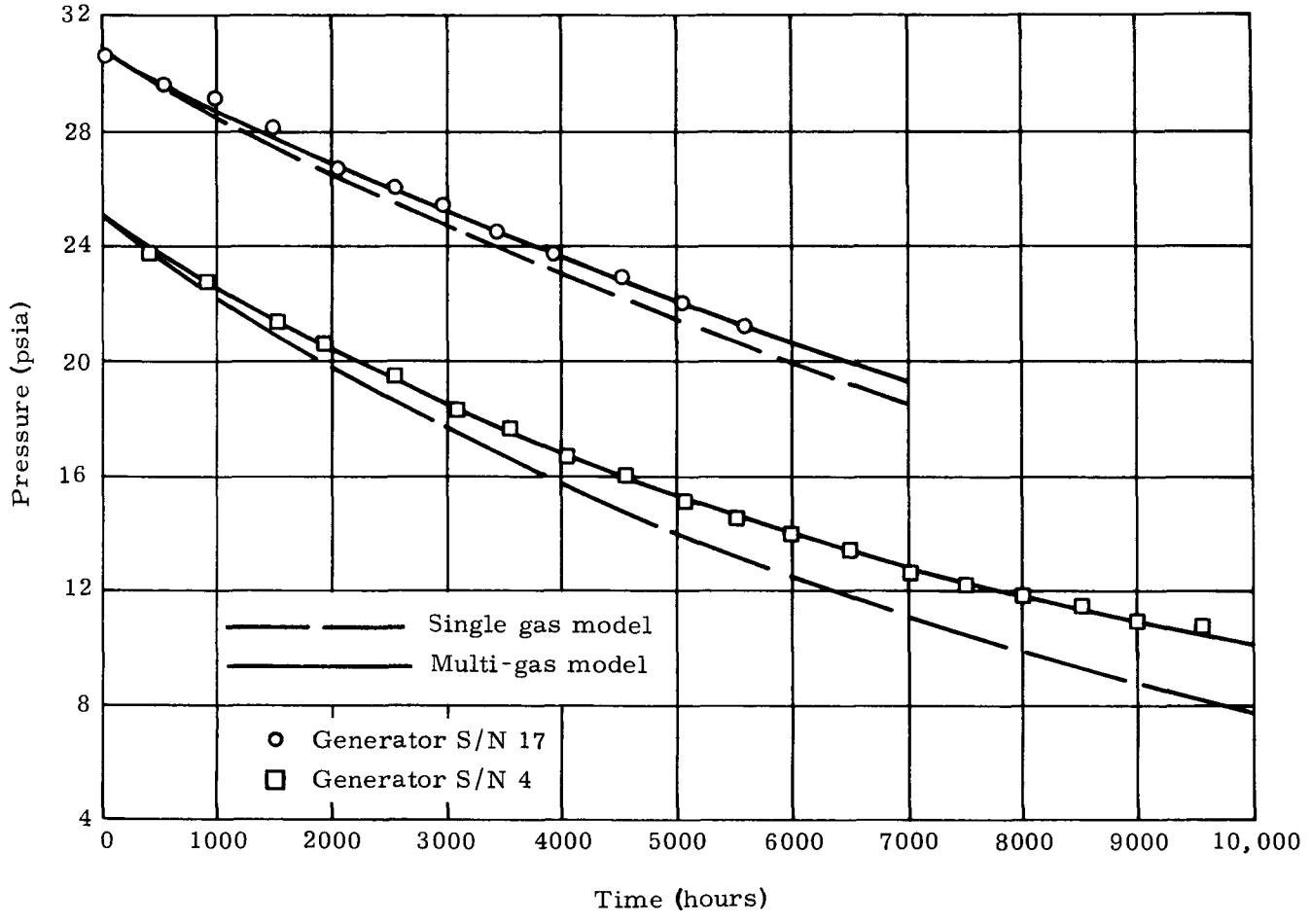

FIG. VII-6. ENDURANCE GENERATOR PRESSURE PREDICTIONS AND EXPERIMENTAL DATA--SINGLE GAS VERSUS MULTIGAS MODELS

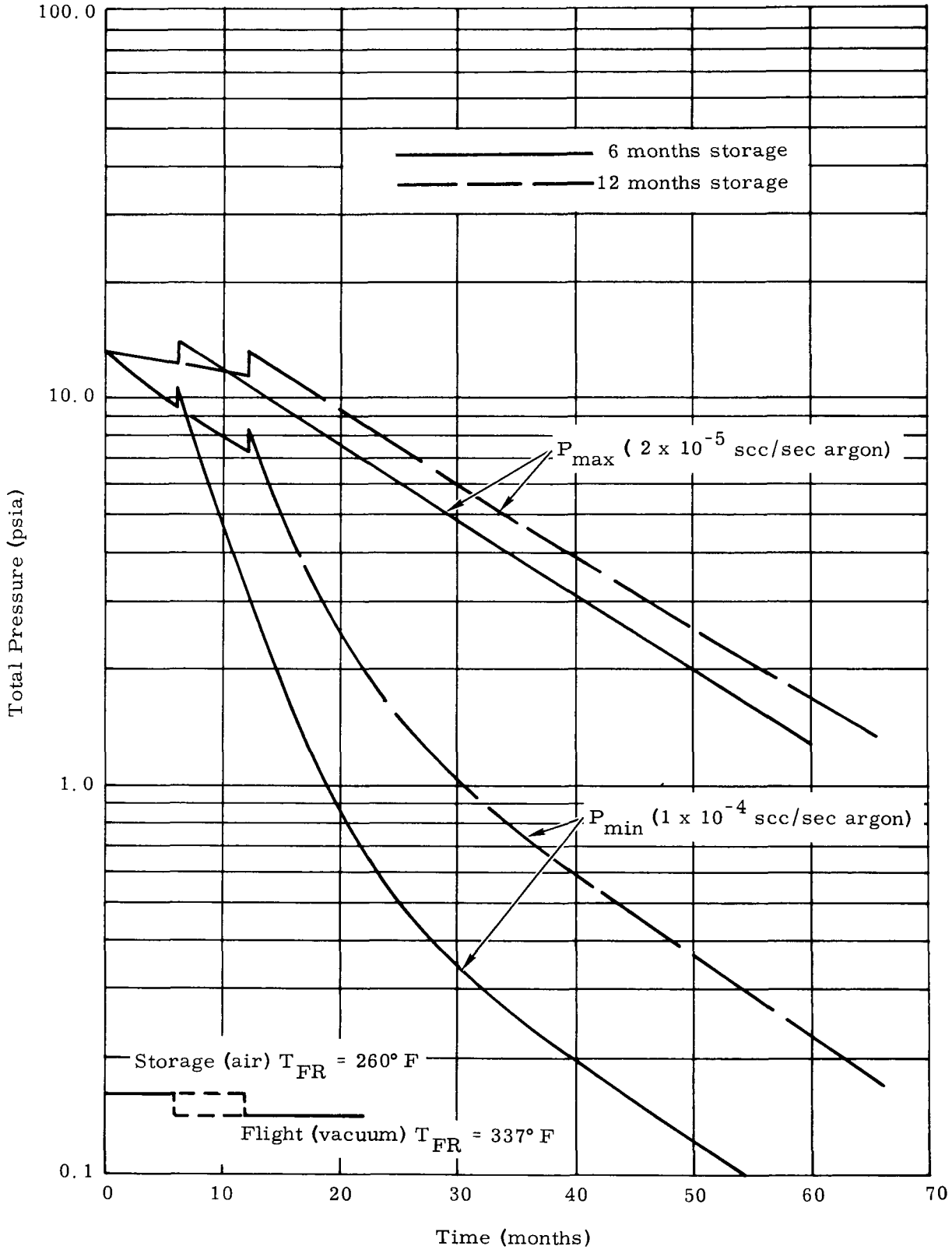

FIG. VII-7. FUELED DISPERSAL GENERATOR PRESSURE PROFILES

and 920° F on the hot junction as the generator is placed on electrical load. It is noted that prior air storage decreases the rate of leakage in space and thereby lengthens generator life from a minimum pressure standpoint. This behavior is attributable to the lower permeability of nitrogen compared to argon.

3. Flight-IRHS Generators

Pressure profiles for generators utilizing the helium emitting IRHS capsule with an initial generator argon fill are illustrated in Figs. VII-8 through VII-10. Total (Fig. VII-8), partial nitrogen (from air storage) and helium (Fig. VII-9) and argon pressures (Fig. VII-10) are shown. The generator ultimately approaches an equilibrium pressure of 1.2 to several psia of helium, depending on seal tightness (i.e., leak rate). The SNAP 19 flight generators, S/N 23A and 22A, have leak rates of 1.7×10^{-5} and 2.5×10^{-5} scc/sec argon, respectively.

Pressure profiles for IRHS generators initially filled with helium may be of interest for future design (Fig. VII-11). Thermal losses, and consequently power output, vary with the inventory of types and quantities of gases within the generator. The helium-filled generator approaches equilibrium pressure conditions at relatively constant gas temperatures, and power output therefore varies less for long missions (e.g., 5 years) than is the case for an argon-filled generator.

4. Oxygen Reactor

The amount of oxygen permeating into the generator per year in air depends on seal tightness and seal temperature. Representative volumes and mass quantities are presented in Table VII-3.

TABLE VII-3

Quantities of Oxygen Entering Generators for Various Test Conditions

Test Condition		Seal Tightness	Oxygen Permeation	
Air Environment	Fin Root (seal) Temperature (° F)	Normalized Argon Leakage Rate (scc/sec)	Volume (scc/yr)	Mass (gm/yr)
Storage	260	2×10^{-5}	50	0.07
Storage	260	1×10^{-4}	250	0.36
Load	337	2×10^{-5}	135	0.19
Load	337	1×10^{-4}	675	0.96
Load	350	2×10^{-5}	155	0.22
Load	350	1×10^{-4}	770	1.10

The largest quantities of oxygen are permeated while the generators are on load at high seal temperatures, a condition existing during endurance tests when generator fins are insulated. The rate of oxygen permeation for this case can be as high as 1.1 gm/yr. The zirconium mass within the generators is capable of reacting 48 grams of oxygen.

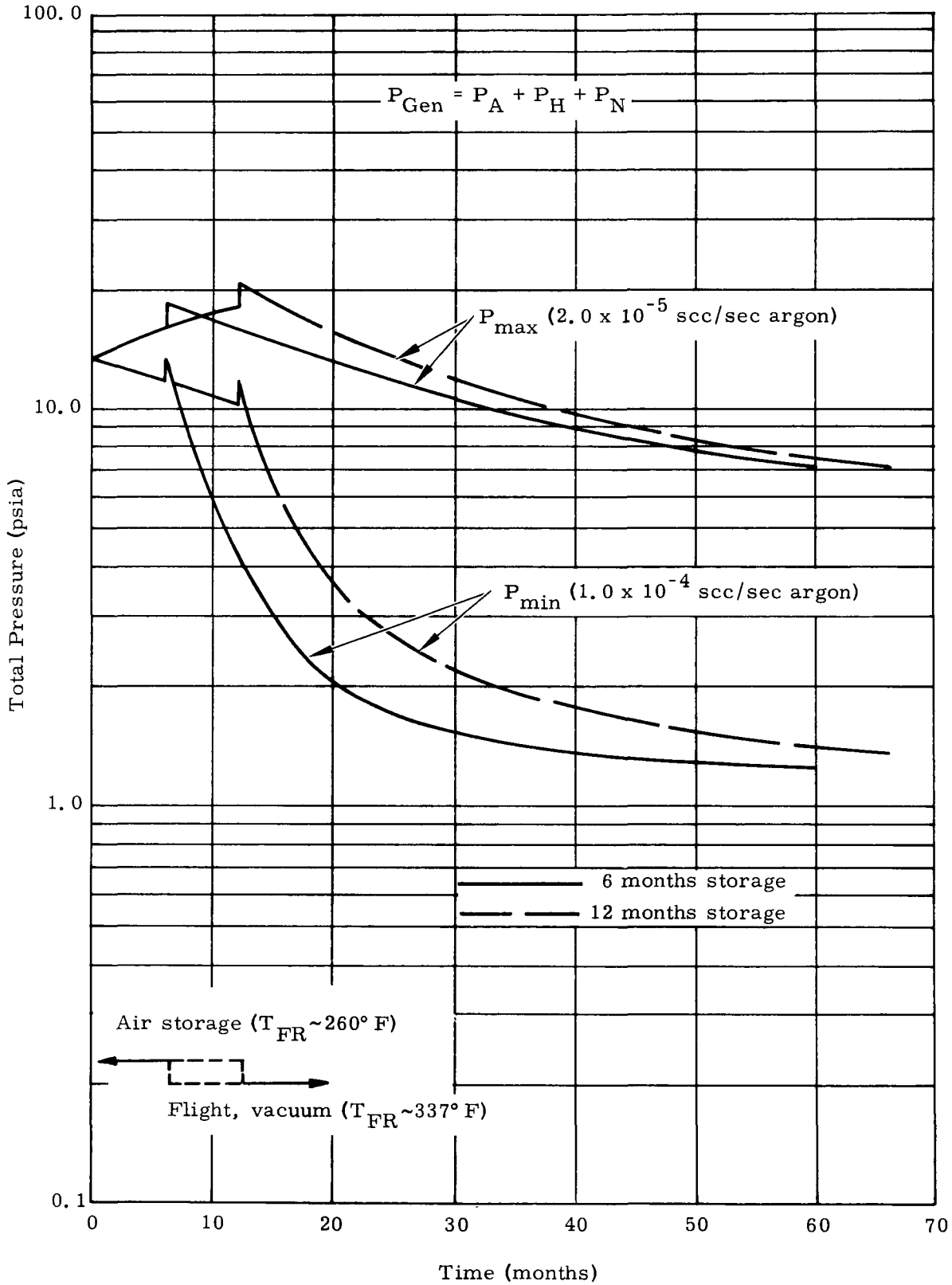

FIG. VII-8. FUELED IRHS GENERATOR PRESSURE PROFILES -- TOTAL PRESSURE

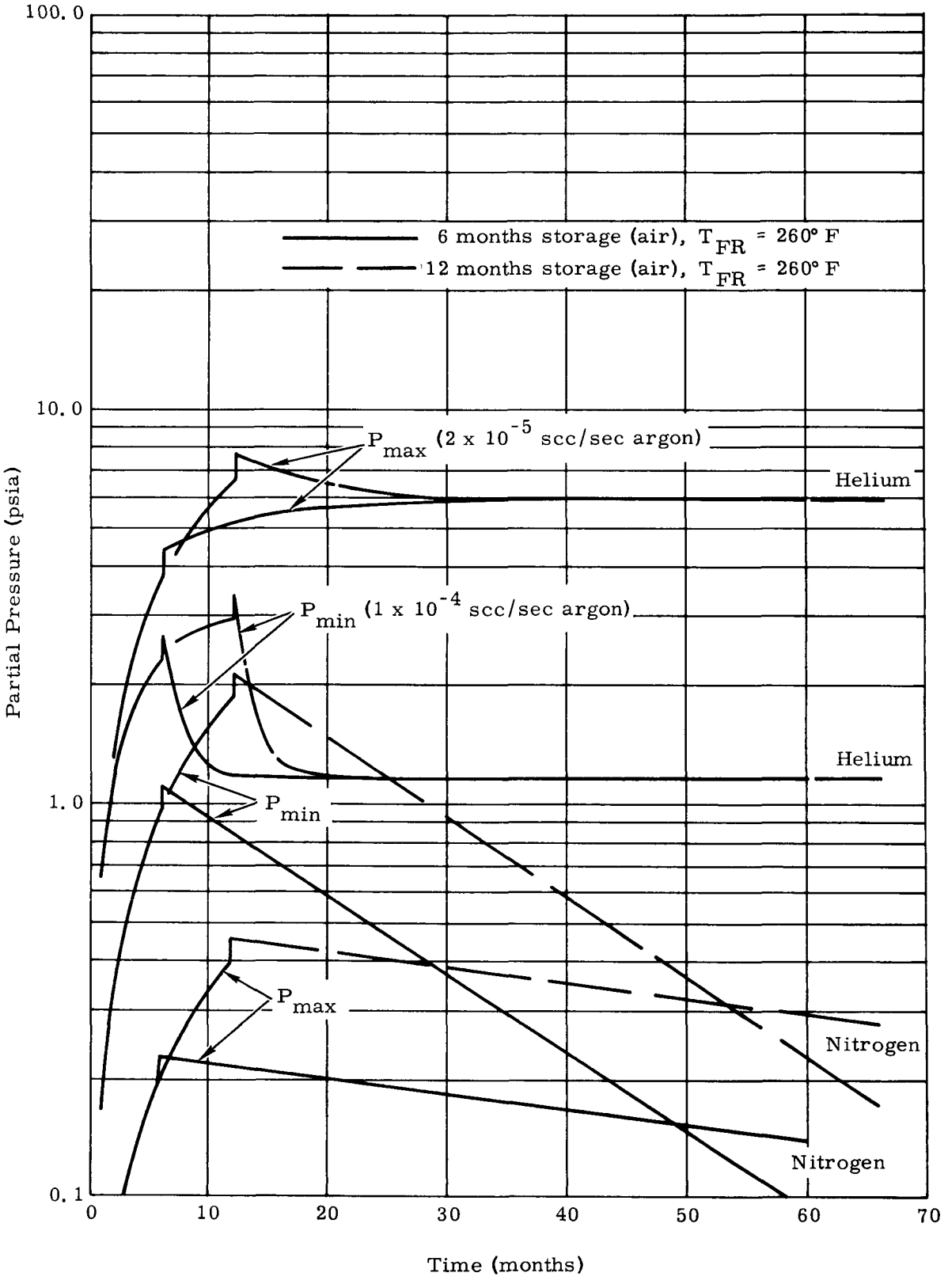

FIG. VII-9. FUELED IRHS GENERATOR PRESSURE PROFILES -- PARTIAL PRESSURES OF NITROGEN AND HELIUM

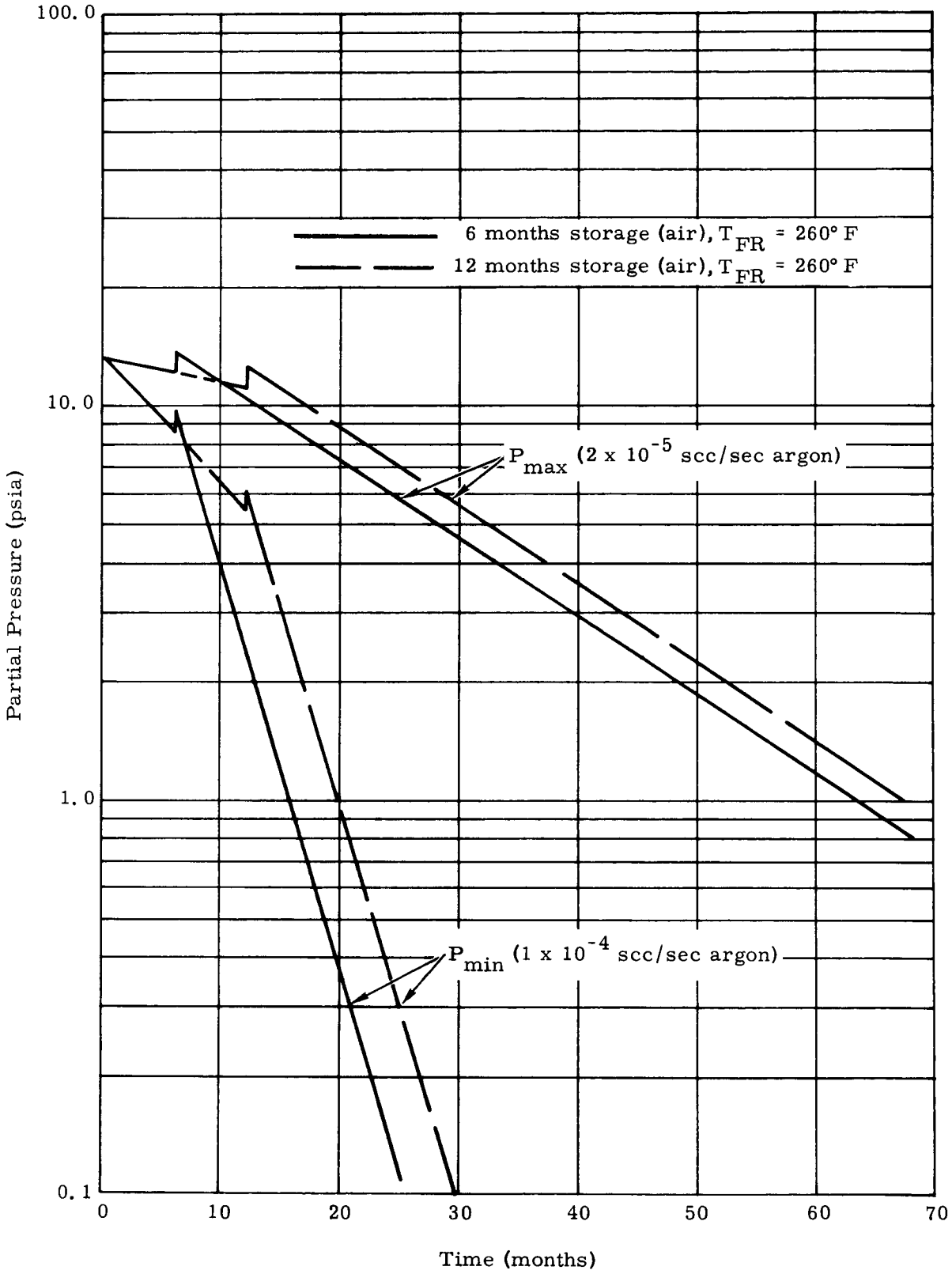

FIG. VII-10. FUELED IRHS GENERATOR PRESSURE PROFILES -- PARTIAL PRESSURE OF ARGON

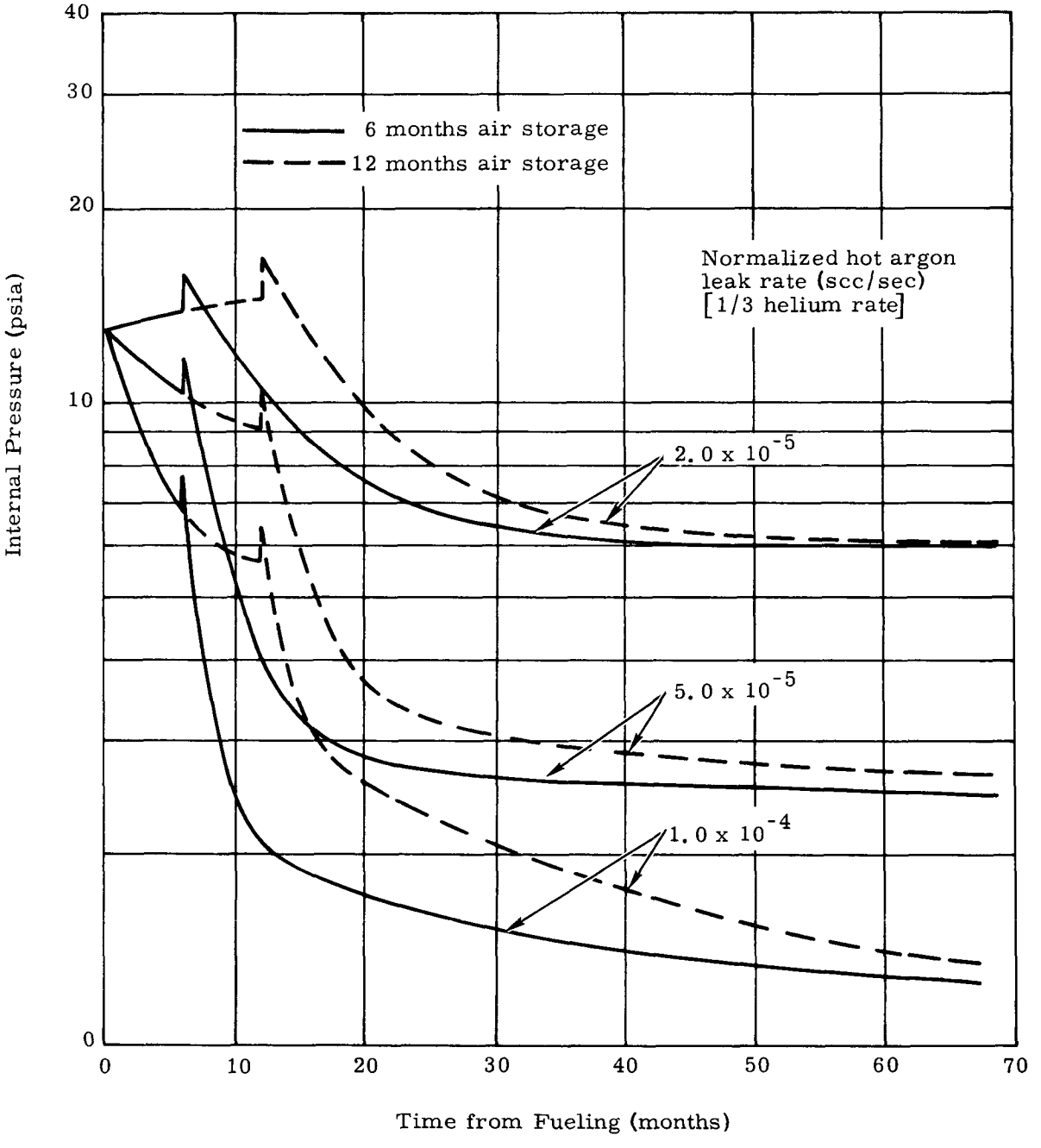

FIG. VII-11. IRHS GENERATOR PRESSURE PROFILES--HELIUM FILL

VIII. HOT JUNCTION TEMPERATURE MEASUREMENT

Thermistors are commonly used in spacecraft for temperature measurements. These are also used in the SNAP 19 system to sense temperatures of the generator housing and the power conditioner. Hot junction temperatures are on the order of 900° F and can range from about 750° to 1050° F, depending on the mode of operation. This is significantly above the upper limit of thermistors.

A resistance element type of sensor is suitable for the application. The resistance temperature device (RTD) was selected because of the following characteristics:

(1) Small size

(2) Low power requirement

(3) Reference temperature junction not required

(4) Extreme accuracy

(5) Fast response

(6) Good repeatability.

The initial RTD used for SNAP 19 (Fig. VIII-1) consisted of a 100-ohm platinum element installed in a 0.25 by 0.25 by 0.030-inch platinum case and electrically insulated from the case with a high temperature ceramic material. This unit was commercially available; the only modification required was an extension of the leads. The temperature range and structural attributes were more than adequate.

The RTD case was spotwelded into a specially prepared slot in the body of the hot shoe as shown in Fig. VIII-2. While this installation gave a good thermal pickup, it also imposed a voltage onto the case of the RTD.

The RTD's were coupled to the telemetry signal conditioning unit (TSCU) as shown in Fig. VIII-3. The bridge circuit for each RTD is balanced so that, with the RTD at 700° F, there is no output signal from the bridge or the amplifier. The circuit was designed to limit the current in the RTD to approximately 1.4 ma. Over the normal 700° F-to-1100° F operating range of the RTD, the output voltage of the bridge varies between 0 and -106 mv. This is the input signal to the operational amplifier and corresponds to a 0 to -6.36 vdc output signal from the amplifier to the telemetry unit. Any signal voltage impressed on the RTD would change the output voltage by the amount of impressed voltage and could be additive or subtractive, depending on the polarity. A resistance shunting the RTD would reduce the current through the RTD and reduce the output voltage of the bridge.

The RTD's were laboratory tested by the supplier and by Martin Marietta with satisfactory results. However, operating experience with the units in generators indicated significant problems. Erratic hot junction temperature measurements were observed. Troubleshooting indicated that a d-c voltage was being impressed onto the RTD's (Ref. VIII-1). It was indicated that this voltage was from the thermoelectric module circuit.

To further analyze the problem, a generator was diagnostically disassembled. This was followed by laboratory testing of the RTD's. It was found that the RTD electrical insulation was breaking down, allowing the element to short to the case and the case voltage to be impressed on the leads. Laboratory testing showed that

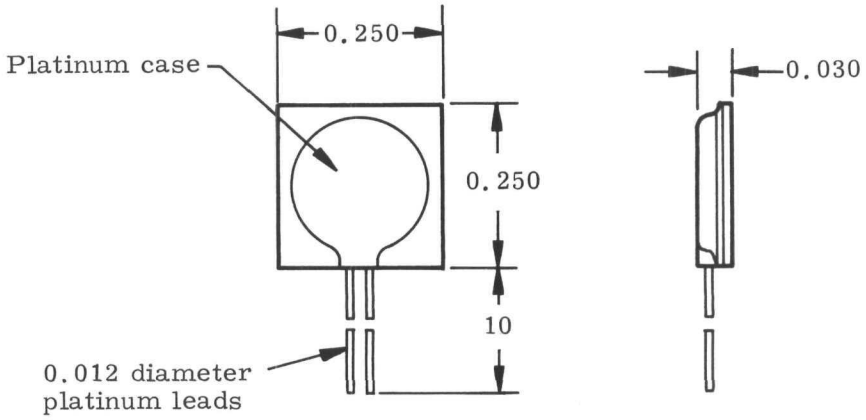

FIG. VIII-1. HOT JUNCTION TEMPERATURE SENSOR (RTD)

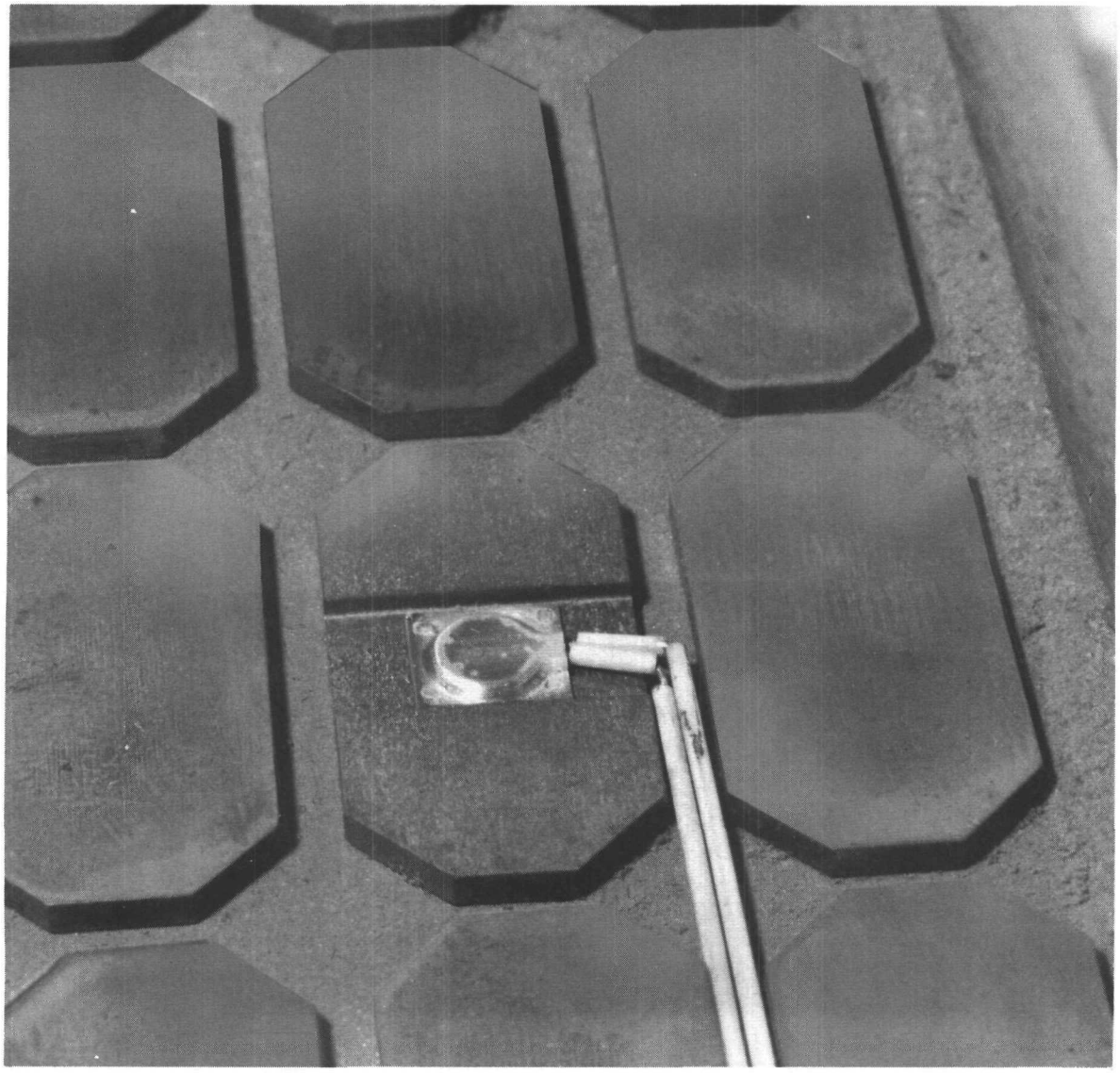

FIG. VIII-2. RTD INSTALLED ON HOT SHOE

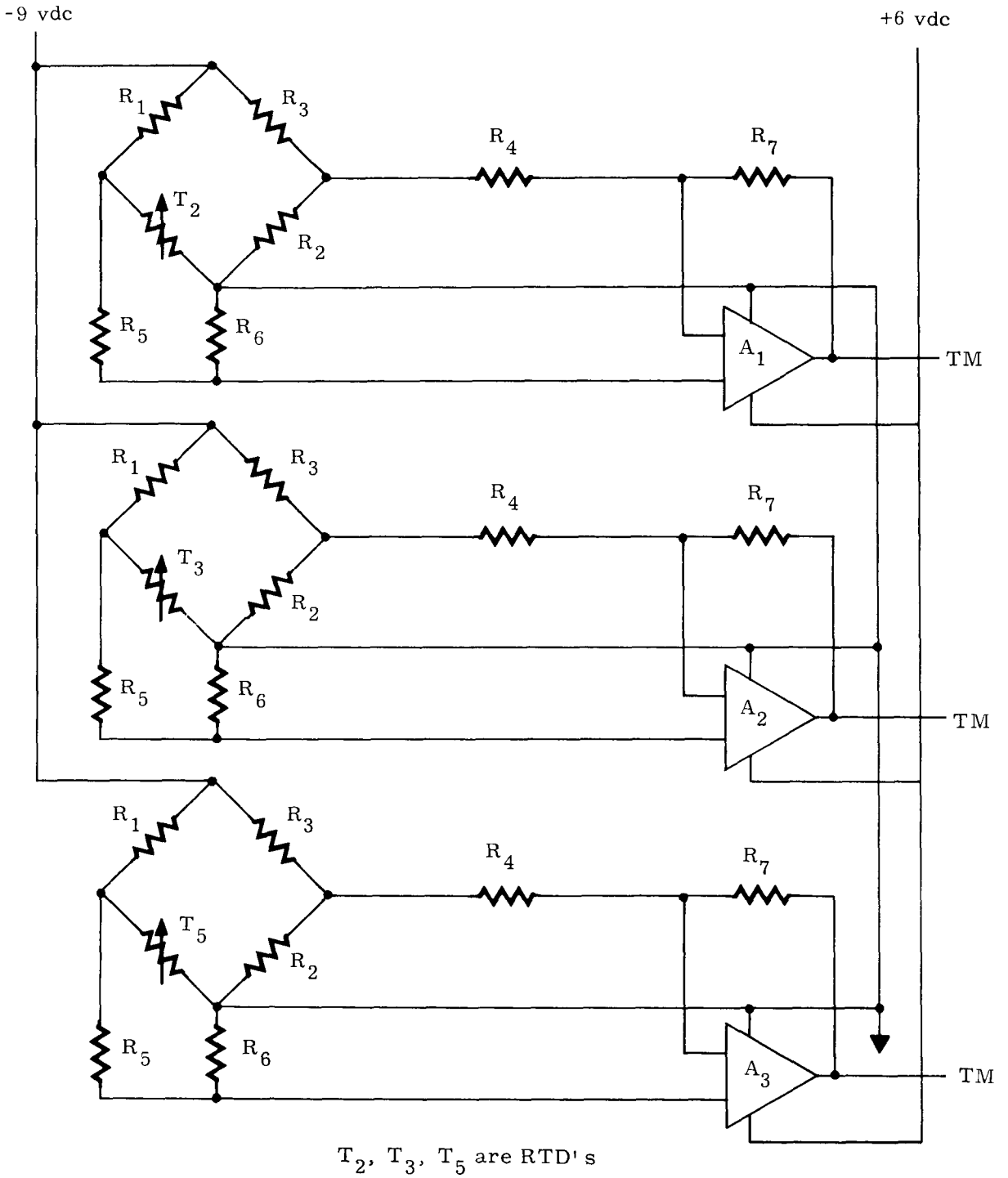

FIG. VIII-3. RTD-TSCU CIRCUIT SCHEMATIC

the insulation breakdown could have been caused by trace amounts of hydrocarbon vapors and/or a reduction of the metal oxides in the RTD insulating material. The process could be reversed by operation at elevated temperatures in the presence of oxygen.

Resolution of the problem was started along two avenues. All generator fabrication processes were reviewed and use of hydrocarbon cleaning agents was deleted, or a further cleaning or "wash" following their use was prescribed to remove traces of hydrocarbon. Trace amounts of hydrocarbons could, however, evolve from thermal insulation material. A sealed RTD was therefore required. Two concurrent technical approaches were taken. An in-house effort to encapsulate the RTD was conducted, and the RTD supplier was to develop hermetically sealed unit.

The encapsulation approach was subject to problems of both encapsulation and of installation. An attempt was made to slip-cast the RTD with glass into a cavity in the hot shoe. This method yielded some success but would have led to complications in thermoelectric couple fabrication. High temperature cements were tested as sealants and for attachment but were proved ineffective as sealants because of porosity.

Encapsulation in a glass enamel proved to be an effective method of sealing. This unit, shown in Fig. VIII-4, was installed in a recess in the hot shoe and held by a stainless steel retainer spotwelded to the hot shoe. It was found that installation could cause cracking of the glass, giving a high rejection rate. Further, vibration testing produced minute cracks in the glass enamel, resulting in ineffective sealing.

The hermetically sealed unit (Fig. VIII-5) developed by the Rosemount Engineering Company proved to be successful. The RTD's were installed on thermoelectric couples at the end of the module. Each device was spotwelded to an extension of the hot shoe. This allowed the RTD's to be installed after the core was installed in the housing. The RTD installation is shown in Fig. VIII-6. The RTD case is Type 304 stainless steel and is equipped with a sealed connector.

For future applications, it is recommended that only hermetically sealed units be considered. Further, if practicable, the unit should be installed on a surface which is not part of an electrical circuit. In SNAP 19, for example, it would have been less costly to attach the RTD to the heater block and determine a correction factor to give hot junction temperature.

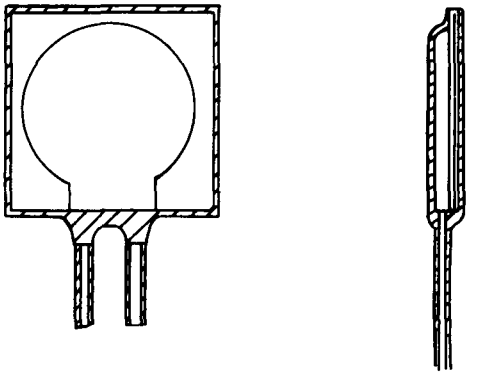

FIG. VIII-4. ENCAPSULATED RTD

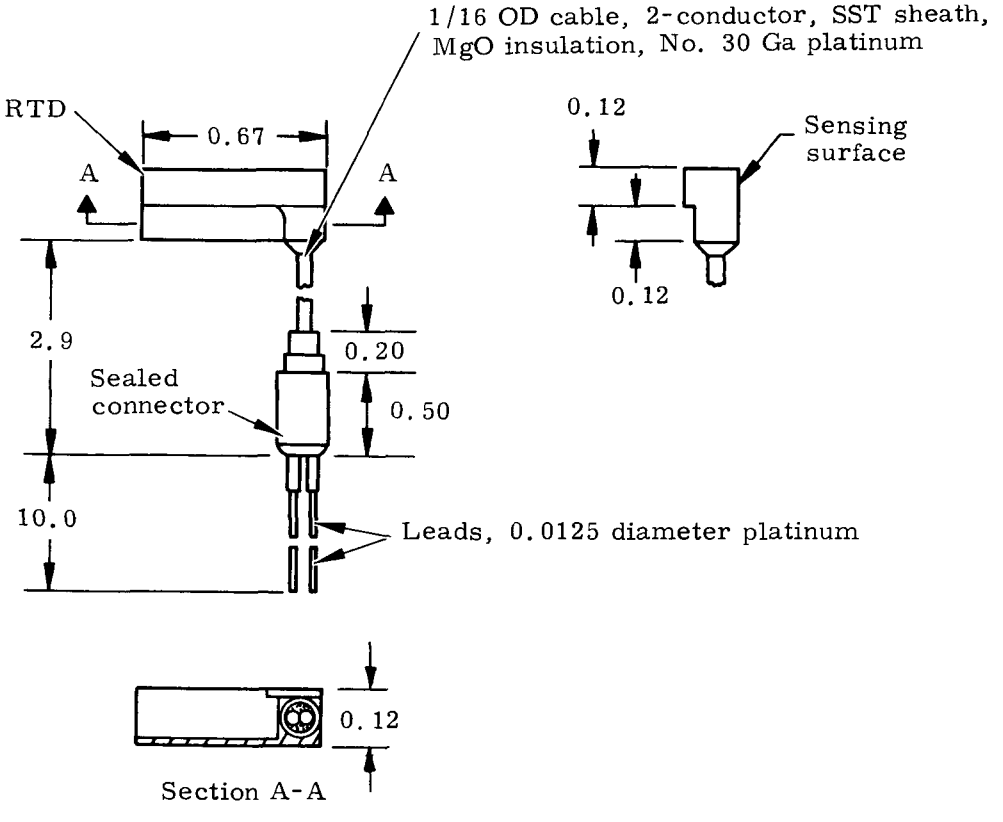

FIG. VIII-5. HERMETICALLY SEALED RTD

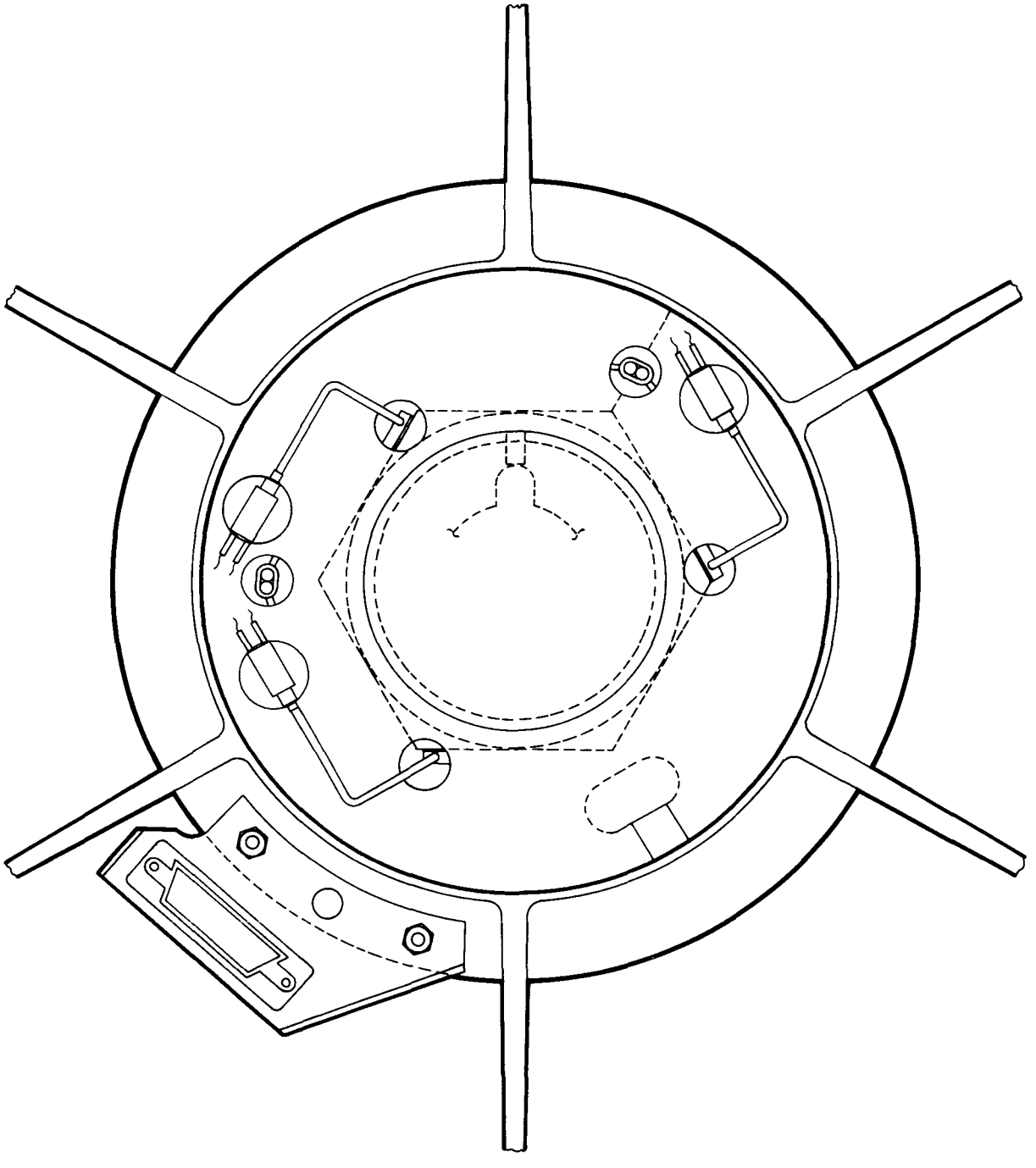

FIG. VIII-6. INSTALLATION OF HERMETICALLY SEALED RTD'S

IX. RADIATION SPECTRA

The energy distribution and the absolute magnitude of the neutron and gamma radiation were determined for the generator subsystem (Ref IX-1). This type of data had not been obtained on previous plutonium-fueled generators. The magnitude of the radiation compared favorably with calculated values and with dose rates measured with health physics techniques. (For dose rates, see Volume I, Chapter III. D.)

A. NEUTRON MEASUREMENTS

The stilbene neutron detection system was used in making neutron measurements. This system measures the amplitude of the light pulses produced by proton recoil resulting from neutron elastic scattering in a hydrogenous medium--a stilbene crystal. The scintillation count rate data can be related to the energy-dependent neutron flux spectrum. A data reduction program for the stilbene system was obtained from Mound Laboratory and modified for use with the IBM 7094 and 360 computers.

Neutron spectra were measured at six locations around the subsystem; generator subsystem S/N 4 (a prototype unit) was used. The spectral shapes for all the locations were essentially the same. The typical spectrum, shown in Fig. IX-1, was obtained at a distance of 29.1 inches from the subsystem axis. The different symbols represent data taken with the two different settings of the photomultiplier necessary to obtain good resolution over the energy range.

B. GAMMA MEASUREMENTS

Conventional gamma spectrometry techniques were employed. This required a scintillation counter using a 1-1/2-inch diameter sodium iodide crystal and a 256-channel pulse height analyzer.

Measurements were made at one location--the same point shown in Fig. IX-1 for the neutron spectrum. The gamma spectrum is given in Figs. IX-2 and IX-3. The gamma dose rate could not be accurately determined because of scattering and the resultant increase in the magnitude of the low-energy spectrum.

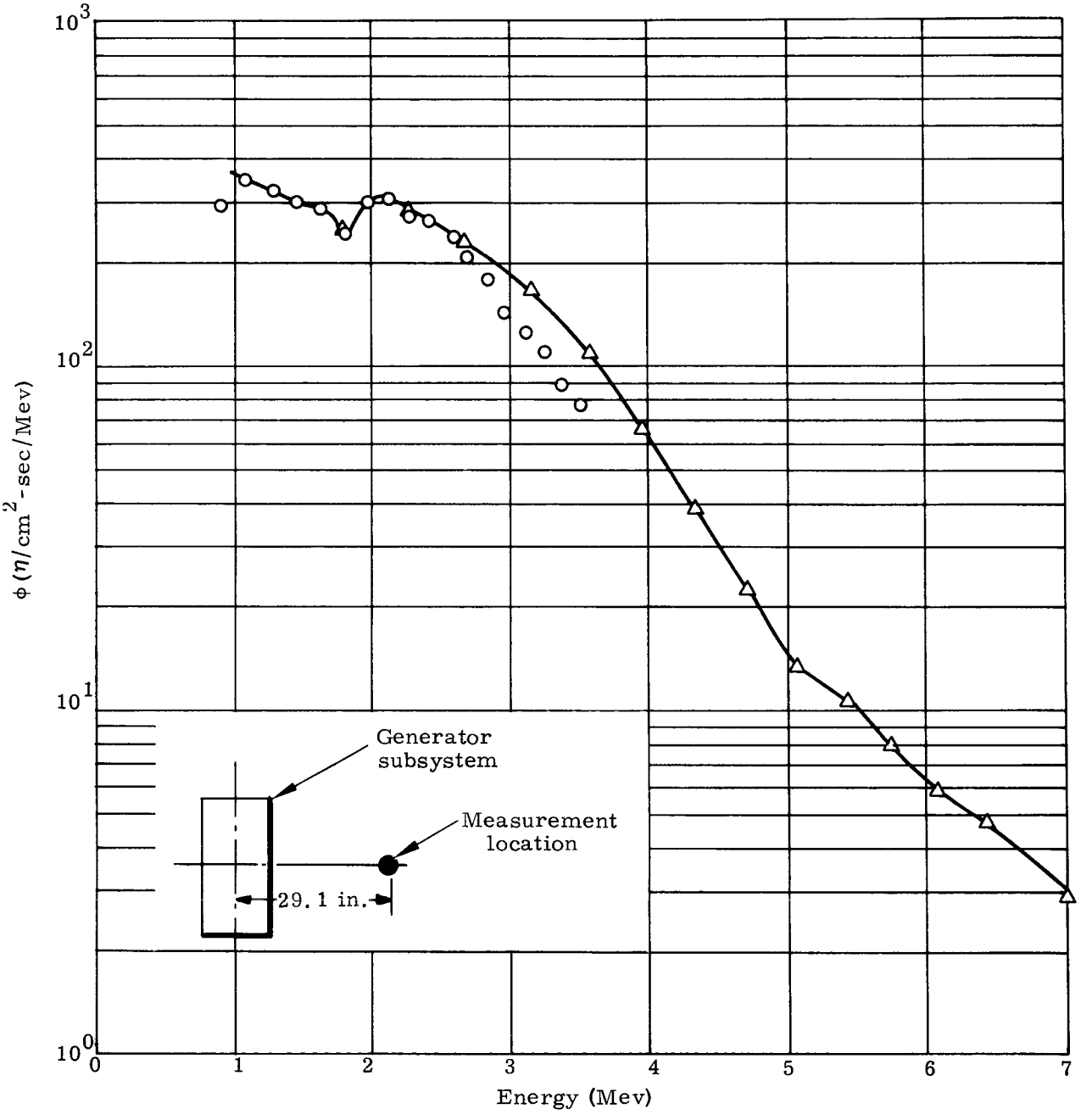

FIG. IX-1. NEUTRON SPECTRAL MEASUREMENT

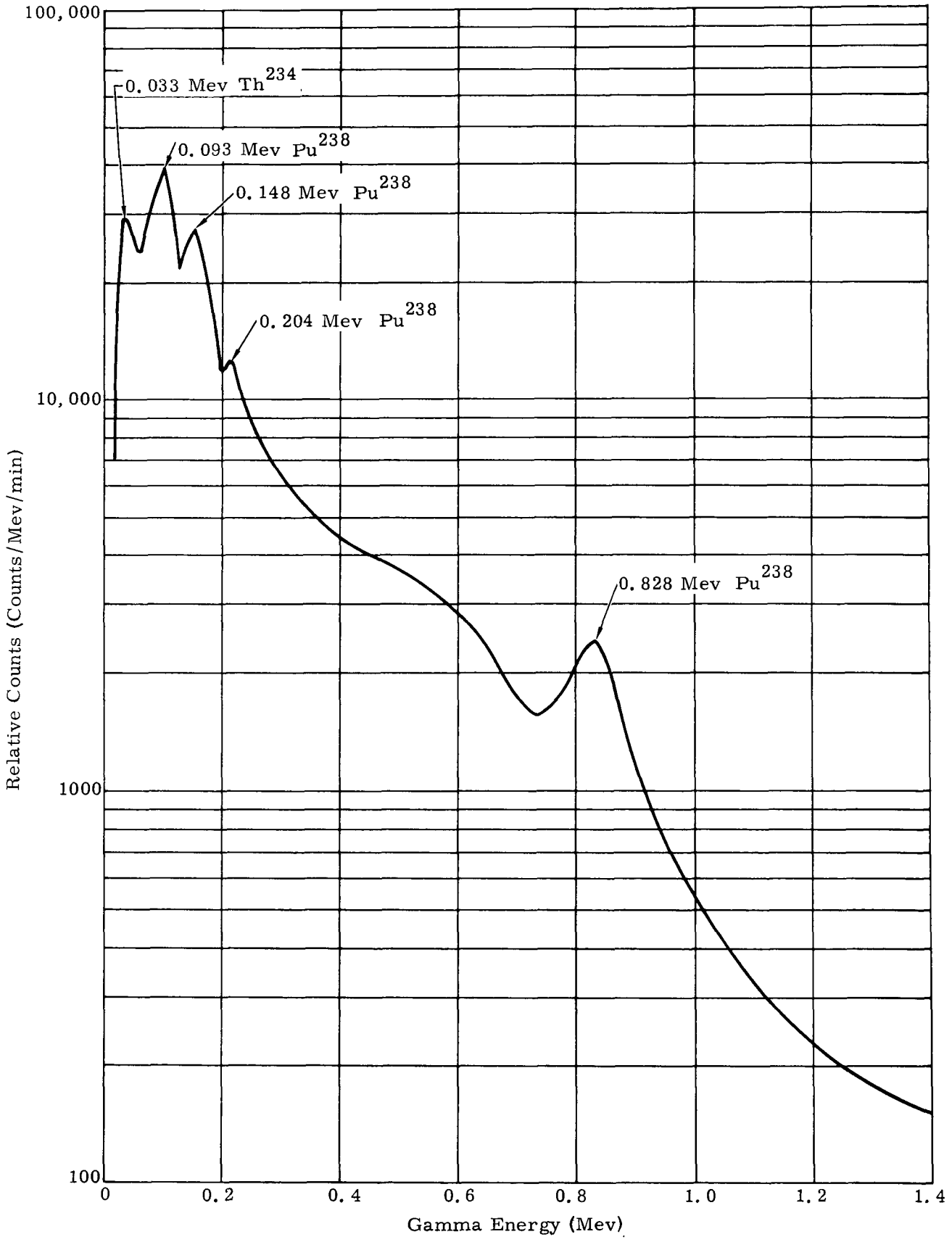

FIG. IX-2. GAMMA SPECTRUM

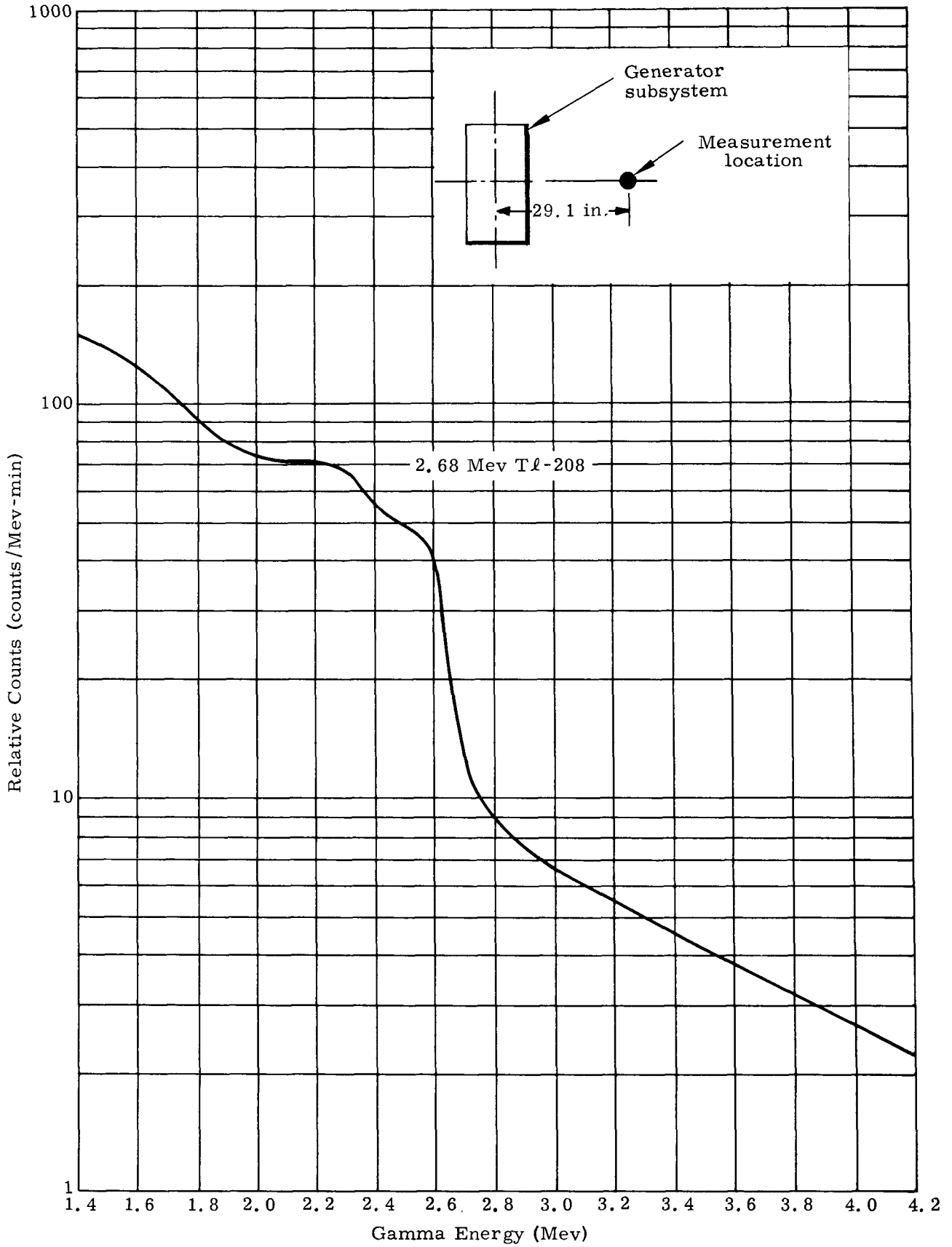

FIG. IX-3. GAMMA SPECTRUM

X. FUEL CAPSULE SUPPORT

Adequate support of the SNAP 19 fuel capsule is essential in order to limit its motion relative to adjacent generator components. Axial displacement of the capsule is constrained by disks of Min-K-1301 (Johns Manville Corporation) thermal insulating material. Because this insulating material is also used as a structural load bearing element in the generator, it was essential that the mechanical properties of Min-K-1301 be within the limits required for practical design considerations. The manufacturer's structural properties data were limited, particularly in the area of dynamic characteristics such as dynamic modulus and damping, and little was known regarding thermal effects on structural properties, either static or dynamic. Therefore, a comprehensive test program was undertaken during Phase II to obtain the required information. The results of this investigation are reported in Ref. X-1. The test program evaluated the effects of temperature, fiber orientation, boundary constraints, load relaxation and static-dynamic loadings. Design guide information was produced in terms of static and dynamic moduli, spring constraints, damping factor and stress limits.

The dynamic loads impressed on the fuel caspule are transmitted through the Min K-1301 support disks. Because of the acceleration levels and the capsule weight, it was necessary to provide a load distribution plate on each end of the dispersal-type capsule to compensate for its cap geometry and the stress limitations of the Min-K-1301.

To preclude hammering of the insulation disks by the capsule during vibration, it was necessary to preload the capsule by an initial compression of the disks, accomplished during the generator fueling sequence. The preload had to be adjusted so that the axial load on both ends of the capsule (hence the load in either disk) never decreased to zero when subjected to dynamic testing The structural properties data provided by Ref. X-1 were used with estimated and measured capsule dynamic loads to specify the size of the load distribution plate and magnitude of displacement required for precompression (preload).

In the IRHS design, the large flat sections at both ends of the heat shield made load distribution plates unnecessary for preloading.

Lateral motion for both cases, dispersal and IRHS, was limited by the graphite heat accumulator block and the friction loads resulting from preloading the heat source.

It was necessary to assure that the defined preload was provided during the fueling operation. Diagnostic disassembly of generator S/N 7 to investigate malfunctioning RTD's disclosed that some of the Min-K details had been pulverized due to hammering during vibration. The problem is discussed in detail in Refs X-2 and X-3. A re-evaluation of preload techniques resulted in a modification to the fueling procedure. The revised procedure calls for measurement of Min-K protrusion beyond generator housing (length to be precompressed) with the heat source installed and adjustment of the protrusion by shims until proper preload can be assured when the generator cover is installed. Adequacy of design and loading technique was demonstrated in prototype testing of generator subsystem S/N 6A and flight testing of generator subsystems S/N 6, 7, 8 and 8A.

The flight generator subsystem, S/N 8A has a total Min-K-1301 precompression displacement of 36 ± 4 mils, resulting in a preload at each end of the IRHS heat source assembly of 360 ± 40 pounds, which provides adequate support up to 120 ± 10 g dynamic loading. Based on vibration transmissibility test measurements, it is estimated that the maximum flight dynamic loads at the capsule will not exceed 30 g.

BLANK

XI. BIBLIOGRAPHY OF TOPICAL REPORTS ON SNAP 19 GENERATOR DEVELOPMENT

A. THERMOELECTRICS

(1) "Thermoelectric Element Data Evaluation," MND-3607-104, T. Conrad, V. Truscello, July 1966.

(2) "SNAP 19 Generator Endurance Test Data and Performance Analysis," MND-3607-236, A. Lieberman, C. Goebel, April 1968.

B. GENERATOR DESIGN AND FABRICATION

(1) "Feasibility Study of Radioisotope Power for the Nimbus B Satellite," MND-3169-2, M. P. Norin, March 1964.

(2) "Thermal Radiator Tests," MND-3169-24, C. Kelly, W. Britton, September 1964.

(3) "Structural Evaluation of Min-K 1301," MND-3169-45, D. Thomas, January 1965.

(4) "SNAP 19 Phase II Final Summary Report," MND-3169-83, August 1965.

(5) "Pressure Transducer Topical Report," MND-3607-108, J. Delp, J. Himes, July 1966.

(6) "Evaluation of SNAP 19/Nimbus B Flight Instrumentation with Special Reference to Measurement of Hot Junction Temperature," MND-3607-117, R. Buxbaum, C. Karr, R. Hemler.

(7) "Electrically Heated Development Generator Subsystem with Redesigned Heater Assembly, Engineering Evaluation Test Report," MND-3607-147, E. Kuhar, C. J. Clemente, H. Porter, February 1967.

(8) "SNAP 19 Heater Failure Investigation," MND-3607-153, C. J. Clemente, L. Piscopink, March 1967.

(9) "Fueling Operation, SNAP 19 Radioisotope Thermoelectric Generators S/N 11 and S/N 12," MND-3607-159, R. Pettigrew, April 1967.

(10) "Test Report on the Hot (Argon) Leak Testing of SNAP 19 Nimbus B Radioisotope Thermoelectric Generators S/N 11 and 12," MND-3607-162, R. Pettigrew, April 1967.

(11) "Test Report, Power Check and Defueling Operation, Prototype, SNAP 19 Subsystem 4," MND-3607-187, R. Pettigrew, June 1967.

(12) "Multigas Permeability Analysis and Pressure Predictions for SNAP 19 Generators," MND-3607-230, C. Goebel, P. Brennan, February 1968.

(13) "Subsystem 6A (IRHS Prototype) Diagnostic Disassembly Report," MND-3607-235, J. Himes, A. Lieberman, W. McDonald, February 1968.

C. FUEL CAPSULE TECHNOLOGY

(1) "Mechanical Test Report, SNAP 19 Fuel Capsule," MND-3169-46, T. Conway, February 1965.

(2) "SNAP 19 Fuel Form Selection and Capsule Configuration," MND-3169-77, T. Dobry, et al., December 1965.

(3) "SNAP 19 Phase II Final Summary Report," MND-3169-83, August 1965.

(4) "SNAP 19 Fuel Capsule Vibration - Engineering Evaluation Test Report," MND-3607-121, W. M. Griffin, November 1966.

(5) "Interim Report--SNAP 19 Fuel Capsule Impact Test," MND-3607-150, D. Caldwell, March 1967.

(6) "Internal Pressure Test Report--Fuel Capsule Assembly with Simulated Fuel," MND-3607-206, D. C. Caldwell, October 1967.

(7) "Filter Development Program for SNAP 19 Intact Re-entry Heat Source," MND-3607-237, J. Gray, III, D. Stoffel, March 1968.

(8) "Intact Re-entry Heat Source Design Development," MND-3607-238, T. H. Cox, March 1968.

D. GENERATOR SUBSYSTEM SUPPORT STRUCTURE

(1) "Structural Analysis of Generator and Mounting Structure for Nimbus B Application," MND-3169-17, R. Gjertsen, F. Schumann, August 1964.

(2) "Dynamics and Loads Analysis of Support Structure for SNAP 19 Generator, Nimbus Application," MND-3169-18, R. Buxbaum, August 1964.

(3) "Dynamic Analysis of SNAP 19 Generator--Nimbus Application," MND-3169-19, R. S. Buxbaum, G. K. Jones, August 1964.

(4) "SNAP 19 Support Structure Design Development and Qualification Tests," MND-3169-52, W. Britton, January 1965.

(5) "Generator Support Structure Transmissibility Test Report," MND-3169-61, G. Numsen, April 1965.

E. GENERATOR PERFORMANCE AND ENDURANCE TESTS

(1) "Test Report, Assembly and Parametric Testing of SNAP 19 Nimbus B Radioisotope Thermoelectric Generator Subsystem S/N 6," MND-3607-163, R. Pettigrew, May 1967.

(2) "Test Report--Parametric Testing of SNAP 19 Nimbus B Radioisotope Thermoelectric Subsystem S/N 5, Generators S/N 15 and S/N 16," MND-3607-164, May 1967.

(3) "Systems Evaluation of Thermal Vacuum Endurance Test for Fueled Prototype SNAP 19 Power Supply--Nimbus B Application," MND 3607 196, C. J. Clemente, May 1967.

(4) "Test Report--Thirty-Day, Non-Cyclic Thermal Vacuum Test, Prototype SNAP 19 Power Supply System No. 4, Nimbus B Application," MND-3607-170, C. Goebel, December 1967.

(5) "Test Report, Pre- and Post-Fueling Power Check and Parametric Test on RTG Subsystem 4, Prototype, SNAP 19 Nimbus B," MND-3607-198, S. Macarevidh, February 1968.

(6) "SNAP 19 Generator Endurance Test Data and Performance Analysis," MND-3607-236, A. Lieberman, C. Goebel, April 1968.

F. GENERATOR SUBSYSTEM ENVIRONMENTAL TESTS

(1) "Systems Evaluation of Thermal Vacuum Endurance Test for Fueled Prototype SNAP 19 Power Supply--Nimbus B Application," MND-3607-196, C. J. Clemente, May 1967.

(2) "Test Report--Thirty-Day, Non-Cyclic Thermal Vacuum Test, Prototype SNAP 19 Power Supply System No. 4, Nimbus B Application," MND-3607-170, C. Goebel, December 1967.

(3) "Environmental Test Report, Subsystem No. 6 Flight Acceptance Vibration Test," MND-3607-175, C. Blechschmidt, R. Pettigrew, August 1967.

(4) "Test Report--Humidity, Vibration and Acceleration Testing with Subsequent Power Checks and Parametric Test, System 4," MND-3607-194, S. Macarevich, December 1966.

(5) "Systems Test and Evaluation Report on Thermal Vacuum Testing of SNAP 19 Power Supply System No. 7 for Nimbus B Application," MND-3607-205, P. Aller, November 1967.

(6) "Test and Evaluation Report on Thermal Vacuum Testing of SNAP 19-IRHS Generator Subsystem 8," MND-3607A-015, J. Toennies, December 1967.

G. MASS PROPERTIES

(1) "Results of a Study into the Feasibility of Using the Compound Pendulum Technique for Accurately Locating the Center of Gravity of the SNAP 19 Subsystem," MND-3607-177, C. Riggen, T. Coughlin, June 1967.

(2) "Environmental Test Report Subsystem No. 5 Mass Properties," MND-3607-172, C. Riggen, et al., August 1967.

(3) "Environment Test Report--Subsystem No. 6, Weight, Center of Gravity and Mass Moments of Inertia Determination," MND-3607-176, C. Blechschmidt, et al., October 1967.

XII. REFERENCES

I-1 "SNAP 19 Safety Analysis Report Volumes I, II, III, Addendum, and Supplement," MND-3607-133-1, 2, -3, -A and -S. Martin Marietta Corporation.

II-1 Goebel, C. and Lieberman, A., "SNAP 19 Generator Endurance Test Data and Performance Analysis." Martin Marietta Corporation, MND-3607-236, April 1968.

II-2 Revision 4, "Martin Marietta Specification for 3M-Type Lead Telluride Elements." MN-10126, July 1966.

II-3 "Martin Marietta Specification for Thermoelectric Couple Fabrication and Testing." MN-10158, February 1967.

V-1 Goebel, C. and Lieberman, A., "SNAP 19 Generator Endurance Test Data and Performance Analysis," MND-3607-236, Martin Marietta Corporation, April 1968.

VI-1 "SNAP 19 Generator Endurance Test Data and Performance Analysis," MND-3607-236, Martin Marietta Corporation, April 1968.

VII-1 van Amerongen, G. J., "The Permeability of Different Rubbers to Gases and Its Relation of Diffusivity and Solubility." Journal of Appl. Physics, November 1946

VII-2 Loats, Harry L., Jr., et al., "Space Station Connection and Seal Study." MR 6635, October 1962

VII-3 "Development of High Temperature Resistant Rubber Compounds." WADC TR 56-331, Part II, February 1958

VII-4 Podlaseck, S. E., "The Behavior of Organic Materials Under Simulated Space Environmental Condition." Martin Research Memorandum 130, November 1963

VII-5 "The Engineering Properties of Viton." E. I. du Pont de Nemours & Co., Elastomer Chemicals Department Bulletin A-29642, February 1963

VIII-1 "A Study of SNAP 19 Nimbus B RTD Anomalies," Gill, R., MND-3607-100, Martin Marietta Corporation, July 1966.

IX-1 "SNAP 19 Radiation Measurements Report," Rosenthal, H. B., Owings, W. D., Hrubovcak, J. M., MND-3607-173, Martin Marietta Corporation, November 1967.

X-1 Thomas, D. R., "Structural Evaluation of Min-K-1301," MND-3169-45, Martin Marietta Corporation, January 1965.

X-2 "SNAP 19 Phase III Quarterly Progress Report No. 8," MND 3607-210, Martin Marietta Corporation, November 1967.

X-3 Truscello, V., "Generator Subsystem S/N 4 Min-K RTD Damage Survey Report and Considerations Relative to Subsystem S/N 5," Martin Marietta Corporation.

APPENDIX A

MULTIGAS PERMEATION ANALYSIS

The following development leads to the closed form equations used to describe multigas permeation through the SNAP 19 elastomeric seals. Nomenclature is given at the end of the appendix.

The basic law of permeation is

$$Q = \frac{A}{d} \Delta p P \equiv k \Delta p \tag{A-1}$$

therefore, the argon leakage out of the generator is given by

$$Q_A = \frac{1}{\rho_{A,\,ST}} \frac{d\,M_A}{dt} = k_A (p_{A,\,At} - p_A) \tag{A-2}$$

where the partial pressure of argon in the atmosphere can be neglected. The factor associated with argon permeation of the Viton A seal is k_A and it varies with temperature. Data from SNAP 19 hot argon leak tests (Fig. VII-2) indicate that

$$\frac{A}{d} P_A = k_A = k_{A,\,R} \exp \left\{ 0.013 \, (T_{FR} - T_{FR,\,R}) \right\} \tag{A-3}$$

Substitution of the Ideal Gas Law into Eq. (A-2) for M_A and $\rho_{A,\,ST}$ gives

$$\frac{d\,p_A}{dt} = -\frac{T_G}{T_{ST}} \, p_{ST} \frac{k_A p_A}{V_G} \tag{A-4}$$

where T_G is the average temperature within the generator and is assumed to be defined by

$$T_G = \frac{T_{HJ} + 1.1\, T_{FR}}{2} + 460° \tag{A-5}$$

Integration of Eq. (A-4) gives

$$P_A = p_{A,\,o} \exp \left\{ - \left(\frac{T_G}{T_{ST}} \right) \frac{k_A \, p_{ST}}{V_G} \quad t \right\}$$

Similarly, the nitrogen leakage into the generator is given by

$$Q_N = \frac{1}{\rho_{N,\,ST}} \frac{d\,M_N}{dt} = k_N (p_{N,\,At} - p_N) \tag{A-7}$$

Analogous to the differential equation for argon leakage

$$\frac{d\,p_N}{dt} = \left(\frac{T_G}{T_{ST}}\right)\frac{k_N\,p_{ST}}{V_G}\;(p_{N,\,At} - p_N) \tag{A-8}$$

Integration of Eq. (A-8) gives

$$\frac{p_N - p_{N,\,At}}{p_{N,\,o} - p_{N,\,At}} = \exp\left\{-\left(\frac{T_G}{T_{ST}}\right)\frac{k_N\,p_{ST}}{V_G}\right\} \tag{A-9}$$

or

$$p_N = p_{N,\,At}\left\{1 - \exp\left(-\frac{T_G}{T_{ST}}\right)\frac{k_N\,p_{ST}}{V_G}\;t\right\} + p_{N,\,o}\exp\left\{-\frac{T_G}{T_{ST}}\;\frac{k_N\,p_{ST}}{V_G}\;t\right\} \tag{A-10}$$

Assuming that all of the oxygen from the atmosphere that permeates the generator is reacted with the zirconium getter, the generator pressure is the sum of the partial pressures of argon and nitrogen.

$$p_G = p_A + p_N \tag{A-11}$$

Substituting Eq. (A-6) and (A-10) into Eq. (A-11) gives

$$p_G = p_{A,\,o}\exp(-\tau_A t) + p_{N,\,At}\left\{1 - \exp(-\tau_N t)\right\} + p_{N,\,o}\exp(-\tau_N t) \tag{A-12}$$

where

$$\tau = \left(\frac{T_G}{T_{ST}}\right)\left(\frac{k\,p_{ST}}{V_G}\right) \tag{A-13}$$

For flight operation in a vacuum, $p_{N,\,At}$ is zero. Thus the analytic expression for the SNAP 19 generator transient pressure during flight operation is

$$p_G = p_{A,\,o}\exp(-\tau_A t) + p'_{N,\,o}\exp(-\tau_N t) \tag{A-14}$$

where $p'_{N,\,o}$ is the partial pressure of nitrogen in the generator at the time the system is launched.

In determining the pressure in the IRHS system, it is correctly assumed that the pressure in the fuel capsule is in equilibrium with the pressure of the generator. (The capsule leak rate is two to three orders of magnitude higher than the seal leak rate.)

The mass balance for the helium in the system is given by

$$\left(\frac{d\,M_H}{dt}\right)_G = \left(\frac{d\,M_H}{dt}\right)_S + \left(\frac{d\,M_H}{dt}\right)_L \tag{A-15}$$

where

$$\left(\frac{d\,M_H}{dt}\right)_S = B \exp(-\lambda t) = m_H N \lambda \qquad \text{(A-16)}$$

The helium leakage is given by

$$\frac{1}{\rho_{H,\,ST}} \left(\frac{d\,M_H}{dt}\right)_L = Q_H = -k_H p_H \qquad \text{(A-17)}$$

Thus

$$\left(\frac{d\,M_H}{dt}\right)_G = B \exp(-\lambda t) - k_H \rho_{H,\,ST}\, p_H \qquad \text{(A-18)}$$

Substituting the Ideal Gas Law and rearranging gives

$$\frac{d\,p_H}{dt} + \left(\frac{T_G}{T_{ST}}\right) \frac{k_H p_{ST}}{V_G}\, p_H = \frac{R_H T_G}{V_G}\, B \exp(-\lambda t) \qquad \text{(A-19)}$$

Equation (A-19) is an ordinary linear differential equation whose solution is

$$p_H = p_{H,\,o} \exp(-\tau_H t) + \frac{E}{\tau_H - \lambda} \exp(-\lambda t) - \exp(-\tau_H t) \qquad \text{(A-20)}$$

where

$$E = B\left(\frac{R_H T_G}{V_G}\right)$$

and τ_H is defined by Eq. (A-13).

The generator pressure for the IRHS system is then given as the sum of the partial pressures of argon, nitrogen and helium

$$p_G = p_A + p_N + p_H \qquad \text{(A-21)}$$

where the partial pressures of argon and nitrogen are as defined for the dispersal system.

NOMENCLATURE

Symbol	Definition
A	Area normal to permeation flow (cm^2)
A/d	Seal geometry constant (cm)
B	Fuel capsule helium generation rate at t' = 0 (gm/sec)
C	Unit conversion constant (0.005085) ($in.^2$-ft/cm^3)
d	Width of seal (cm)
E	Unit conversion constant (psi/sec)
k	Proportionality constant ($in.^2$-cm^3/lb-sec)
m	Atomic mass (gm/atom)
M	Mass of gases (lb)
N	Number of atoms
p	Pressure (lb/$in.^2$)
Δp	Partial pressure difference between generator and environment (lb/$in.^2$)
P	Permeability constant (cm^2/sec-atm)
Q	Volumetric flow (leakage) rate (scc/sec)
R	Gas constant (ft-lb/lb-°R)
t	Time (sec)
t'	Fuel decay time (yr)
T	Temperature (°R)
V	Volume (cm^3)
W	Mass flow rate (lb/hr)
τ	Time constant (sec^{-1})
λ	Fuel decay constant (yr^{-1})
ρ	Density (lb/ft^3)

NOMENCLATURE (continued)

Subscripts	Definition
A	Argon
At	Atmosphere
FR	Fin root
G	Generator
H	Helium
HJ	Hot junction
L	Leakage
m	Measured value
N	Nitrogen
o	Initial condition
O	Oxygen
R	At referenced condition, (Fin root temperature = 337° F, and generator pressure = 14.7 psia argon)
S	Source
ST	Standard pressure and temperature (14.7 psia, 32° F)